QUALITATIVE STUDY OF THE PLANAR ISOSCELES THREE-BODY PROBLEM

CARLES SIMÓ

Facultat de Matemàtiques, Universitat de Barcelona, Barcelona, Spain.

and

REGINA MARTÍNEZ

Secció de Matemàtiques, Facultat de Ciènces, Universitat Autònoma de Barcelona, Bellaterra, Barcelona, Spain.

(Received: 4 May, 1987; accepted 21 August, 1987)

Abstract. We consider the particular case of the planar three body problem obtained when the masses form an isosceles triangle for all time. Various authors [1, 2, 12, 8, 9, 13, 10] have contributed in the knowledge of the triple collision and of several families of periodic orbits in this problem. We study the flow on a fixed level of negative energy. First we obtain a topological representation of the energy manifold including the triple collision and infinity as boundaries of that manifold. The existence of orbits connecting the triple collision and infinity gives some homoclinic and heteroclinic orbits. Using these orbits and the homothetic solutions of the problem we can characterize orbits which pass near triple collision and near infinity by pairs of sequences. One of the sequences describes the regions visited by the orbit, the other refers to the behaviour of the orbit between two consecutive passages by a suitable surface of section. This symbolic dynamics which has a topological character is given in an abstract form and after it is applied to the isosceles problem. We try to keep globality as far as possible. This strongly relies on the fact that the intersection of some invariant manifolds with an equatorial plane ($v = 0$) have nice spiraling properties. This can be proved by analytical means in some local cases. Numerical simulations given in Appendix A make clear that these properties hold globally.

1. Triple Collision Manifold

We consider, in the plane, three masses m_1, m_2 and m_3 at the vertices of an isosceles triangle. Let x_1 the distance between m_1 and m_2 and x_2 the (signed) distance between the center of masses (c.o.m.) of m_1, m_2 and m_3 (see Fig. 1.1). We fix the c.o.m. of m_1, m_2, m_3 at the origin and we take $m_1 = m_2$ and the suitable velocities of the three masses in order to maintain the isosceles configuration. We introduce the parameter of masses $\varepsilon = m_3/m_1$ and after a suitable scaling we suppose $m_1 = 1$. The equations of motion are

$$\ddot{x}_1 = -\frac{2}{x_1^2} - \frac{8\varepsilon x_1}{(x_1^2 + 4x_2^2)^{3/2}},$$
$$\ddot{x}_2 = -\frac{8(2+\varepsilon)x_2}{(x_1^2 + 4x_2^2)^{3/2}}. \tag{1.1}$$

The energy integral is given by the function

$$H = \frac{\dot{x}_1^2}{4} + \frac{\varepsilon}{2+\varepsilon}\dot{x}_2^2 + V(x_1, x_2) \tag{1.2}$$

Celestial Mechanics **41** (1988) 179–251.

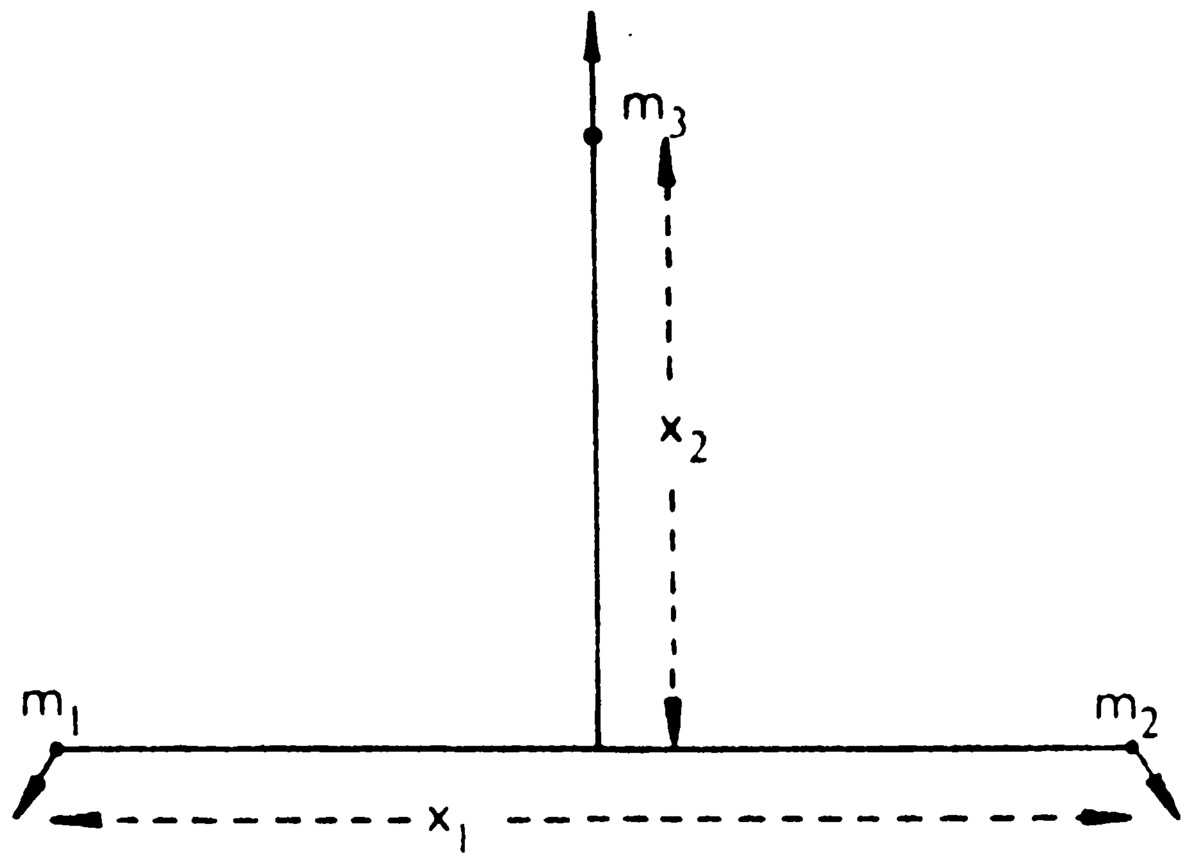

Fig. 1.1.

where

$$V(x_1,x_2) = -\frac{1}{x_1} - \frac{4\varepsilon}{(x_1^2 + 4x_2^2)^{1/2}}$$

is the potential.

If we fix a value h of the energy, the motion takes place in a 3-dimensional manifold $\mathscr{V}$. When the energy is positive or zero, it is known (see [4]) that for all the initial conditions the three masses escape to infinity. We study the case where energy $h < 0$. After a suitable scaling of variables and time we can restrict at the level $h = -1$. Therefore from now on we suppose that $\mathscr{V}$ is the manifold of constant energy -1.

The zero velocity curve (see Fig. 1.2) given by

$$-V(x_1,x_2) - 1 = 0 \tag{1.3}$$

is the boundary of the region where the motion takes place. The projection of this region on the position plane is called Hill's region and given by $-V(x_1,x_2) - 1 \geqslant 0$.

The system (1.1) has two singularities: for $x_1 = 0$, which corresponds to double collisions, and for $x_1 = x_2 = 0$, that is, at triple collision.

In order to study the behaviour of the orbits passing near triple collision we use the blow up method due to McGehee [6]. The suitable transformations of the blow up in the isosceles problem have been made by Devaney [2]. In the remaining part of this section, we present a summary of known results about triple collision in the isosceles case.

Let us introduce some notation: $\mathbf{x}^T = (x_1,x_2)$, $\mathbf{p} = A\dot{\mathbf{x}}, A = \text{diag}(1/2,\ 2\varepsilon/(2+\varepsilon))$.

We define new variables $r, \mathbf{s}, v, \mathbf{u}, \theta, u, w$ by

$$r = (\mathbf{x}^T A\mathbf{x})^{1/2},$$
$$\mathbf{s} = r^{-1}\mathbf{x} = (A^{-1})^{1/2}(\cos\theta,\ \sin\theta), \quad \theta\in[-\pi/2,\ \pi/2],$$

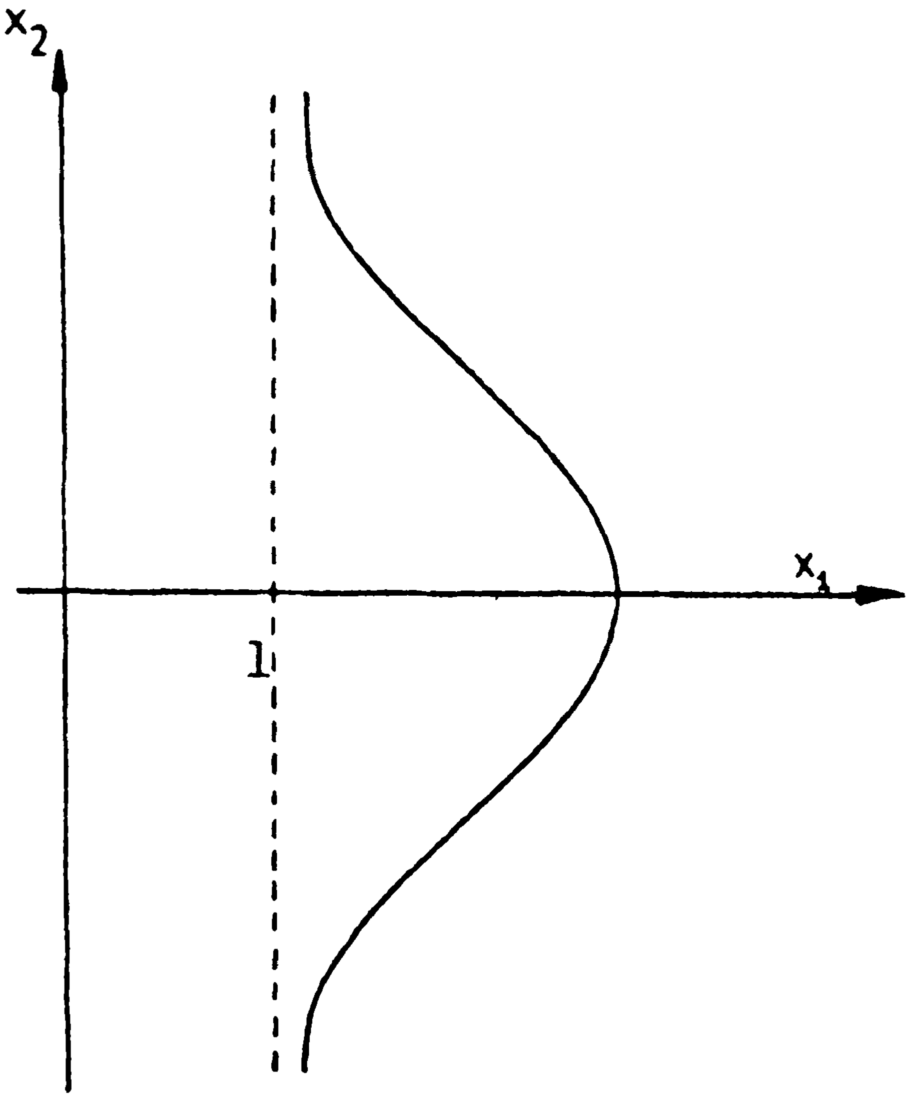

Fig. 1.2.

$$\begin{aligned} v &= r^{1/2}(\mathbf{s},\mathbf{p}), \\ \mathbf{u} &= r^{1/2}(A^{-1}\mathbf{p} - (\mathbf{s},\mathbf{p})\mathbf{s}) = u(A^{-1})^{1/2}(-\sin\theta, \cos\theta), \\ w &= u\cos\theta\,(W(\theta))^{-1/2}, \end{aligned} \tag{1.4}$$

where

$$V(\theta) = -1/(\sqrt{2}\cos\theta) - 4\varepsilon^{3/2}/(2\varepsilon + 4\sin^2\theta)^{1/2}, \quad W(\theta) = -\cos\theta V(\theta).$$

Scaling the time by $\mathrm{d}t/\mathrm{d}\tau = r^{3/2}$ and $\mathrm{d}\tau/\mathrm{d}\bar{\tau} = \cos\theta/(W(\theta))^{1/2}$, we get from (1.1)

$$\begin{aligned} r' &= rv\cos\theta(W(\theta))^{-1/2}, \\ v' &= \sqrt{W(\theta)}\,(1 - \cos\theta(v^2 - 4rh)/(2W(\theta))), \\ \theta' &= w, \\ w' &= \sin\theta(-1 + \cos\theta(v^2 - 2rh)/W(\theta)) - vw\cos\theta/(2\sqrt{W(\theta)}) + \\ &\quad + (\cos\theta - w^2/2)\,W'(\theta)/W(\theta). \end{aligned} \tag{1.5}$$

In (1.5) the prime $'$ means differentiation with respect to $\bar{\tau}$, except in $W'(\theta)$ where $W'(\theta)$ denotes $\mathrm{d}W(\theta)/\mathrm{d}\theta$. We rename $t = \bar{\tau}$. After (1.4) the energy integral becomes

$$\frac{w^2}{2\cos\theta} - 1 = \frac{\cos\theta}{W(\theta)}\left(rh - \frac{v^2}{2}\right). \tag{1.6}$$

The transformation (1.4) is analytic at $r > 0$ and defines a vector field which is analytic at the points of the phase space with $r > 0$. This vector field can be extended analytically at the points with $r = 0$, that is, at triple collision.

We define the triple collision manifold $\mathscr{C}$ as the set of points $(r, v, \theta, w) \in [0, \infty) \times \mathbb{R} \times [-\pi/2, \pi/2] \times \mathbb{R}$ with $r = 0$ such that

$$\frac{w^2}{2\cos\theta} + \frac{v^2\cos\theta}{2W(\theta)} = 1. \tag{1.7}$$

$\mathscr{C}$ is a two dimensional invariant manifold, topologically equivalent to a sphere with four holes (see Fig. 1.3). The flow defined by putting $r = 0$ in (1.5) is gradient-like with respect to v and it is easy to prove that there are six critical points, $(v, \theta, w) = (\pm\sqrt{-2V(\theta)}, \theta, 0)$ where θ is one of the central configurations. In fact, these are the unique critical points of the global system (1.5).

The Euler configuration corresponds to $\theta = 0$ which is a local minimum of $V(\theta)$. There are 2 configurations of Lagrange type for the local maximum of $V(\theta), \theta = \pm\,\theta_L(\varepsilon) = \pm\arctan\,((3\varepsilon/(2+\varepsilon))^{1/2})$. We put $\theta_L = \theta_L(\varepsilon)$ if there is no confusion.

On $\mathscr{C}$, the Lagrange points $L^{i,s}$, $M^{i,s}$ are saddles and the Euler points are sink (E^s) or source (E^i) with respect to the flow restricted to $\mathscr{C}$, with complex eigenvalues for $\varepsilon < 55/4$ and real ones for $\varepsilon \geqslant 55/4$. From now on we assume $\varepsilon < 55/4$. First of all we recall some properties of the flow on $\mathscr{C}$.

Let P be one of the Lagrange points. We denote by W_p^a with $a \in \{s, u\}$, the stable ($a = s$) or unstable ($a = u$) invariant manifold of P. We denote by $W_p^{a,b}$ with $b \in \{1, 2\}$ the branch which reaches or leaves P with $w > 0$ ($b = 1$) or $w < 0$ ($b = 2$).

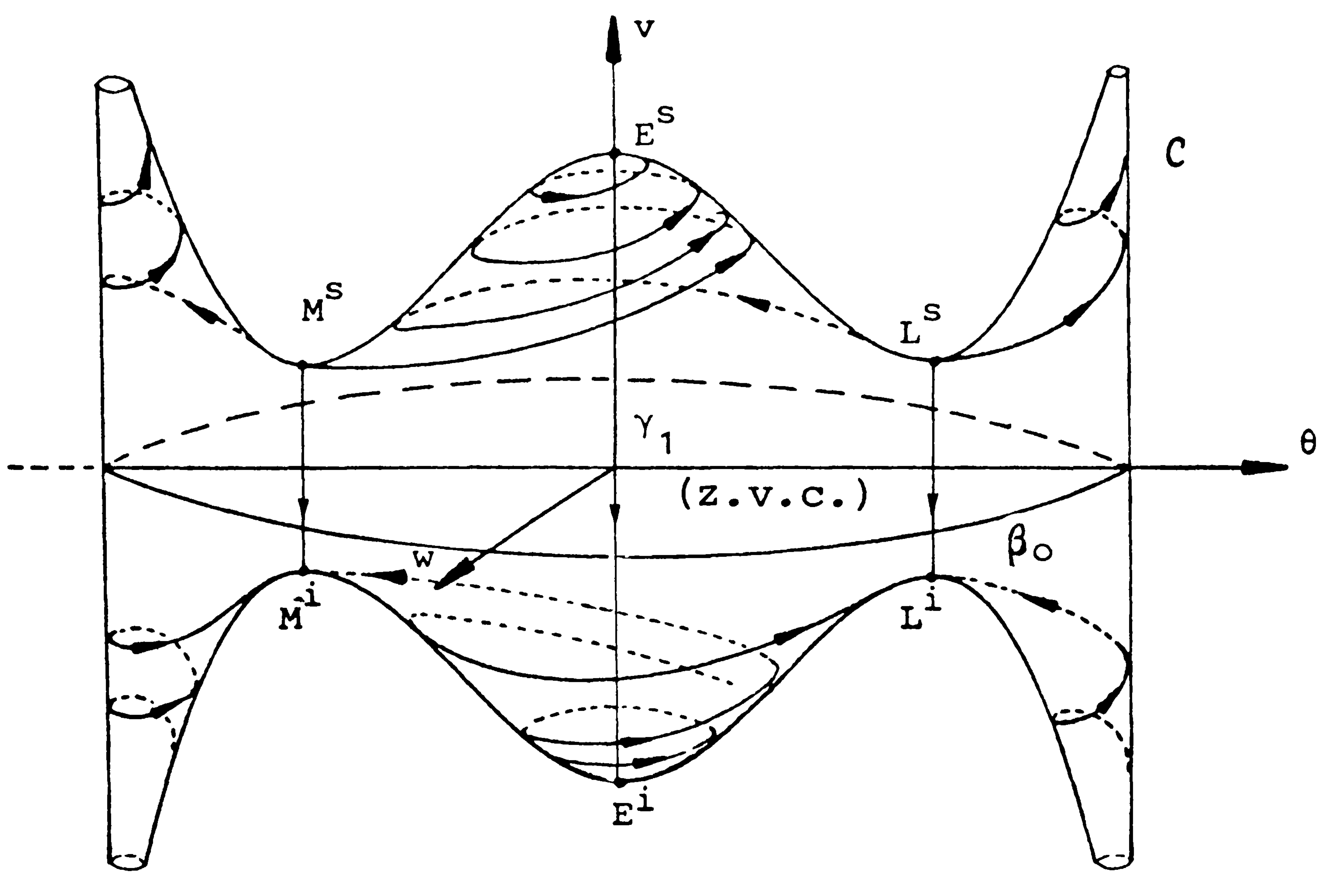

Fig. 1.3.

We define $W^1_{E^i}(W^2_{E^i})$ as the open set in $\mathscr{C}$ bounded by $W^{s,2}_{M^i}$, $W^{s,1}_{L^i}$, $W^{u,1}_{M^i}$ and $W^{u,1}_{L^i}$ ($W^{s,1}_{L^i}$, $W^{s,2}_{M^i}$, $W^{u,2}_{L^i}$ and $W^{u,2}_{M^i}$ respectively). $W^1_{E^s}$ and $W^2_{E^s}$ are defined in a similar way.

The behaviour of $W^{s,1}_{L^i}$ and $W^{s,2}_{L^i}$ is shown in Figure 1.3. We can obtain $W^u_{L^s}$, $W^u_{M^s}$ and $W^s_{M^i}$ using the symmetries of the flow in $\mathscr{C}$

$$L^1: (r, v, \theta, w, \tau) \rightarrow (r, -v, \theta, -w, -\tau),$$
$$L^2: (r, v, \theta, w, \tau) \rightarrow (r, -v, -\theta, w, -\tau).$$

restricted to $\mathscr{C}$.

The intersection of $W^{u,1(2)}_{L^i}$ ($W^{s,1(2)}_{L^s}$) with $v = 0$ will be called $l^{i,1(2)}$ ($l^{s,1(2)}$). We use $m^{i,1(2)}$ and $m^{s,1(2)}$ for the corresponding intersections of $W^{u,1(2)}_{M^i}$ and $W^{s,1(2)}_{M^s}$, respectively.

Next proposition was proved by Simó in [10].

PROPOSITION 1.1. *There exist two critical values of* ε, ε_1, *and* ε_2 *with* $\varepsilon_1 < \varepsilon_2$ *such that:*

(i) if $\varepsilon = \varepsilon_1$ *(case II), then* $m^{i,1} = (\pi/2, 0)$ *and so* $W^{u,1}_{M^i} = W^{s,2}_{M^s}$, *and for* $\varepsilon = \varepsilon_2$ *(case IV),* $l^{i,1} = (0, -\sqrt{2})$ *and* $W^{u,1}_{L^i} = W^{s,1}_{M^s}$;

(ii) *for* $0 < \varepsilon < \varepsilon_1$ *(case I)* $m^{i,1} = (\theta, w)$ *with* $\theta > 0$, $w > 0$ *and* $l^{i,1} = (\theta, w)$ *with* $\theta > 0$, $w < 0$, *so* $W^{u,1}_{M^i}$ *dies at* E^s *and* $W^{u,1}_{L^i}$ *escapes around the upper branch of binary collision with* $\theta = -\pi/2$;

(iii) *for* $\varepsilon > \varepsilon_2$ *(case V),* $m^{i,1} = (\theta, w)$ *with* $\theta > 0$, $w < 0$, *and* $l^{i,1} = (\theta, w)$ *with* $\theta < 0$, $w < 0$. *Then* $W^{u,1}_{L^i}$ *ends at* E^s *and* $W^{u,1}_{M^i}$ *escapes through the upper branch of* $\theta = -\pi/2$;

(iv) *for* $\varepsilon_1 < \varepsilon < \varepsilon_2$ *(case III),* $l^{i,1}$ *and* $m^{i,1}$ *have coordinates* $\theta > 0$ *and* $w < 0$. *Therefore* $W^{u,1}_{L^i}$ *and* $W^{u,1}_{M^i}$ *turn around the upper branch of* $\theta = -\pi/2$.

The values $\varepsilon_1 = 0.378\,532 \ldots$ and $\varepsilon_2 = 2.661\,993 \ldots$ are obtained numerically. They determine the five different cases mentioned above.

Now we consider $\mathscr{C}$ in the total phase space. $\mathscr{C}$ is in the boundary of $\mathscr{V}$ and contains the critical points of the global system (1.5). We give the dimensions of W^a_p on $\mathscr{C}$ and on $\mathscr{V} \cup \mathscr{C}$ in the Table I.1

TABLE I.1

	$W^u_{E^s}$	$W^s_{E^s}$	$W^u_{E^i}$	$W^s_{E^i}$	$W^u_{L^s,M^s}$	$W^s_{L^s,M^s}$	$W^u_{L^i,M^i}$	$W^s_{L^i,M^i}$
$\mathscr{C}$	0	2	2	0	1	1	1	1
$\mathscr{V} \cup \mathscr{C}$	1	2	2	1	2	1	1	2

We refer to [2] for the computations.

The collision (ejection) orbits are the union of $W^{s(u)}_{E^{i(s)}}$, $W^{s(u)}_{L^{i(s)}}$ and $W^{s(u)}_{M^{i(s)}}$ on $\mathscr{V} \cup \mathscr{C}$.

There are 3 homothetic solutions (see Fig. 1.4) corresponding to $\theta = 0$ (collinear), $\theta = \theta_L$ and $\theta = -\theta_L$ (equilateral triangle). They are contained in the plane $w = 0$

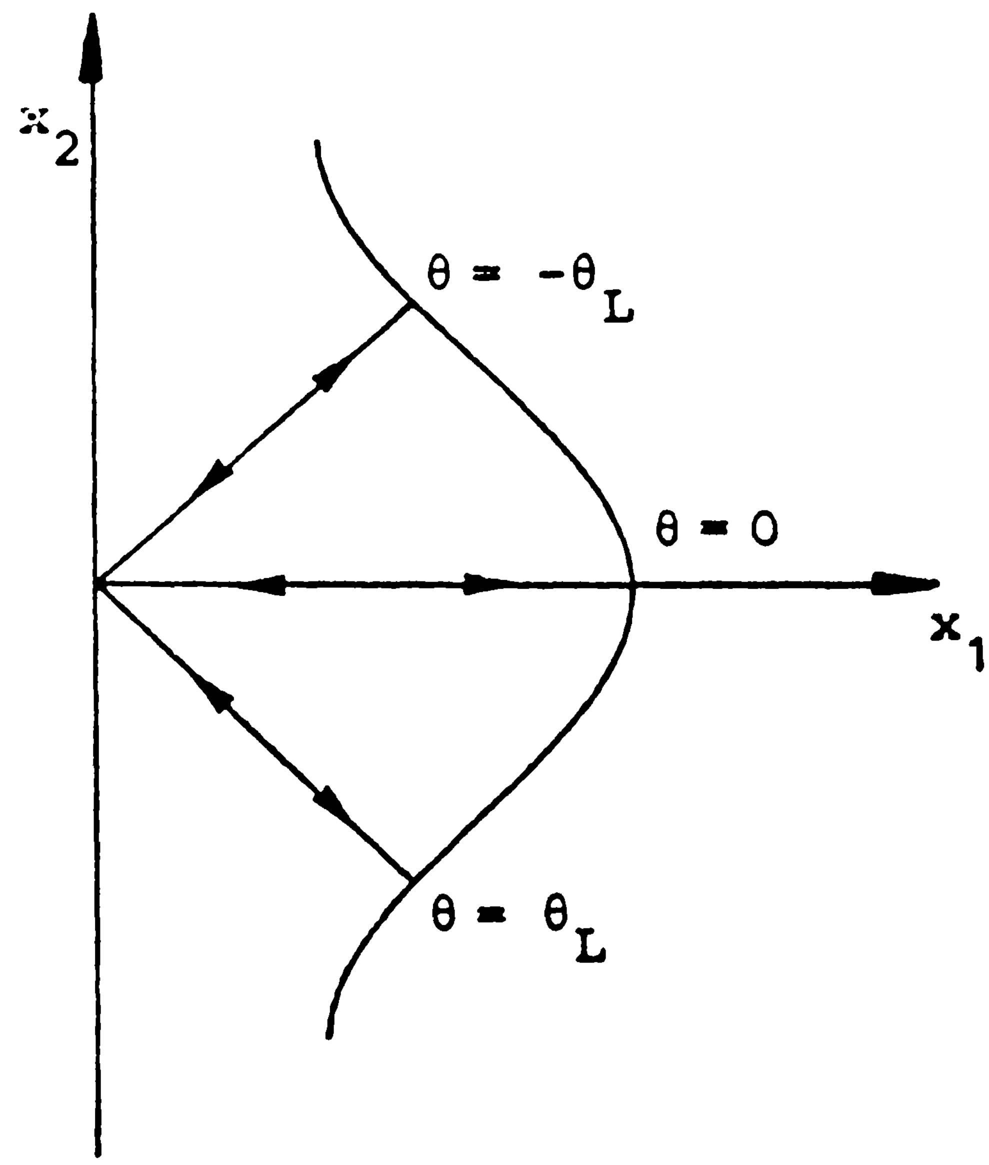

Fig. 1.4.

(see Fig. 1.3). We note that both $W^u_{E^s}$ and $W^s_{E^l}$ coincide with the Euler homothetic orbit for $\theta = 0$.

THEOREM 1.1. *$W^u_{L^s}$ $(W^u_{M^s})$ cuts transversally to $W^s_{L^l}(W^s_{M^l})$ along the Lagrange homothetic orbit for $\theta = \theta_L(-\theta_L)$.*

Theorem 1.1 is proved in a more general form in [11].

We note that in the variables (1.4) the zero velocity curve is reduced to the segment

$$\gamma_1 = \{(r, v, \theta, w) \in \mathcal{V} \mid v = 0,\ w = 0,\ -\pi/2 < \theta < \pi/2\}.$$

We define

$$\begin{aligned} S^+ &= \{(r, v, \theta, w) \in \mathcal{V} \mid \theta = \pi/2\}, \\ S^- &= \{(r, v, \theta, w) \in \mathcal{V} \mid \theta = -\pi/2\}, \\ S_1 &= \{(r, v, \theta, w) \in \mathcal{V} \mid \theta = 0\}, \\ \gamma_2 &= \{(r, v, \theta, w) \in \mathcal{V} \mid \theta = 0,\ v = 0\}. \end{aligned}$$

We can represent the points of $S^+ \cup S^-$ by (r, v) because $w = 0$ if $\theta = \pm\pi/2$.

We note that the points on S^+ and S^- represent the binary collisions and S_1 is the set of collinear configurations.

2. The Flow Near Infinity

Let $p \in \mathcal{V}$, $(x_1(t),\ x_2(t),\ \dot{x}_1(t),\ \dot{x}_2(t))$ or shortly $\varphi(t, p)$, will be the orbit which passes by p at $t = 0$.

An orbit escapes at (arrives from) infinity if $x_2(t)$ tends to $\pm\infty$ when t tends to $+\infty(-\infty)$. This is the only way to escape at (arrive from) infinity when the energy is negative due to the existence of the zero velocity curve (1.3).

The escape (arrival) is parabolic if $\dot{x}_2(t)$ tends to zero when t tends to $+\infty(-\infty)$. If $\dot{x}_2(t)$ tends to a constant different from zero when t tends to $+\infty$ or $-\infty$, we say that the orbit is hyperbolic.

We use the transformations introduced by McGehee [7] in the collinear three body problem.

Let be

$$\begin{aligned} x_2 &= 2(2+\varepsilon)^{1/3}x^{-2}, \\ \dot{x}_2 &= (2+\varepsilon)^{1/3}y, \\ x_1 &= \xi^2, \\ \dot{x}_1 &= 2\eta\xi^{-1}, \\ dt &= \xi^2 d\kappa \quad \text{and} \quad {}' = d/d\kappa. \end{aligned} \tag{2.1}$$

Inserting (2.1) in (1.2) we obtain the new expression for the energy integral

$$\eta^2 + \xi^2 + 4d\xi^2(y^2 - x^2) - 4\varepsilon u f(u) = 1, \tag{2.2}$$

where $d = \varepsilon(4(2+\varepsilon)^{1/3})^{-1}$, $u = d\xi^2 x^2/\varepsilon$ and $f(u) = (1+u^2)^{-1/2} - 1$.

Now we get the following system which is regular at infinity ($x = 0$)

$$\begin{aligned} x' &= -\xi^2 y x^3/4, \\ y' &= -\xi^2 x^4(1+g(u))/4, \\ \xi' &= \eta, \\ \eta' &= \xi\left(-1 + 4dx^2 f(u) - 4d(y^2 - x^2) - \frac{G_1(u)}{\xi^2}\right), \end{aligned} \tag{2.3}$$

where $g(u) = (1+u^2)^{-3/2} - 1 = O(u^2)$, $G_1(u) = 4\varepsilon u^3(1+u^2)^{-3/2}$ and for the last equation we have used (2.2).

We use a Levi–Civita regularization (ξ, η) for the binary collision. If we take polar coordinates $(R, \bar{\varphi})$ in the plane (ξ, η) given by $\xi = R\cos\bar{\varphi}$, $\eta = R\sin\bar{\varphi}$, then, from (2.2) we obtain

$$R^2 = 1 + \bar{R}(x, y, \bar{\varphi}),$$

where $\bar{R}$ is a function of order 2 in x, y and 2π-periodic in $\bar{\varphi}$.

The points $x = 0$ form an invariant manifold that we call the infinity manifold.

Let

$$X = x\sqrt{\frac{4d}{1+4dx^2}}, \quad Y = y\sqrt{\frac{4d}{1+4dy^2}}, \quad \bar{\eta} = \eta\sqrt{1-Y^2}.$$

Inserting $X, Y, \bar{\eta}$ in (2.2) we have for $X = 0$

$$\bar{\eta}^2 + \xi^2 + Y^2 = 1.$$

This is a sphere except two points $(Y, \xi, \bar{\eta}) = (\pm 1, 0, 0)$. Really the infinity manifold is the union of two spheres taking out the two poles in both of them. We call these spheres I_+ and I_- depending on the sign of x_2.

As in the collinear three body problem [7], (2.3) has a 2π-periodic solution for $(x, y) = (0,0)$ (P.O.$_+$ in I_+ and P.O.$_-$ in I_-). The flow near $(x, y) = (0,0)$ is obtained by rotation of Figure 2.1 around the y axis. In this way the Figure 2.2 is obtained. The point $(x, y) = (0,0)$ can be seen as a hyperbolic fixed point (despite the fact that this is a degenerate case) for the Poincaré map; that is, there exist stable and unstable invariant manifolds which are analytic in a neighbourhood of $(0,0)$ (except, perhaps, at $(0,0)$, see [7]).

To compute the stable manifold we put

$$x = F(y,\bar{\varphi}) = \sum_{1 \leqslant n < \infty} a_n(\bar{\varphi})\, y^n,$$

as the expression for such manifold. We rewrite (2.3) using $\bar{\varphi}$ as the independent variable to get

$$\frac{dx}{d\bar{\varphi}} = -\tfrac{1}{4}\cos^2(\bar{\varphi})\, y x^3 (1 + O_2),$$

$$\frac{dy}{d\bar{\varphi}} = -\tfrac{1}{4}\cos^2(\bar{\varphi}) x^4 (1 + O_2),$$

where O_n means terms of order n in x, y. We should have

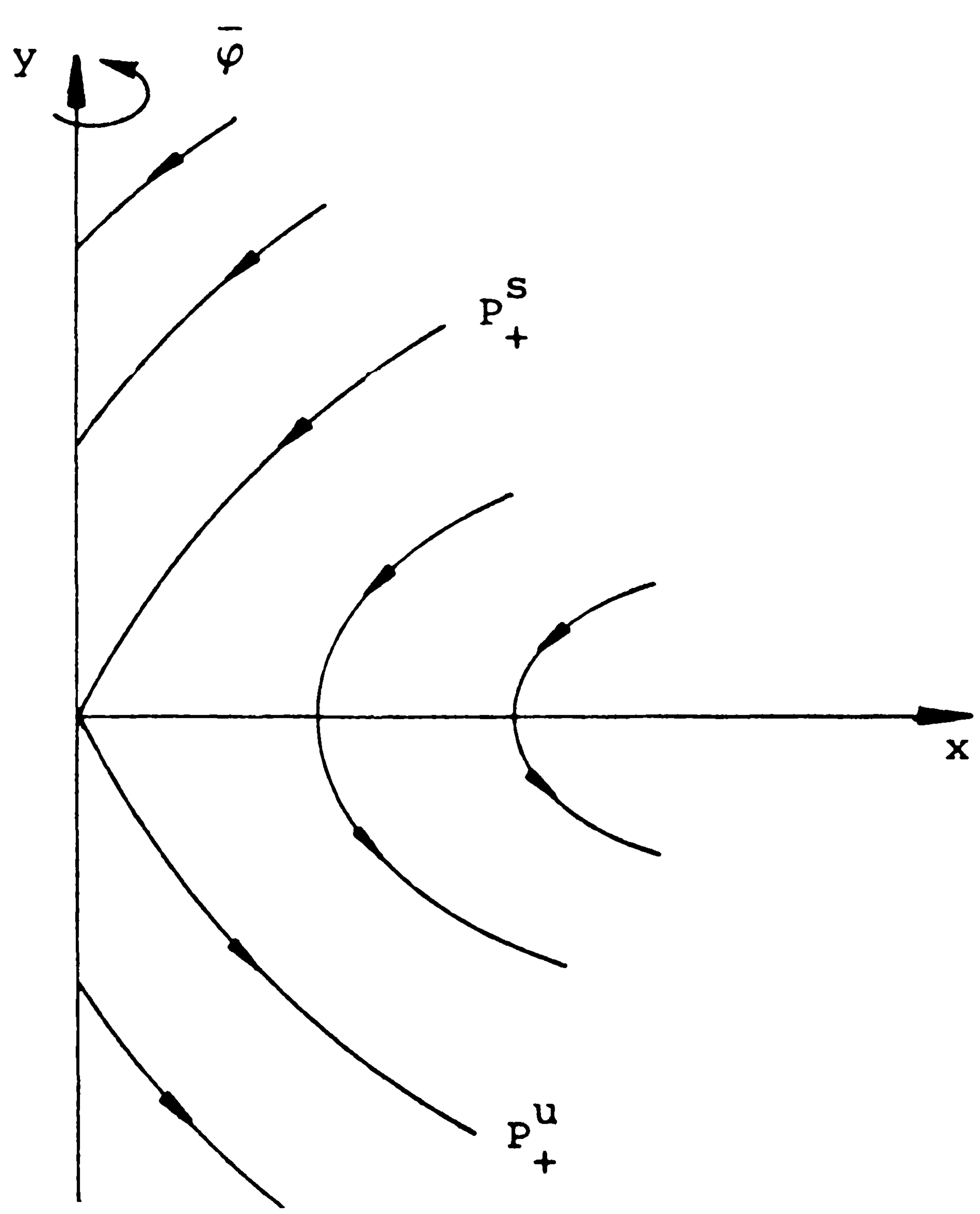

Fig. 2.1.

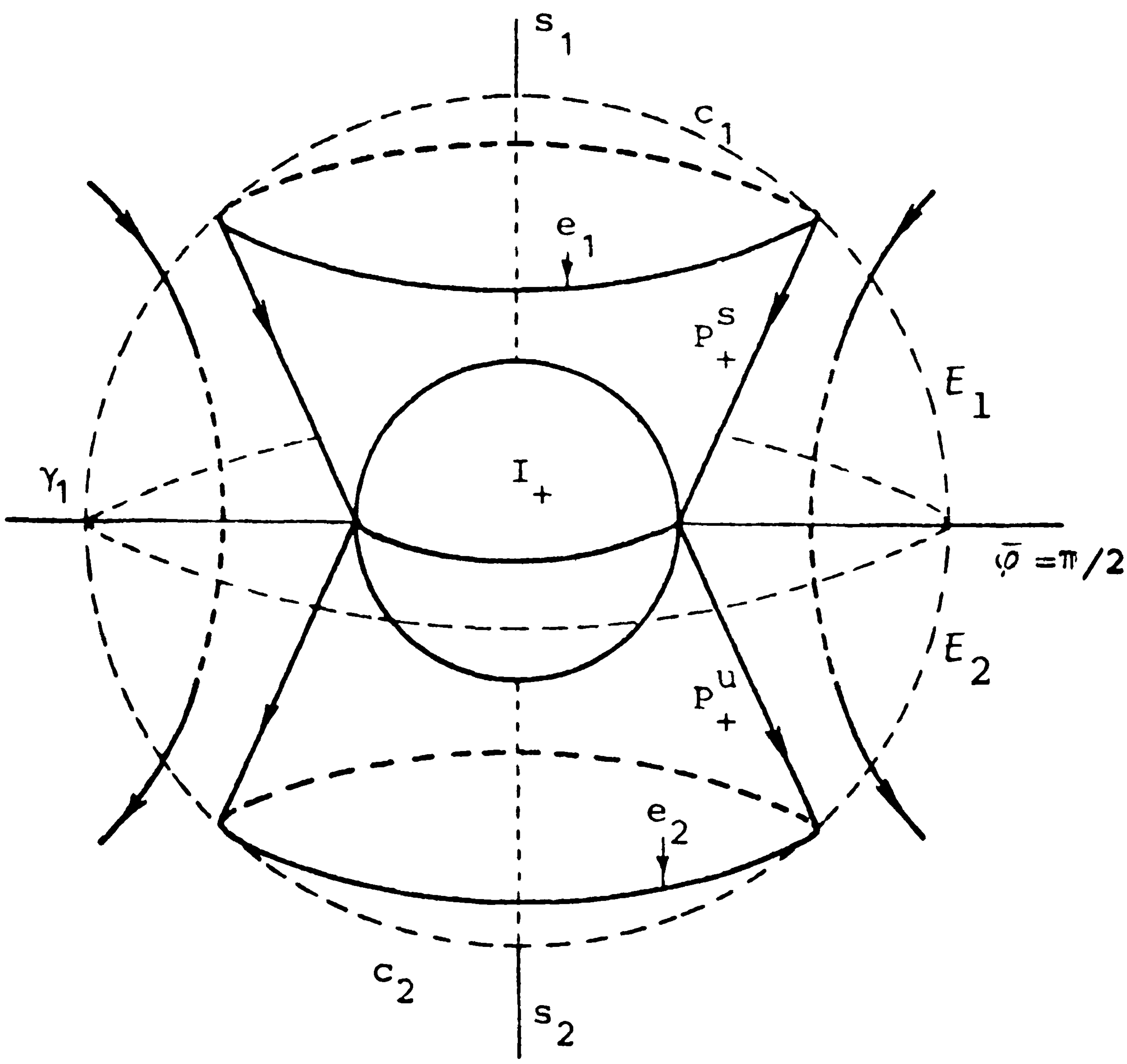

Fig. 2.2.

$$\frac{\mathrm{d}x}{\mathrm{d}\bar\varphi}=\frac{\partial F}{\partial y}\frac{\mathrm{d}y}{\mathrm{d}\bar\varphi}+\frac{\partial F}{\partial \bar\varphi},$$

where in $\mathrm{d}x/\mathrm{d}\bar\varphi$ and $\mathrm{d}y/\mathrm{d}\bar\varphi$ we substitute x by $F(y,\bar\varphi)$. Equating the coefficients of the different powers of y we obtain a sequence of differential equations for $a_n(\bar\varphi)$, $n \geqslant 1$. We remark that the expressions $\mathrm{d}a_n(\bar\varphi)/\mathrm{d}\bar\varphi$, $n \geqslant 1$, contain $\cos^2(\bar\varphi)$ as a factor. In this way all the coefficients $a_n(\bar\varphi)$ can be obtained by recurrence. For $n \leqslant 10$ the only nonzero terms are $a_1(\bar\varphi)=1$, $a_5(\bar\varphi)=5/(512(2+\varepsilon)^{2/3})$, $a_8(\bar\varphi)=3\sin(2\bar\varphi)((1/3)\sin^2(2\bar\varphi)-(3/2)(\cos(2\bar\varphi)+1))/(2048(2+\varepsilon)^{2/3})$, $a_9(\bar\varphi)=43/(2^{18}(2+\varepsilon)^{4/3})$.

The translation of symmetry L^1 to the new variables (2.1) gives

$$(x,y,\bar\varphi,\kappa)\to(x,-y,-\bar\varphi,-\kappa). \tag{2.4}$$

Using (2.4) we obtain for the unstable manifold $x=F(-y,-\bar\varphi)$. Furthermore, from (2.3) it is clear that the equations remain unchanged if x changes sign. Therefore the unstable manifold is given also by $x=-F(y,\bar\varphi)$. From this it follows that $a_n(\bar\varphi)$ is an odd function of $\bar\varphi$ for n even, and an even function for n odd.

The orbits of the invariant manifolds of P.O.$_+$ and P.O.$_-$ are parabolic. We call

$P^s_{+(-)}$ and $P^u_{+(-)}$ the manifolds of parabolic orbits at $I_{+(-)}$ when t tends to $+\infty$ and t tends to $-\infty$, respectively (see Fig. 2.1).

Let B_+ and B_- two spheres near I_+ and I_- respectively (see Fig. 2.2). The circle $e_1 = P^s_+ \cap B_+$ determines on the northern hemisphere of B_+ two regions, c_1 corresponding to hyperbolic orbits, and $\mathscr{E}_1$ whose orbits are elliptic. In this context an elliptic orbit means an orbit which enters in a neighbourhood of infinity but it goes out after a positive time. In a similar way, the circles $e_2 = P^u_+ \cap B_+$, $e_3 = P^s_- \cap B_-$ and $e_4 = P^u_- \cap B_-$ determine the regions c_2 and $\mathscr{E}_2, c_3$ and $\mathscr{E}_3, c_4$ and $\mathscr{E}_4$ in B_+, B_- and B_-, respectively.

The flow near infinity crosses the surface

$$S_2 = \{(x, y, \xi, \eta) \in \mathscr{V} \mid y = 0\}.$$

Therefore we can define the following diffeomorphisms

$$i^1_{+(-)}\colon \mathscr{E}_{1(3)} \to S_2; \quad i^2_{+(-)}\colon S_2 \to \mathscr{E}_{2(4)},$$

obtained following the flow. Then we define $i_+\colon \mathscr{E}_1 \to \mathscr{E}_2$ and $i_-\colon \mathscr{E}_3 \to \mathscr{E}_4$ as $i_+ = i^2_+ i^1_+$ and $i_- = i^2_- i^1_-$, respectively.

LEMMA 2.1. *Let γ be an arc in $\mathscr{E}_{1(2)}$ with an endpoint on $e_{1(2)}$. Then $i_+(\gamma)$ $(i_+^{-1}(\gamma))$ is an arc spiraling towards $e_{2(1)}$, that is, if $\gamma' \subset \mathscr{E}_{2(1)}$ is an arc which ends in a point of $e_{2(1)}$, then $i_+(\gamma)$ cuts γ' at infinite points in any neighbourhood of $e_{2(1)}$.*

An analogous result is true in $\mathscr{E}_3$ and $\mathscr{E}_4$.

Lemma 2.1 follows immediately from the next Lemma whose proof is essentially inspired by [5], p. 170.

LEMMA 2.2. *Let γ be an arc in $\mathscr{E}_1$ with an endpoint on e_1. Then the image of γ by the forward flow until it cuts the plane $y = 0$ (the equatorial plane in* Fig. 2.2) *is an arc spiraling towards* P.O.$_+$.

Proof. From (2.3), again using t as independent variable and $\dot{} = \mathrm{d}/\mathrm{d}t$, we have

$$\begin{aligned} \dot{x} &= -yx^3/4, \\ \dot{y} &= -x^4(1 + O_4)/4, \\ \dot{\bar{\varphi}} &= (-1 + O_2)/\cos^2(\bar{\varphi}), \end{aligned} \tag{2.5}$$

and, introducing a new variable b defined by

$$\dot{b} = -\cos^2(\bar{\varphi})\dot{\bar{\varphi}}, \tag{2.6}$$

we have $\dot{b} = 1 + O_2$ and

$$\bar{\varphi} + \sin(\bar{\varphi})\cos(\bar{\varphi}) = -2b + \text{constant}. \tag{2.7}$$

From (2.5) and (2.6) it follows

$$\begin{aligned} \frac{\mathrm{d}x}{\mathrm{d}b} &= -yx^3(1 + O_2)/4, \\ \frac{\mathrm{d}y}{\mathrm{d}b} &= -x^4(1 + O_2)/4. \end{aligned} \tag{2.8}$$

Finally we introduce a new independent variable c defined by $\mathrm{d}c/\mathrm{d}b = x^3/4$, and hence, from (2.8), we obtain

$$\frac{\mathrm{d}x}{\mathrm{d}c} = -y(1 + O_2),$$
$$\frac{\mathrm{d}y}{\mathrm{d}c} = -x(1 + O_2). \tag{2.9}$$

Now we change the dependent variables through $u = x - F(y,\bar{\varphi}) = x - y + O_5$, $v = x + F(y,\bar{\varphi}) = x + y + O_5$. Hence $u = 0$ and $v = 0$ correspond to the stable and unstable manifolds, respectively. The differential equation for u,v is

$$\frac{\mathrm{d}u}{\mathrm{d}c} = \frac{\mathrm{d}x}{\mathrm{d}c} - \frac{\partial F}{\partial y}\frac{\mathrm{d}y}{\mathrm{d}c} - \frac{\partial F}{\partial \bar{\varphi}}\frac{\mathrm{d}\bar{\varphi}}{\mathrm{d}c} = u(1 + O_2),$$
$$\frac{\mathrm{d}v}{\mathrm{d}c} = \frac{\mathrm{d}x}{\mathrm{d}c} + \frac{\partial F}{\partial y}\frac{\mathrm{d}y}{\mathrm{d}c} + \frac{\partial F}{\partial \bar{\varphi}}\frac{\mathrm{d}\bar{\varphi}}{\mathrm{d}c} = -v(1 + O_2), \tag{2.10}$$

where we have made use of (2.9), the remark about $\mathrm{d}a_n(\bar{\varphi})/\mathrm{d}\bar{\varphi}$ and the fact that $u = 0$ and $v = 0$ are invariant manifolds. It is not restrictive to consider the arc γ on $v = a$ (simply using a diffeomorphism). The initial conditions on γ can be taken as $u_0 = \alpha z$, $v_0 = a$, $\bar{\varphi}_0 = \bar{\varphi}^* + \beta z + O(z^2)$, $0 \leqslant z \leqslant z_0$, where $\alpha^2 + \beta^2 = 1$ $\alpha > 0$ and z is a parameter of the arc such that the end point corresponds to $z = 0$.

For any $\delta > 0$ we can choose a and z_0 small enough such that the following inequalities hold:

$$(1 - \delta)u \leqslant \frac{\mathrm{d}u}{\mathrm{d}c} \leqslant (1 + \delta)u,$$
$$-(1 + \delta)v \leqslant \frac{\mathrm{d}v}{\mathrm{d}c} \leqslant -(1 - \delta)v. \tag{2.11}$$

From (2.11) we obtain, in so far as u and v remain smaller than a,

$$u_0 e^{(1-\delta)c} \leqslant u \leqslant u_0 e^{(1+\delta)c},$$
$$v_0 e^{-(1+\delta)c} \leqslant v \leqslant v_0 e^{-(1-\delta)c}, \tag{2.12}$$

We suppose that the origin of the new variables, $b = 0$, $c = 0$ is taken when $v_0 = a$.

The plane $y = 0$ can be written $u - v = 0$. From (2.12) we have $v - u \geqslant v_0 e^{-(1+\delta)c} - u_0 e^{(1+\delta)c}$. Hence $v - u$ remains non-negative for $c \leqslant c_1 = (1/2)(1 + \delta)^{-1}\ln(v_0/u_0)$. Let b_1 be the minimum positive value of b for which $v - u = 0$. The corresponding values of $\bar{\varphi}$ and x will be denoted by $\bar{\varphi}_1$ and x_1. Then

$$b_1 \geqslant 32 \int_0^{c_1} (u_0 e^{(1+\delta)c} + v_0 e^{-(1-\delta)c})^{-3}\,\mathrm{d}c$$

$$= 32(u_0 v_0)^{-3/2} \int_0^{c_1} e^{-3\delta/c} (e^{c-(1+\delta)c_1} + e^{(1+\delta)c_1 - c})^{-3} \, dc.$$

Introducing the new variable $w = c_1 - c$, one has

$$b_1 > 32(u_0 v_0)^{-3/2} \left(\frac{u_0}{v_0}\right)^{3\delta(2+\delta)/(2+2\delta)} \int_0^{c_1} (e^w + e^{-w})^{-3} \, dw.$$

Let $\rho > 0$. Then for a and z_0 small enough we have

$$b_1 > C(1-\rho) u_0^{-(3/2)(1-\rho)},$$

where $C = 32 v_0^{-3/2} \int_0^\infty (e^w + e^{-w})^{-3} \, dw$. Hence b_1 (and therefore $\bar{\varphi}_1$) goes to infinity when z goes to zero. This ends the proof of the Lemma. ■

Remark 2.1 We should note that spiraling means here that the angle, $\bar{\varphi}_1$, of the image point on $y = 0$ goes to infinity when z goes to zero. We do not claim for monotonicity. However lots of numerical simulations (see Fig. A.1) make it apparent, i.e., $d\bar{\varphi}_1/dz > 0$ and $dx_1/dz > 0$. Using the suitable inequalities we obtain $b_1 < C(1+\rho) u_0^{-(3/2)(1+\rho)}$. In fact, if we only keep the dominant terms in the equations we can easily obtain $\bar{\varphi}_1 = -2Cu_0^{-(3/2)}(1 + o(1))$ and the value x_1 of x when the image of a point in γ reaches $y = 0$ is $(u_0 v_0)^{1/2}$. From this it follows that, using only the dominant terms, $\lim_{z \to 0} \bar{\varphi}_1 x_1^3 =$ constant. This is indeed observed in the numerical computations (see Appendix A).

3. Blow Up of the Lines $\theta = \pm\pi/2$

The blow up of triple collision and infinity has the effect of glueing two boundaries to $\mathscr{V}$, one for $r = 0$, the other for $r = \infty$. We look for a good topological representation of $\mathscr{V}$ with the two boundaries.

We introduce some notation. Let $c \in \mathbb{R}$; we define

$$\mathscr{P}_c = \{(r, v, \theta, w) \in \mathscr{V} \mid v = c\},$$
$$\beta_c = \{(r, v, \theta, w) \in \mathscr{C} \mid v = c\}.$$

If we fix $c \in \mathbb{R}$, β_c is a curve in the plane (θ, w) defined by

$$w^2 = 2\cos\theta\left(1 - \frac{c^2 \cos\theta}{2W(\theta)}\right). \tag{3.1}$$

Let $\omega^c = \{(r, v, \theta, w) \in \mathscr{P}_c \mid v' = 0\}$.

Using (1.5) and (1.6), we can see that ω^c is given by

$$w^2 = \cos\theta\left(1 - \frac{c^2 \cos\theta}{2W(\theta)}\right). \tag{3.2}$$

The points of $\mathscr{P}_c, \beta_c$ and ω^c, will be represented by coordinates (θ, w) when this not leads to confusion.

Moving the real constant c in (3.2) we obtain a surface which separates in $\mathscr{V}$ two components, one with $v' < 0$, another near $\mathscr{C}$ with $v' > 0$.

The curve ω^0 given by $w^2 = \cos\theta$, defines in $\mathscr{P}_0$ an inner region (containing the origin) corresponding to maxima of r along the orbits, and an outer one, $\mathscr{M}$, (near $\mathscr{C}$) whose points are minima of r.

We fix $c \in \mathbb{R}$. We take two constants w_0, θ_0 such that $w_0 > 0$ and $\pi/2 - \theta_0 > 0$ are sufficiently small. We define (see Fig. 3.1)

$$Q_c = \{(r, v, \theta, w) \in \mathscr{P}_c \mid |w| \leqslant w_0, \theta_0 \leqslant \theta \leqslant \pi/2\}.$$

For a fixed value of $w, |w| \leqslant w_0$, we can define $r_w(\theta, c)$ as the function of θ obtained from (1.6) with $h = -1$, that is

$$r_w(\theta, c) = -\frac{c^2}{2} + \frac{W(\theta)}{\cos\theta} - \frac{w^2 W(\theta)}{2\cos^2\theta}. \tag{3.3}$$

When $w = 0$, $r_0(\theta, c) = -(c^2/2) - V(\theta)$ increases near $\theta = \pi/2$ and $r_0(\theta, c)$ tends to infinity when θ tends to $\pi/2$ (see Fig. 3.2). Therefore there is a discontinuity at this point. The variables given by (1.4) are not good out of $\mathscr{C}$ in a neighbourhood of binary collision. So we will make a blow up of the two lines $\theta = \pm\pi/2$.

First we study the function $r_w(\theta, c)$ for different values of w.

LEMMA 3.1. *If $w \neq 0, r_w(\theta, 0)$ has a maximum at $\theta_m(w) < \theta^w$, where (θ^w, w) is a point of $\omega^0 \cap Q_0$*

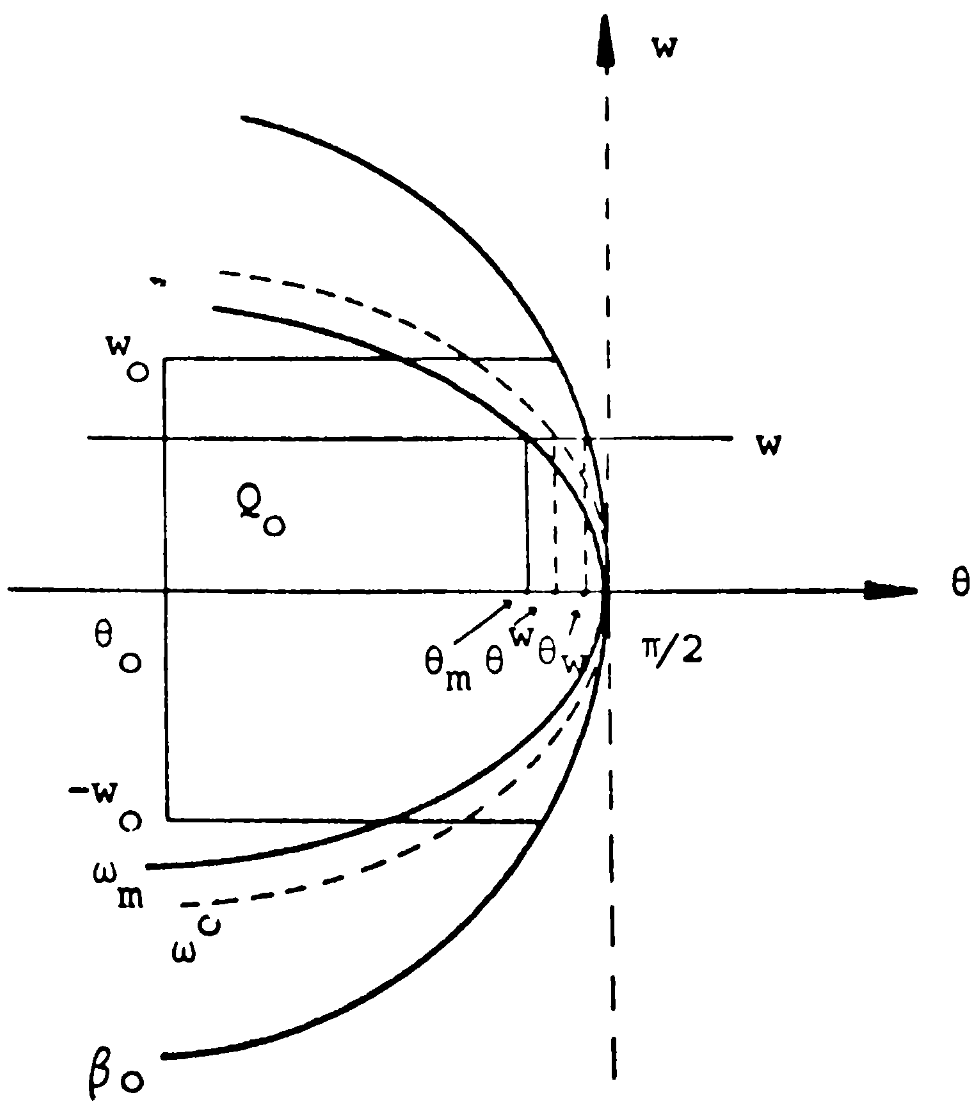

Fig. 3.1a.

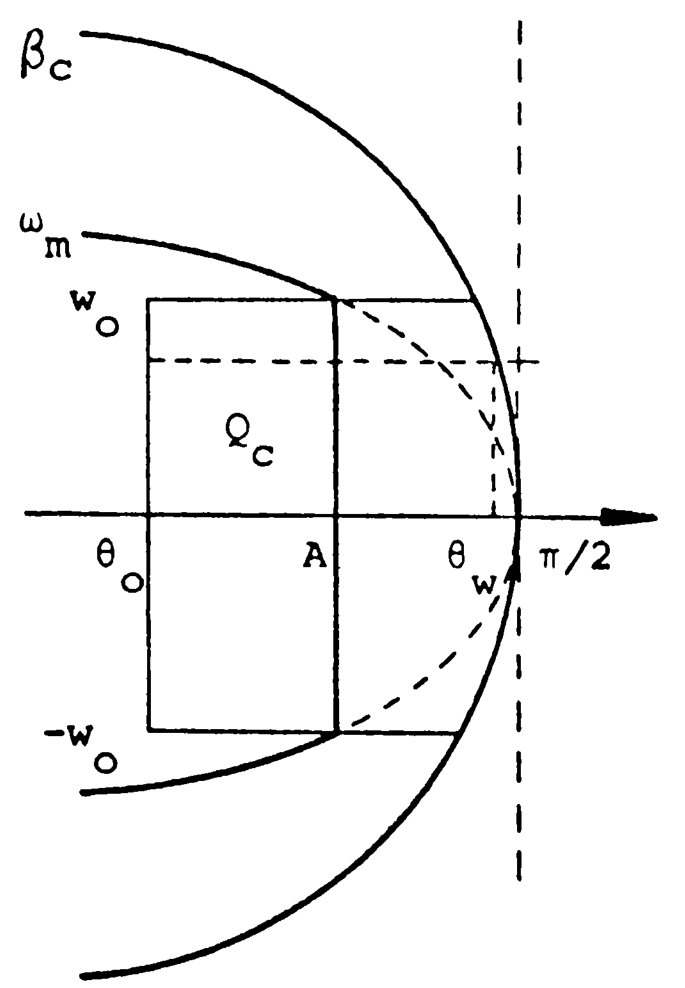

Fig. 3.1b.

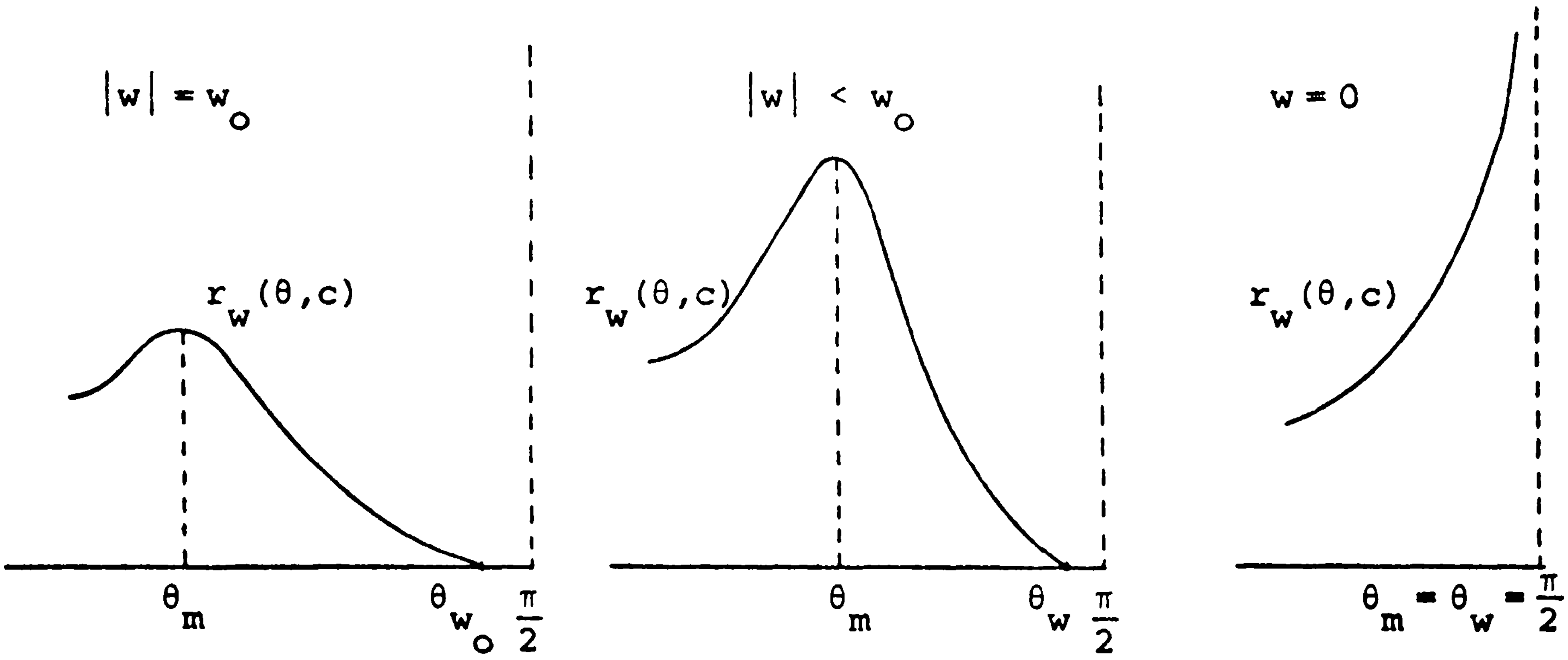

Fig. 3.2.

Proof. By derivation of (3.3) we obtain

$$\frac{\mathrm{d}r_w}{\mathrm{d}\theta}(\theta,0) = \frac{W'(\theta)}{\cos\theta}\left(1 - \frac{w^2}{2\cos\theta}\right) + \frac{W(\theta)\sin\theta}{\cos^2\theta}\left(1 - \frac{w^2}{\cos\theta}\right). \tag{3.4}$$

We fix w, $0 < w < w_0$ (the case $-w_0 < w < 0$ is symmetrical). The points $(\theta, w) \in Q_0$ with $\theta^w < \theta < \theta_w$ where $(\theta_w, w) \in \beta_0$ are between β_0 and ω^0, so $\cos\theta < w^2 < 2\cos\theta$. Furthermore $W(\theta)$ is a positive strictly decreasing function near $\pi/2$. Then $\mathrm{d}r_w(\theta,0)/\mathrm{d}\theta < 0$ if $\theta^w < \theta < \theta_w$.

It is clear that $\mathrm{d}r_w(\theta,0)/\mathrm{d}\theta < 0$ for $\theta = \theta^w$ and $\theta = \theta_w$. This ends the proof. ■

Now we consider values of c that are different from zero and we define

$$\omega_m = \left\{(\theta, w) \in Q_c \,\middle|\, \frac{\mathrm{d}r_w}{\mathrm{d}\theta}(\theta,c) = 0\right\}.$$

For $c \neq 0$ we have $\mathrm{d}r_w(\theta,c)/\mathrm{d}\theta = \mathrm{d}r_w(\theta,0)/\mathrm{d}\theta$. Then from (3.4) we obtain for ω_m

$$w^2 = 2\cos\theta\left(\frac{W'(\theta)\cos\theta + W(\theta)\sin\theta}{W'(\theta)\cos\theta + 2W(\theta)\sin\theta}\right), \tag{3.5}$$

where

$$W'(\theta) = \frac{\mathrm{d}W(\theta)}{\mathrm{d}\theta} = -\frac{4\varepsilon^{3/2}(2\varepsilon+4)\sin\theta}{(2\varepsilon + 4\sin^2\theta)^{3/2}}. \tag{3.6}$$

Using $W(\theta) = -\cos\theta\, V(\theta)$ and (3.6), some computations give the following expression for ω_m near $\pi/2$

$$w^2 = \cos\theta\left(1 - \frac{8\varepsilon^{3/2}\cos^3\theta}{(\varepsilon + 2\sin^2\theta)^{3/2}}\right)\left(\frac{1}{1 + C\cos\theta}\right) \tag{3.7}$$

where

$$C = \frac{2\varepsilon^{3/2}(\varepsilon - 2 + 4\sin^2\theta)}{(\varepsilon + 2\sin^2\theta)^{3/2}}.$$

The curve ω_m is independent of c.

From (3.7) next Lemma follows immediately.

LEMMA 3.2. (i) *$\theta_m(w)$ tends to $\pi/2$ when w tends to zero.*

(ii) *If $w(\theta)$ is the function defined by* (3.7), *then* $\mathrm{d}w(\theta)/\mathrm{d}\theta$ *tends to* $\pm\infty$ *when θ tends to $\pi/2$.*

Figure 3.2 shows the evolution of $r_w(\theta, c)$ in Q_c.

LEMMA 3.3. *Let w_0 and θ_0 be real constants such that $w_0 > 0$ and $\pi/2 - \theta_0 > 0$ are sufficiently small. Then,* $\mathrm{Int}(Q_c) \cap \omega_m \neq \emptyset$, *for all* $c \in \mathbb{R}$.

Proof. From (3.1) and (3.5) we obtain, after some computations, that for all values of θ near to $\pi/2$, ω_m intersects β_c and β_{-c} where

$$c^2 = \frac{2W^2 \sin\theta}{\cos\theta(W'(\theta)\cos\theta + 2W(\theta)\sin\theta)}. \tag{3.8}$$

Moreover $W(\theta)$ tends to $1/\sqrt{2}$ and $W'(\theta)$ tends to $-4\varepsilon^{3/2}(2\varepsilon+4)^{-1/2}$ when θ tends to $\pi/2$. From (3.8) c^2 tends monotonically to $+\infty$ when θ tends to $\pi/2$. Then, for all $c \in \mathbb{R}$, ω_m intersects to β_c and β_{-c} at points different from $\pi/2$. ■

The main idea in the blow up of the lines of binary collisions $\theta = \pm\pi/2$, is as follows. We fix a constant level c of v. We make a change of variables in a suitable set Q_c in order to blow up the point $(\pi/2, 0)$ to a segment $[A, \pi/2]$ on $w = 0$. Over this segment the momentum of inertia will go from zero to ∞. After that, the change can be extended to a neighbourhood of the line $\theta = \pi/2$. The blow up can be made C^∞.

In the plane (θ, w), the curve β_c has two components diffeomorphic to circles when $|c|$ is sufficiently large. One component tends to the point $(\pi/2, 0)$ and the other tends to $(-\pi/2, 0)$ if $|c|$ grows to the infinity. Therefore it is necessary to modify Q_c when v goes to $\pm\infty$. Following Lemma 3.3, this can be done by taking suitable constants w_0 and θ_0 which depend on $|c|$. It is easily computed that w_0 and $\pi/2 - \theta_0$ can be taken going to zero as $1/|c|$ and $1/c^2$, respectively, when $|c| \to \infty$. We define the set $Q = \cup_{c \in \mathbb{R}} Q_c$. In the next construction we suppose that Q_c is fixed.

Let $A = \theta_m(w_0)$ (see Fig. 3.1b). We define a family of functions $\alpha_w(\theta)$ for $|w| \leqslant w_0$ (see Fig. 3.3) by

$$\alpha_w(\theta) = \theta \quad \text{if} \quad w = w_0,$$

$$\left.\begin{aligned} \alpha_i = \alpha_w(\theta_0) &= \theta_0 \\ \alpha_w(\theta_m(w)) &= A \\ \alpha_f = \alpha_w(\theta_w) &= \theta_w \end{aligned}\right\} \quad \text{if} \quad 0 < |w| < w_0, \tag{3.9}$$

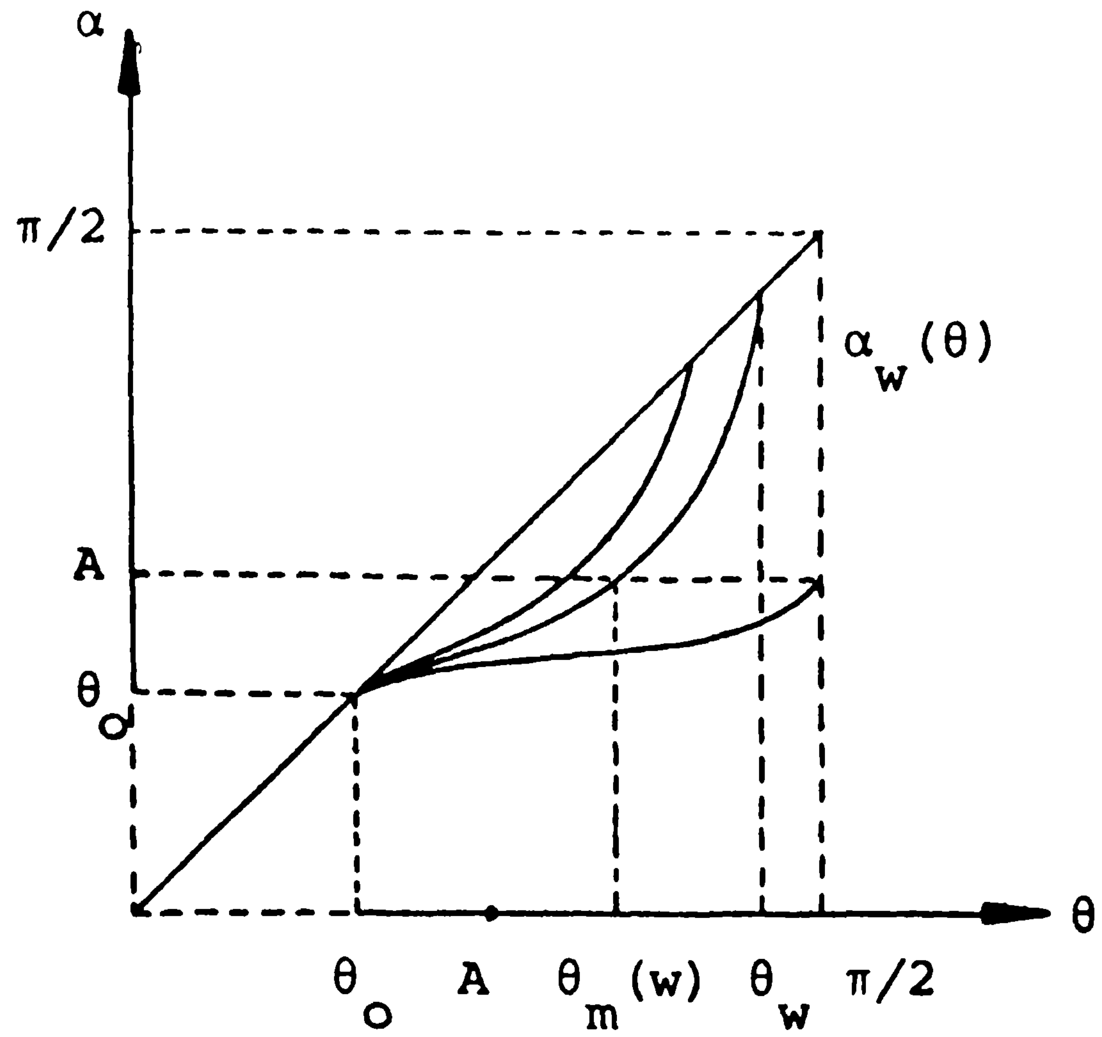

Fig. 3.3.

$$\alpha_0(\theta)=\begin{cases}\lim\limits_{w\to 0}\alpha_w(\theta) & \text{if}\quad \theta\neq\pi/2,\\ A & \text{if}\quad \theta=\pi/2.\end{cases}$$

It is sufficient to take piecewise linear functions.

We have from (3.9) a new variable α which goes from α_i to α_f for all $0<|w|\leqslant w_0$. The variable α will be used instead of θ. When $w=0$, α takes values only defined between α_i and A.

Let $a^0=\operatorname{arc\,cot} r_w(\theta_0,c)$ and $a=(w_0\operatorname{arc\,cot} r_w(\theta_m(w),c)-w\operatorname{arc\,cot} r_w(A,c))/(w_0-w)$. We remark that $\lim_{w\to w_0}a=\operatorname{arc\,cot}(r_{w_0}(A,c))$.

We introduce $\varphi_w(\alpha)$ as the family of piecewise linear functions defined for $0\leqslant w<w_0$ by

$$\varphi_w(\alpha)=\begin{cases}a+\dfrac{a^0-a}{\alpha_i-A}(\alpha-A) & \alpha_i\leqslant\alpha\leqslant A,\\[2ex] a+\dfrac{\pi/2-a}{\alpha_f-A}(\alpha-A) & A<\alpha\leqslant\alpha_f.\end{cases}$$

Now we consider the following family of functions $\psi_w(\alpha)$ with $0\leqslant w\leqslant w_0$ (for negative values of w the construction is symmetrical)

$$\psi_w(\alpha)=\begin{cases}r_w(\theta(\alpha),c) & \text{if}\quad w=w_0,\\ \cot\left(\dfrac{w}{w_0}\operatorname{arc\,cot} r_w(\theta(\alpha),c)+\dfrac{w_0-w}{w_0}\varphi_w(\alpha)\right) & \text{if}\quad 0<w<w_0,\\ \cot\varphi_w(\alpha) & \text{if}\quad w=0.\end{cases}$$

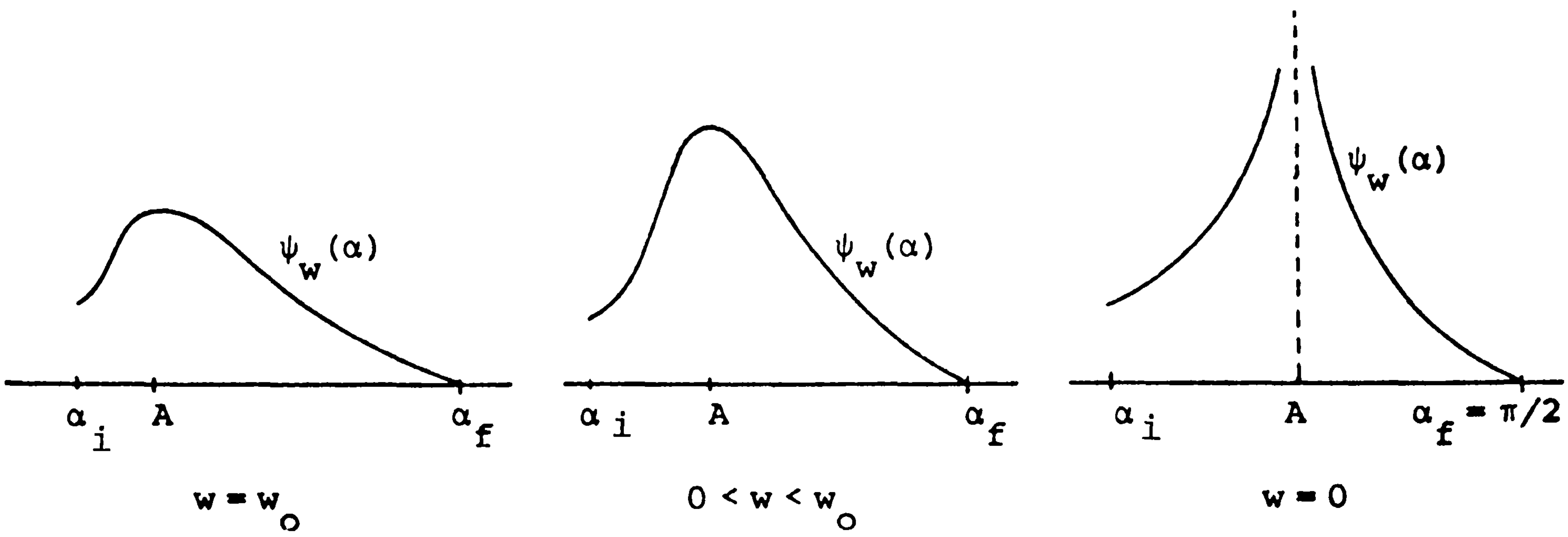

Fig. 3.4.

Then

$$\begin{aligned} \varphi_w(\alpha_i) &= a^0, \\ \varphi_w(A) &= a, \\ \varphi_w(\alpha_f) &= \pi/2. \end{aligned} \tag{3.10}$$

Using (3.10) we get for the family $\psi_w(\alpha)$, $0 < w < w_0$ (see Fig. 3.4)

$$\begin{aligned} \psi_w(\alpha_i) &= r_w(\theta_0, c), \\ \psi_w(A) &= r_w(\theta_m(w), c), \\ \psi_w(\alpha_f) &= 0. \end{aligned}$$

Using α instead of θ and ψ instead of r, the state of the system is completely determined in Q.

4. The Manifold $\mathscr{V}$

The line of points in Q which have r unbounded can be blown up to a sphere I_+ with 2 holes. The equator is the periodic orbit P.O.$_+$. The parabolic orbits are asymptotic to P.O.$_+$, so we can put this orbit on $\mathscr{P}_0 \setminus \mathrm{Int}(\mathscr{M})$. This fact needs some comments that will be made in section 7 showing the behaviour of the orbits near infinity with respect to $\mathscr{P}_0$.

$\mathscr{V}$ can be represented as in Figure 4.1 if we think that the points with $r > 0$ are 'contained in' $\mathscr{C}$. The pointed strips are the points of S^+ and S^- after the blow up of binary collision lines. We define

$$\gamma_+ = S^+ \cap \mathscr{P}_0 \quad \text{and} \quad \gamma_- = S^- \cap \mathscr{P}_0. \tag{4.1}$$

There is in Figure 4.1 a fictitious orbit s_1 which goes from triple collision to infinity with infinite velocity. s_2, s_3 and s_4 are the symmetrical orbits of s_1. More information about these orbits is given in Appendix B.

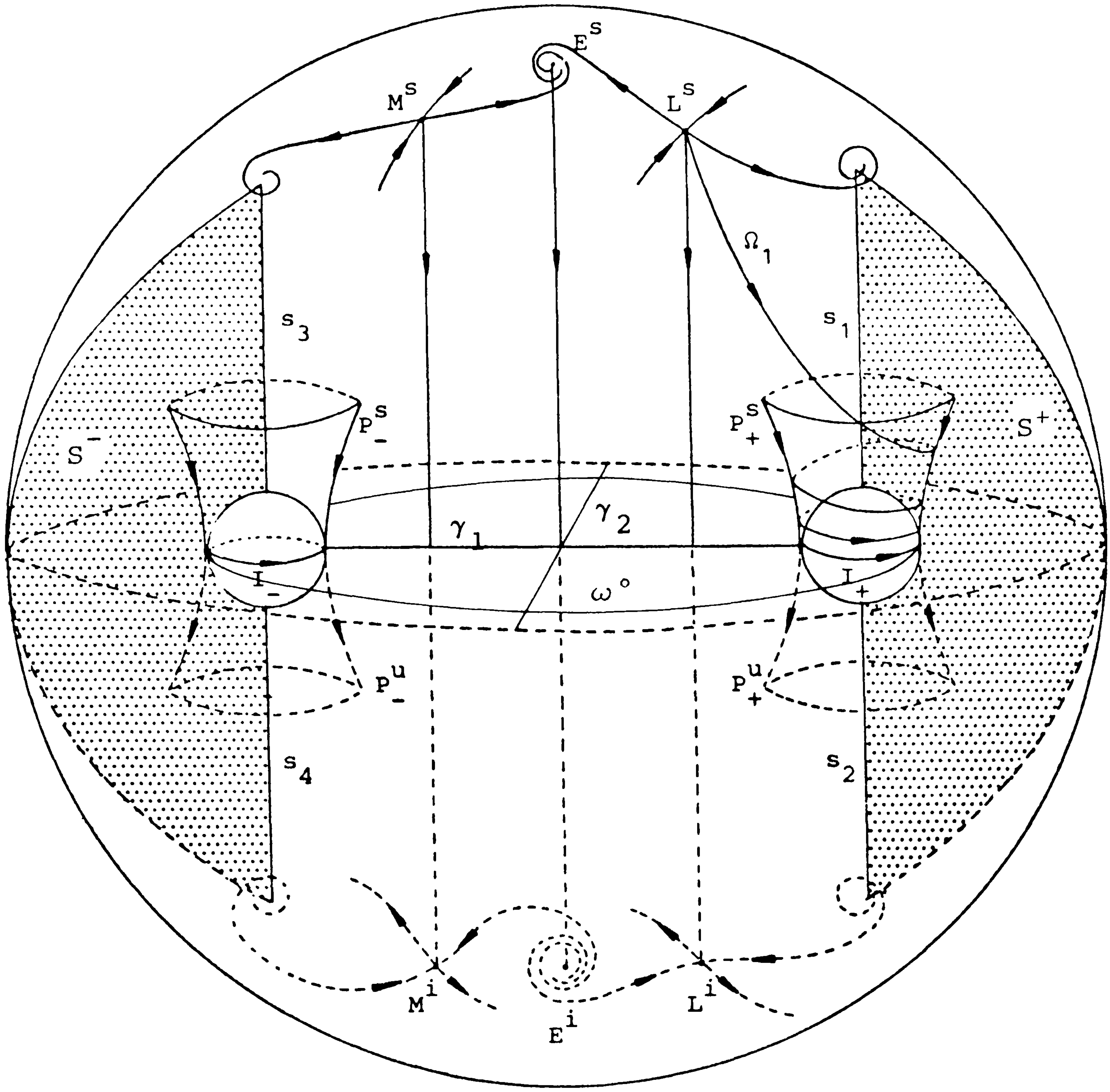

Fig. 4.1.

LEMMA 4.1. *If* $p \in (S^+ \cup S^-) \setminus (\gamma_+ \cup \gamma_-)$, *the orbit* $\varphi(t, p)$ *has at* p *an inflexion point of* r. *If* $p \in \gamma_+ \cup \gamma_-$, $\varphi(t, p)$ *has at* p *a minimum of* r.

Proof. Differentiating the first equation of (1.5) we obtain

$$\ddot{r} = ((-\sin\theta) W^{-1/2} - \tfrac{1}{2}\cos\theta\, W'W^{-3/2})\, rvw$$
$$+ rv^2 \tfrac{1}{2}\cos^2\theta\, W^{-1} + r\cos\theta - 2r^2\cos^2\theta\, W^{-1}.$$

If $\theta = \pi/2$ and $w = 0$, $\dot{r} = \ddot{r} = 0$. A new differentiation shows that $\dddot{r} = rvW^{-1/2}$ for $\theta = \pi/2$. Then, if $v \neq 0$, we have $\dddot{r} \neq 0$. For $v = 0$ and keeping $\theta = \pi/2$, $w = 0$, $\ddddot{r} = 3r > 0$. ∎

The orbits can not reach a maximum of r in binary collision. Therefore, the curve ω^0 tends to infinity when θ tends to $\pi/2$ or $-\pi/2$ (see Fig. 4.1).

5. Ejection – Parabolic Orbits

Some ejection orbits leave a neighbourhood of $\mathscr{C}$ with arbitrarily large velocity. We use this fact to show the existence of hyperbolic and parabolic orbits which begin at triple collision.

The subsystem m_1, m_2 has an energy $h_{12} = (\dot{x}_1^2/4) - (1/x_1)$. We define $h_{123} = h - h_{12}$; h is the total energy that we suppose to be fixed and negative ($h = -1$ after some scaling).

LEMMA 5.1. *There exist ejection orbits which go out from triple collision with an energy h_{123} arbitrarily large.*

This is shown using ideas of McGehee [6].

Proof. From (1.4) we get

$$x_1 = \sqrt{2}\, r \cos\theta,$$

$$\dot{x}_1 = \sqrt{2}\, r^{-1/2}\left(v\cos\theta - w\frac{\sin\theta}{\cos\theta}\sqrt{W}\right).$$

Then, using (1.6) we obtain

$$h_{12} = \frac{W}{r}\left[\frac{v^2(\cos^2\theta - \sin^2\theta)}{2W} - \frac{vw\sin\theta}{\sqrt{W}}\right.$$

$$\left. + \frac{rh\sin^2\theta}{W} - \cos\theta + \frac{1}{\cos\theta}\left(1 - \frac{1}{\sqrt{2}\,W}\right)\right].$$

Let $p = (r, v) \in S^+$. Using $W(\pi/2) = 2^{-1/2}$ and the fact that $(1/\cos\theta) \times [1 - (1/\sqrt{2}\,W)]$ tends to $4\varepsilon^{3/2}/\sqrt{2+\varepsilon}$ when θ tends to $\pi/2$, we have at p

$$h_{12} = \frac{1}{r}\left[-\frac{v^2}{2} + \frac{4\varepsilon^{3/2}}{\sqrt{2(2+\varepsilon)}}\right] + h.$$

Let N be a constant such that $N > |h|$. If (r, v) is such that

$$v^2 > \frac{8\varepsilon^{3/2}}{\sqrt{2(2+\varepsilon)}} \tag{5.1}$$

and

$$r < \left(\frac{v^2}{2} - \frac{4\varepsilon^{3/2}}{\sqrt{2(2+\varepsilon)}}\right)(N+h)^{-1},$$

then $h_{12} < -N$.

The orbit of $W_{L^s}^{u,1}$ contained in $\mathscr{C}$ has an infinity of points in S^+ with v arbitrarily large. We fix $v = v_0$ as in (5.1). $W_{L^s}^{u,1}$ has dimension 2 and the flow is transversal to

S^+, so there exist orbits of $W^{u,1}_{L^s}$ which intersect S^+ with r arbitrarily small. At this points we have $h_{12} < -N$. ∎

Let $(x_1(t), x_2(t), \dot{x}_1, (t), \dot{x}_2(t))$ an ejection orbit given by Lemma 5.1. There exists t_0 such that $x_1(t_0) = 0$ and $h_{123} > M$ for some large M. We can write this inequality as

$$\frac{(\dot{x}_2(t_0))^2}{2} - \frac{(2+\varepsilon)}{x_2(t_0)} > B, \tag{5.2}$$

where $B = (2+\varepsilon)M/2\varepsilon$. The left side of (5.2) is the energy of a two body problem with masses 1 and $2+\varepsilon$. The distance x_2 has a larger negative acceleration than the corresponding 2-body problem because

$$\ddot{x}_2 = -\frac{8(2+\varepsilon)x_2}{(x_1^2 + 4x_2^2)^{3/2}} > -\frac{(2+\varepsilon)}{x_2^2}.$$

We conclude that for all values of the energy h there exist ejection orbits which escape to infinity hyperbolically. By continuity we get the following Lemma.

LEMMA 5.2. *There exists an orbit $\Omega_1 \subset P^s_+ \cap W^{u,1}_{L^s}$ which goes out from triple collision in configuration θ_L and escapes parabolically to infinity without crossing the axis* $x_2 = 0$. (see Fig. 5.1)

It is clear that there exist the symmetrical orbits to Ω_1, that is, $\Omega_2 \subset P^u_+ \cap W^{s,2}_{L^i}$, $\Omega_3 \subset P^s_- \cap W^{u,2}_{M^s}$ and $\Omega_4 \subset P^u_- \cap W^{s,1}_{M^i}$. These orbits do not intersect $\mathscr{P}_0$; in the position plane m_3 never cuts the axis $x_2 = 0$.

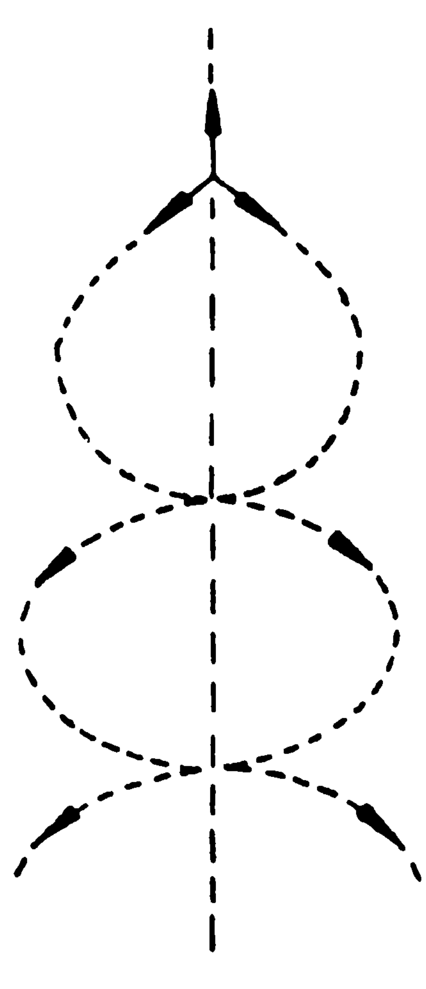

Fig. 5.1.

6. Ejection – Collision Orbits

We are interested in the intersection of the invariant manifolds to equilibrium points. These intersections will give orbits which tend to triple collision when t tends to $-\infty$ and $+\infty$. To do that we cut the invariant manifolds by a suitable plane.

First we consider $\mathscr{P}_0$. The flow is transversal to $\mathscr{P}_0$ except at the points of ω^0. Some computations show on ω^0, $v'' = wW^{-1/2}\cos\theta\ (-V'(\theta))$, so $\operatorname{sgn}(v'') = \operatorname{sgn}(-wV'(\theta))$ changes at $\theta = 0$, $\theta = \pm\theta_L$ and $\theta = \pm\pi/2$. More precisely, if we define

$$X_1 = \{(\theta, w) \in \omega^0 \mid w < 0,\ \theta \in (-\theta_L, 0) \cup (\theta_L, \pi/2)\},$$

$$X_2 = \{(\theta, w) \in \omega^0 \mid w > 0,\ \theta \in (-\pi/2, -\theta_L) \cup (0, \theta_L)\},$$

$$X_3 = \{(\theta, w) \in \omega^0 \mid w < 0,\ \theta \in (-\pi/2, -\theta_L) \cup (0, \theta_L)\},$$

$$X_4 = \{(\theta, w) \in \omega^0 \mid w > 0,\ \theta \in (-\theta_L, 0) \cup (\theta_L, \pi/2)\},$$

then, $v(t)$ has a local maximum at the points of $X_1 \cup X_2$ and a local minimum at $X_3 \cup X_4$. For the third derivative on ω^0 we get

$$v''' = \tfrac{1}{2} W^{-1/2}(-W^{-1}(W')^2 \cos\theta + 2W'' \cos\theta - W' \sin\theta + 2W \cos\theta).$$

Then, if $\theta = 0$, $v''' = -7(1+4\varepsilon)^{-1/2} 2^{1/4} < 0$ and for $\theta = \pm\theta_L$, $v''' = 9(2^{7/4}(2+\varepsilon)^{1/2})^{-1} > 0$. At the points of $\omega^0 \setminus X_1 \cup X_2 \cup X_3 \cup X_4$, $v(t)$ has inflexion points.

LEMMA 6.1. *Let $p \in \mathscr{P}_0 \setminus \mathrm{cl}(\mathscr{M})$. If $v(t) \neq 0$ or $\theta(t) \neq \pm\pi/2$ for all $t > 0$, then $\varphi(t, p)$ is a collision orbit, that is, $r(t)$ tends to zero when t tends to ∞.*

Proof. $r(t)$ has a maximum at $p = \varphi(0, p)$, so for positive and small time, $r(t)$ decreases. Then we can assume $v(t) < 0$ for all $t > 0$. $r(t)$ should be a decreasing function tending to a nonnegative constant r_0 when t tends to $+\infty$. If $r_0 \neq 0$ then $v(t)$ will tend to zero when t tends to $+\infty$, but this is impossible because $\varphi(t, p)$ should tend to an equilibrium point out of the collision manifold.

From (1.4), $x_1 = \sqrt{2}\, r \cos\theta$. Along the orbits, $x_1(t)$ is a positive and bounded function and $\ddot{x}_1(t) < k$, where $k = -2(1+4\varepsilon)^{-2}$ for all t. Then there exists $t^\star$ such that $x_1(t^\star) = 0$. Therefore either $t^\star$ is finite or $t^\star = \infty$. If $t^\star$ should be finite we reach binary collision, which is an absurdity. ■

We define

$$\sigma^u_+ = \{p \in \mathscr{P}_0 \cap W^{u,1}_{M^s} \mid \varphi(t, p) \text{ does not intersect } \mathscr{P}_0 \text{ for any } t < 0\},$$

$$\sigma^u_- = \{p \in \mathscr{P}_0 \cap W^{u,2}_{L^s} \mid \varphi(t, p) \text{ does not intersect } \mathscr{P}_0 \text{ for any } t < 0\}.$$

Let $\mathscr{U} \subset \mathscr{P}_0$ a neighbourhood of $(0, 0)$. It is proved in [8] that $\sigma^u_+ \cap \mathscr{U}$ is a curve spiraling to $(0, 0)$ if $\mathscr{U}$ is sufficiently small. Of course, we suppose $\varepsilon < 55/4$. In this case, σ^u_+ is a continuous curve as shown in Lemma 6.2. In fact, numerical computations show that σ_+^u has, globally, nice spiralling properties (see Appendix A).

LEMMA 6.2. *We parametrize σ_+^u by a parameter $l \in [0, \infty)$ such that $\sigma_+^u(0) = (-\theta_L, 0)$ and $\sigma_+^u(l)$ tends to $(0,0)$ when l tends to ∞. Then, σ_+^u is a continuous curve and there exists an increasing sequence $\{l_i\}_{i \in \mathbb{N}}$ with $l_1 = 0$ such that, if $q_i = \sigma_+^u(l_i) = (\theta_i, 0)$ then $\sigma_+^u \cap \{w=0\} \supseteq \cup_{i \in \mathbb{N}} \{q_i\}$ and $\theta_i > 0$ for i even and $\theta_i < 0$ for i odd. A similar assertion holds for σ_-^u.*

Proof. The homothetic orbit associated to configuration $-\theta_L$ intersects $\mathscr{P}_0$ at the point σ_+^u (0). Therefore, for $l > 0$ sufficiently small, σ_+^u (l) is a continuous curve contained in the semiplane $w > 0$. This fact can be shown using variational equations near the homothetic Lagrange solution (see [11] for details). σ_+^u will be a continuous arc if $\sigma_+^u \subset \mathscr{P}_0 \setminus \mathrm{cl}(\mathscr{M})$ that is, σ_+^u has not intersection with ω^0.

Let $l_2 = \min\{l > 0 \mid \sigma_+^u(l) = (\theta_i, 0)$ with $\theta_i > 0\}$. This number exists because σ_+^u is a spiral near the origin (use variational equations near the homothetic Euler solution as in [8]. From (1.5) $\dot{w} > 0$ if $w = 0$ and $\theta \in (-\theta_L, 0)$. Therefore the arc $B = \{\sigma_+^u(l) \mid 0 < l < l_2\}$ is contained in the semi-plane $w > 0$. In order to prove that $\sigma_+^u \cap \omega^0 = \emptyset$ it is sufficient to show that $B \cap \omega^0 = \emptyset$ because σ_-^u and σ_+^u have no intersection and $\sigma_-^u = L^2 \circ L^1(\sigma_+^u)$. The orbits of $W_{M^s}^{u,1}$ can not arrive, for the first time, to a point of $X_1 \cup X_2$ so it is sufficient that B does not cut ω^0 at a point (θ, w) with $w > 0$ and $-\theta_L < \theta < 0$.

If binary collision is not regularized, from (1.4) the curve ω^0 is $u^2 = -V(\theta)$ and for $-\theta_L < \theta < 0, u^2 = -V(\theta) > -V(-\theta_L)$. From (1.4) and (1.5) $\mathrm{d}u/\mathrm{d}\tau = \frac{1}{2}vu - V'(\theta)$. Then $\mathrm{d}u/\mathrm{d}\theta = -\frac{1}{2}v - V'(\theta)/u$ and $\mathrm{d}u/\mathrm{d}\theta < -V'(\theta)/u$ if $v > 0$. Integrating

$$u_1^2 < 2 \int_{-\theta_L}^{0} -V'(\theta)\,\mathrm{d}\theta = 2(-V(0) + V(-\theta_L)).$$

The values $V(0) = -(1+4\varepsilon)/\sqrt{2}$ and $V(-\theta_L) = -(1+2\varepsilon)^{3/2}(2+\varepsilon)^{-1/2}$ prove $u_1^2 < -V(-\theta_L)$. Hence $B \cap \omega^0 = \emptyset$.

The existence of a sequence $\{l_i\}$ in the conditions of the lemma follows from the changes of sign $(\dot{w})$ on $w = 0$. The last equation of (1.5) gives, on $w = 0$, $\dot{w} > 0$ if $\theta \in (-\theta_L, 0) \cup (\theta_L, \pi/2)$ and $\dot{w} < 0$ if $\theta \in (-\pi/2, -\theta_L) \cup (0, \theta_L)$. ■

We define $\sigma_+^s = L^1(\sigma_+^u)$ and $\sigma_-^s = L^1(\sigma_-^u)$ (see Fig. 6.1), so $\sigma_+^s \subset W_{M'}^{s,2}$ and $\sigma_-^s \subset W_{L'}^{s,1}$. In Figure 6.1 we have assumed nice global spiraling properties according to the numerical computations (see Appendix A). For these properties we refer to the Remark 2.1. However, in this case, the radius of the spiral is not necessarily a monotone function but the numerical computations show that the curves σ_+^s, σ_-^s, σ_+^u and σ_-^u have only intersections on $w = 0$ or $\theta = 0$. If we do not consider the numerical results this behaviour is only guaranted in a neighborhood of (0 0). Let $D \subset \mathscr{P}_0 \setminus \mathrm{cl}(\mathscr{M})$ the set bounded by arcs of σ_+^s, σ_-^u, σ_+^u and σ_-^s as in Figure 6.1. After a positive time, the orbits passing through D near $(-\theta_L, 0)$ escape from a

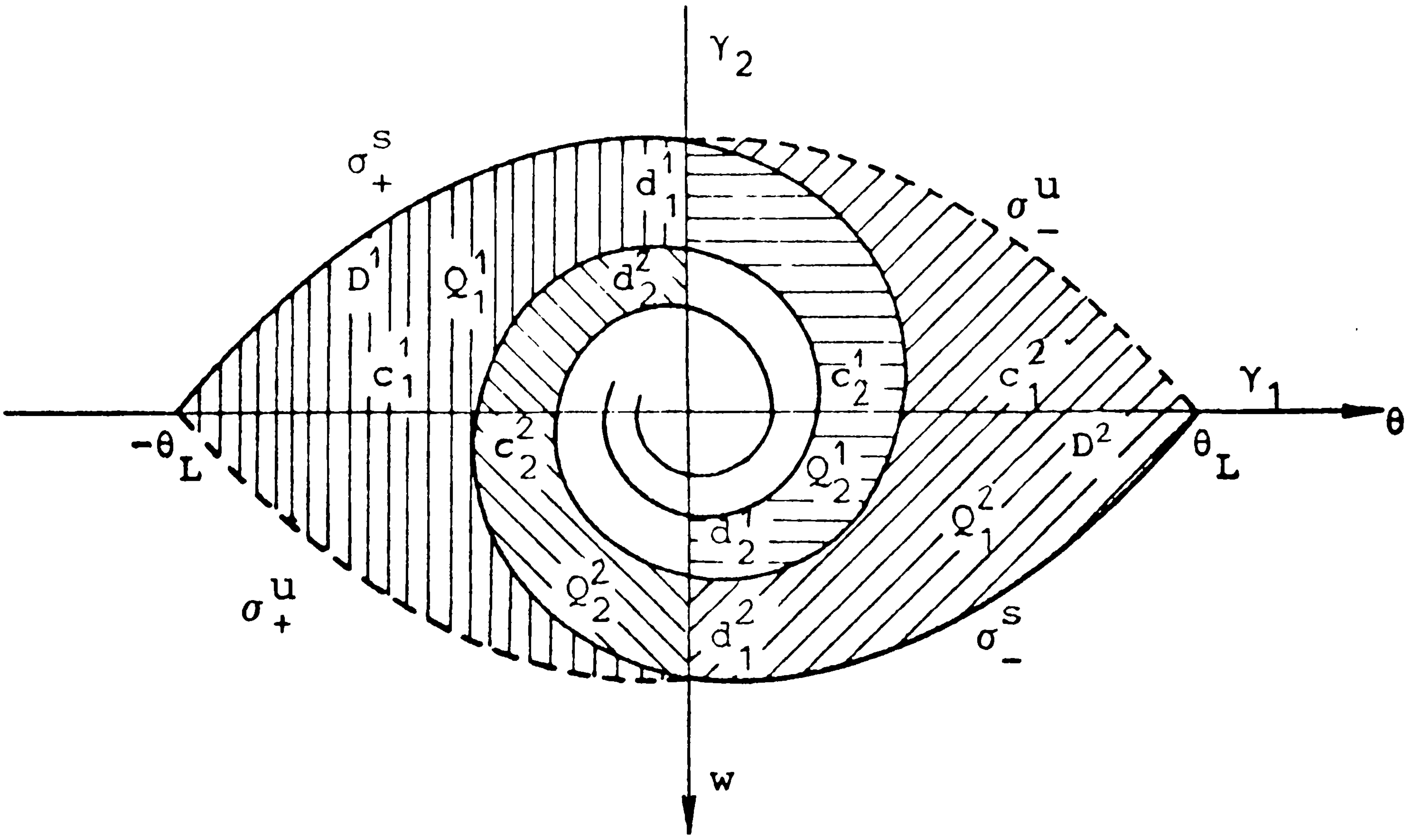

Fig. 6.1.

neighbourhood of M^i following $W^1_{E'}$. We call D^1 the component of $D \setminus (\sigma^s_+ \cup \sigma^s_- \cup \{(0,0)\})$ which contains these kind of orbits. D^2 will be the other component of $D \setminus (\sigma^s_+ \cup \sigma^s_- \cup \{(0,0)\})$. We define $D^3 = L^2(D^1)$ and $D^4 = L^1(D^1)$. D^1 determines two families of segments $\{c^1_j\}$ and $\{d^1_j\}$ in γ_1 and γ_2 respectively as in Figure 6.1. The corresponding families in D^2 are called $\{c^2_j\}$ and $\{d^2_j\}$.

For positive integers $j \geqslant 2$ we define Q^1_j as the closed set in D^1 bounded by d^1_{j-1} and d^1_j (see Fig. 6.1), and $Q^1_1 = D^1 \setminus \bigcup_{j \geqslant 2} Q^1_j$. Let us define three more families of sets $\{Q^2_j\}$, $\{Q^3_j\}$ and $\{Q^4_j\}$ in $\mathrm{cl}(D^2)$, $\mathrm{cl}(D^3)$ and $\mathrm{cl}(D^4)$ respectively by $Q^2_j = L^2L^1(Q^1_j)$, $Q^3_j = L^2(Q^1_j)$ and $Q^4_j = L^1(Q^1_j)$ for all $j \in \mathbb{N}$.

Given $p \in D$, we define $t_b(p) = \min\{t > 0 | \varphi(t,p) \in S^+ \cup S^-\}$, $t_{-b}(p) = \max\{t < 0 | \varphi(t,p) \in S^+ \cup S^-\}$. (We will use t_b and t_{-b} if there is not confusion). From Lemma 6.1 t_b exists for every point $p \in D \setminus (\sigma^s_+ \cup \sigma^s_- \cup \{(0,0)\})$ and t_{-b} exists for $p \in D \setminus (\sigma^u_+ \cup \sigma^u_- \cup \{(0,0)\})$.

We note that if $p \in \mathrm{Int}(Q^1_j \cup Q^2_j)$ ($p \in \mathrm{Int}(Q^3_j \cup Q^4_j)$), $j \in \mathbb{N}$, then $\{\varphi(t,p) | t \in \mathrm{Int} < 0, t_{b(-b)}(p) >\}$, where $\langle \ , \ \rangle$ is the convex closure, has j points in S_1. The arcs of $D^1 \cap \sigma^u_-$ and $D^1 \cap \sigma^u_+$ determine in D^1 a collection of closed sets that we number P^1_2, P^1_3, $P^1_4, \ldots$ as in Figure 6.2. The symmetrical sets $P^2_j = L^2L^1(P^1_j)$ are contained in D^2. Really the family $\{P^1_j\}$ is the intersection of families $\{Q^1_j\}$, $\{Q^2_j\}$, $\{Q^3_j\}$ and $\{Q^4_j\}$ as follows: $P^1_{2j} = Q^1_j \cap Q^4_j$ and $P^1_{2j+1} = (Q^1_j \cap Q^3_{j+1}) \cup (Q^1_{j+1} \cap Q^3_j)$ for $j \geqslant 1$. We restrict P^1_2 to the set bounded by c^1_1 and the corresponding arcs of σ^u_+ and σ^s_-. A similar property restricts P^2_2.

Therefore, if $p \in \mathrm{Int}\ (P^1_j)$ or $p \in \mathrm{Int}\ (P^2_j)$, $j \geqslant 2$, $\{\varphi(t,p) | t_{-b} < t < t_b\}$ has j points in

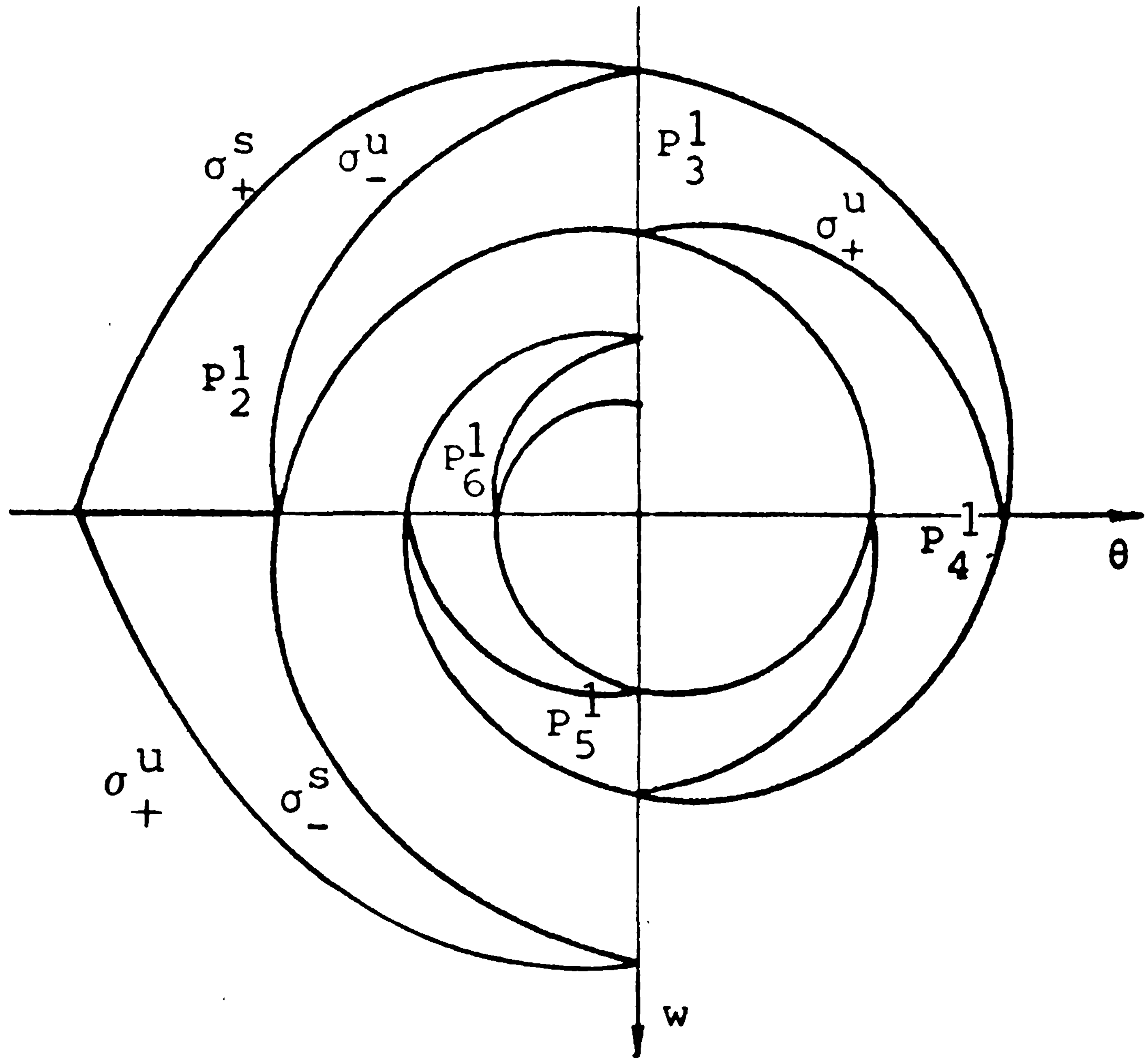

Fig. 6.2.

S_1. We note that points of open segments $(d_j^1\}$ and $\{d_j^2\}$ are in the boundary of families Q but they are in the same conditions of points in the interior of sets P.

PROPOSITION 6.1. *For every positive integer n there exist two symmetrical ejection-collision orbits* ($E - C$) *between Lagrange configurations such that* m_3 *crosses n times the axis* $x_2 = 0$ *and there are not binary collisions. For n even the initial and final configurations are equal, and they are different when n is odd.* (See Fig. 6.3.).

Proof. The points of $\sigma^u_+ \cap \sigma^s_+$ and $\sigma^u_- \cap \sigma^s_-$ correspond to $E - C$ orbits with n even. It is clear (see Fig. 6.3) that these orbits have a point on the zero velocity curve. For n odd the orbits are obtained from $\sigma^u_+ \cap \sigma^s_-$ and $\sigma^u_- \cap \sigma^s_+$. ■

The orbits of Proposition 6.1 were given by Simó in [10].

Now we study the invariant branches attached to Lagrange points which turn around some branch of binary collision. We consider the surface S_2 near infinity. In variables $(x, y, \bar{\varphi}, R)$ the periodic orbit P.O.$_+$ has two points of γ_1 for $\bar{\varphi} = 0$ and $\bar{\varphi} = \pi$. The two points correspond to one real point because of the Levi–Civita regularization. We will assume that the necessary identifications are done. Then, in S_2 and near infinity, $\bar{\varphi} = 0$ will be the zero velocity curve and by the same reason $\bar{\varphi} = \pi/2$ will be the binary collisions.

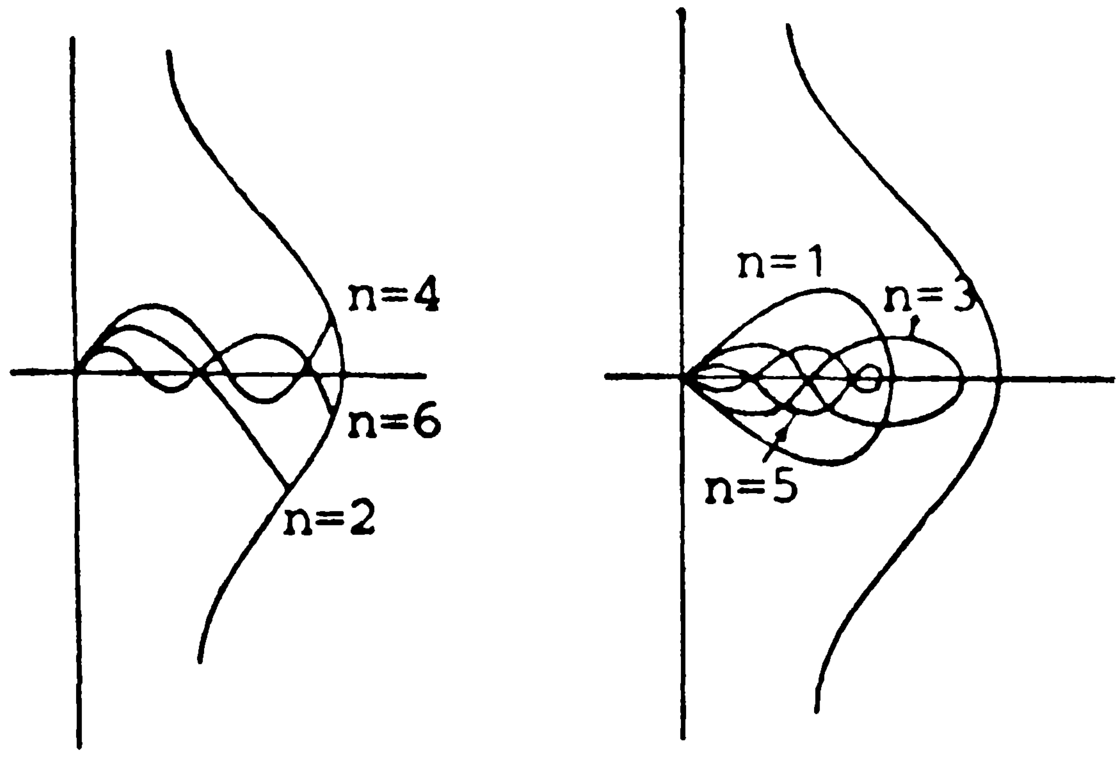

(a) (b)

Fig. 6.3.

We proved in Section 5 the existence of hyperbolic ejection orbits belonging to $W^{u,1}_{L^s}$. Then there is an arc $\gamma \in W^{u,1}_{L^s} \cap \mathscr{E}_1$ in the hypothesis of Lemma 2.1. The arc $\sigma^\infty_{L^s} = i^1_+(\gamma \cap \mathscr{E}_1)$ spirals around P.O.$_+$. We refer to the Remark 2.1 concerning the spiraling properties of $\sigma^\infty_{L^s}$. So we obtain the following Lemma.

LEMMA 6.3. *We parametrize $\sigma^\infty_{L^s}$ by a parameter $l \in [0, \infty)$ such that $\sigma^\infty_{L^s}(l)$ tends to* P.O.$_+$ *when l tends to $+\infty$. Then, there exists an increasing sequence $\{l_i\}_{i\in\mathbb{N}\cup\{0\}}$ such that $\sigma^\infty_{L^s} \cap \gamma_1 \supseteq \bigcup_{i\in\mathbb{N}\cup\{0\}} \{p_{2i}\}$ and $\sigma^\infty_{L^s} \cap S^+ \supseteq \bigcup_{i\in\mathbb{N}} \{p_{2i-1}\}$ where $p_i = \sigma^\infty_{L^s}(l_i)$.*

In the same way, there is an arc $\gamma \subset W^{u,2}_{M^s} \cap \mathscr{E}_3$ which gives by i^3_+ an arc $\sigma^\infty_{M^s}$ spiraling towards P.O.$_-$. $\sigma^\infty_{L^l}$ and $\sigma^\infty_{M^l}$ will be the symmetrical arcs of $\sigma^\infty_{L^s}$ and $\sigma^\infty_{M^s}$ respectively by the symmetry L^1. We define x_j, for $j \geqslant 0$, as the open segment of γ_1 bounded by points p_{2j} and p_{2j+2} given by Lemma 6.3 (see Fig. 6.4). x'_j for $j \geqslant 0$, will be the open segment of binary collisions bounded by p_{2j-1} and p_{2j+1}. We define D_+ as the region of S_2 bounded by the arc $\{\sigma^\infty_{L^s}(l) | l_0 \leqslant l \leqslant l_2\}$, x_0 and P.O.$_+$. We call $\{y_j\}$ and $\{y'_j\}$ the families of open segments which are symmetrical by L^2 to $\{x_j\}$ and $\{x'_j\}$ respectively. If $D'_+ = L^1(D_+)$ we can define $D_- = L^2(D'_+)$ and $D'_- = L^2(D_+)$.

As we did before near $(0,0) \in \mathscr{P}_0$, we can now define in $D_+ \cup D'_+$ a family of closed sets $\{Q^+_j\}$ as in Figure 6.4. We have a symmetrical picture in $D_- \cup D'_-$ for the symmetrical sets $\{Q^-_j\}$ when $j \geqslant 1$. In Figure 6.4 (and the related Figures 11.1 and 11.4) we have assumed nice spiraling properties. This is supported by the numerical evidence as stated before (see Appendix A).

Let $p \in \mathscr{V}$. We define $t_{-x}(p) = \max \{t < 0 | \varphi(t, p) \in S_1\}$ and $t_x(p) = \min \{t > 0 | \varphi(t, p) \in S_1\}$. We will use t_{-x} and t_x if there is not confusion. Then, t_x exists for every point $p \in (D_+ \cup D'_+) \setminus \sigma^\infty_{L^l}$ or $p \in (D_- \cup D'_-) \setminus \sigma^\infty_{M^l}$ and t_{-x} exists for $p \in (D_+ \cup D'_+) \setminus \sigma^\infty_{L^s}$ or $p \in (D_- \cup D'_-) \setminus \sigma^\infty_{M^s}$.

We note that if $p \in \operatorname{Int}(Q^+_j)$ $(p \in \operatorname{Int}(Q^-_j))$ for some $j \geqslant 1$, the arc

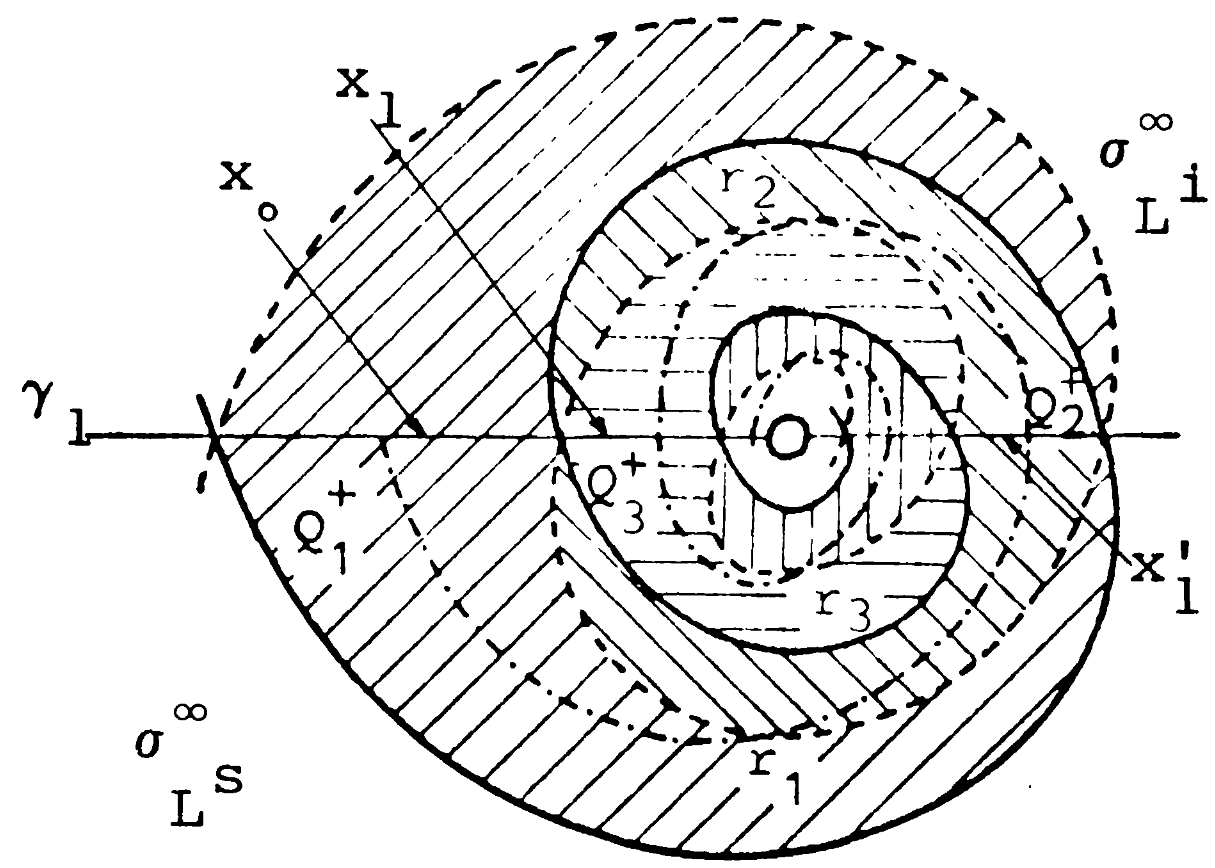

Fig. 6.4.

$a = \{\varphi(t, p) | t_{-x} < t < t_x\}$ crosses $j + m^1$ times $S^+(S^-)$. m^1 is a constant which depends essentially on the size of the neighbourhood used near infinity. It is related to a fixed number of binary collisions. In order to simplify we renumber the sets $\{Q_j^+\}$ and $\{Q_j^-\}$ beginning in the constant m^1. Then the subindex j of the set will represent exactly the number of binary collisions of the arc a.

PROPOSITION 6.2. *For every positive integer n large enough, there exist two ejection – collision orbits with initial and final configurations of Lagrange type such that m_3 does not cross the axis $x_2 = 0$ and m_1 has n binary collisions with m_2.* (See Fig. 6.5).

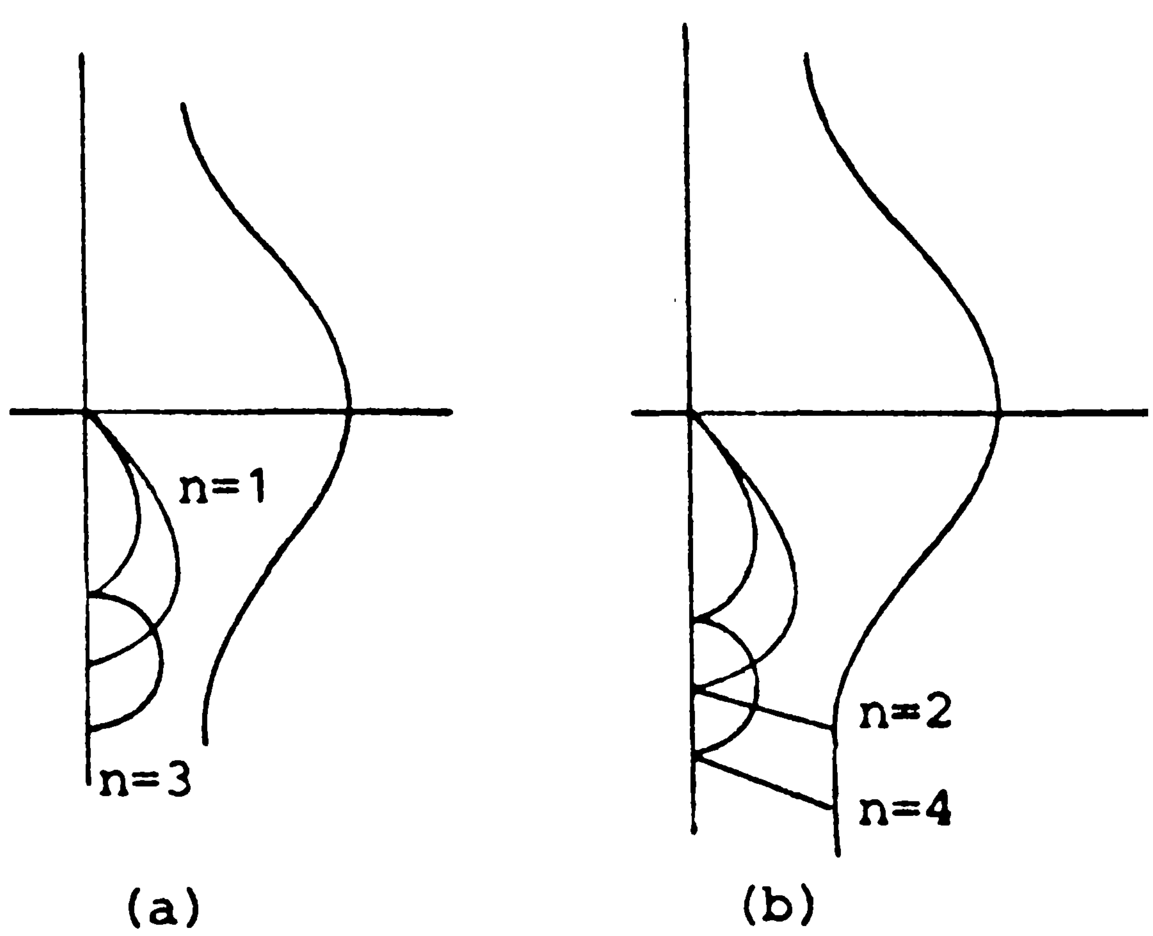

Fig.6.5

Proof. These orbits are obtained from the intersections $\sigma^{\infty}_{L^s} \cap \sigma^{\infty}_{L^u}$ and $\sigma^{\infty}_{M^s} \cap \sigma^{\infty}_{M^u}$, respectively (see Fig. 6.4) ■

7. The Surface of Section S_0

We have used two surfaces of section $\mathscr{P}_0$ and S_2. The surface S_2 ($y = 0$) is not a good global surface of section, but it is good for $\theta_L \leqslant \theta \leqslant \pi/2$. Any orbit cuts S_2 except the hyperbolic and parabolic ones and the Euler homothetic orbit.

The surface $\mathscr{P}_0$ is also a bad surface of section near infinity. This means that there are orbits which cut $\mathscr{P}_0$ tangencially in any neighbourhood of infinity. To show this we write $v = 0$ in (x, y, ξ, η) coordinates. From (1.4)

$$v = r^{-1/2}(\tfrac{1}{2}x_1\dot{x}_1 + (2\varepsilon/(2+\varepsilon))x_2\dot{x}_2),$$

and using (2.1)

$$v = (\xi^4 x^4/2 + 8\varepsilon/(2+\varepsilon)^{1/3})^{-1/4}(\xi\eta x + 4\varepsilon(2+\varepsilon)^{-1/3}y/x) \tag{7.1}$$

Then, for $v = 0$ *and* $x \neq 0$ we have

$$y = -\frac{(2+\varepsilon)^{1/3}}{4\varepsilon}\xi\eta x^2. \tag{7.2}$$

The periodic orbit $(x, y) = [0, 0]$ is contained in $\mathscr{P}_0$. Moreover, $\mathscr{P}_0$ cuts S_2 at the zero velocity curve ($\eta = 0$) and at the binary collisions corresponding to $\xi = 0$. Using polar coordinates in the plane (ξ, η) we can write $\xi\eta = R^2 \sin(2\bar{\varphi})/2$. For x, y sufficiently small, R is near 1. Then, if we fix $\bar{\varphi}$, (7.2) is close to a parabola of second degree in the plane (x, y), with positive coefficient if $\xi\eta < 0$ and negative one if $\xi\eta > 0$. Figure 7.1 shows $\mathscr{P}_0$ respect S_2 near P.O.$_+$ after Levi–Civita identifications.

Another way to make apparent that the variable v is not suitable near the infinity is that the periodic orbit P.O.$_+$ is contained in $v = 0$ but the related invariant manifolds have values of v going to $\pm 4\varepsilon(8\varepsilon(2+\varepsilon))^{-1/4}$ ($+$ for the stable manifold and $-$ for the unstable one).

When the elliptic orbits close enough to the parabolic orbits enter into B_+ we claim that they have a first intersection with $\mathscr{P}_0$ in the region $\xi\eta < 0$, that is, when $w > 0$. To prove the claim it is enough to consider the Poincaré map $\bar{F}$ near the infinity through $\bar{\varphi} = 3\pi/4$ (mod π). $\bar{F}$ is given by $\bar{F}(x, y) = (x - \frac{1}{4}\pi x^2(y + r_1),$ $y - \frac{1}{4}\pi x^3(x + r_2))$ where r_1 and r_2 are real analytical functions of third order in x, y (see [6]). If the first intersection with $\mathscr{P}_0$ of an elliptic orbit takes place in the $y < 0$ region (i.e. with $\xi\eta > 0$), this orbit should reach the Poincaré section with $y < 0$. It is enough to prove that the preimage of the line $y = 0$, in the given section has a negative value of v. But the preimage is $y = \frac{1}{4}\pi x^3(x + r_2) < (2+\varepsilon)^{1/3}R^2x^2/(8\varepsilon)$ if x is small enough.

Using

$$w = u\cos\theta/\sqrt{W} = r^{-1/2}(\varepsilon/(2+\varepsilon))^{1/2}(-x_2\dot{x}_1 + x_1\dot{x}_2)\cos\theta/\sqrt{W},$$

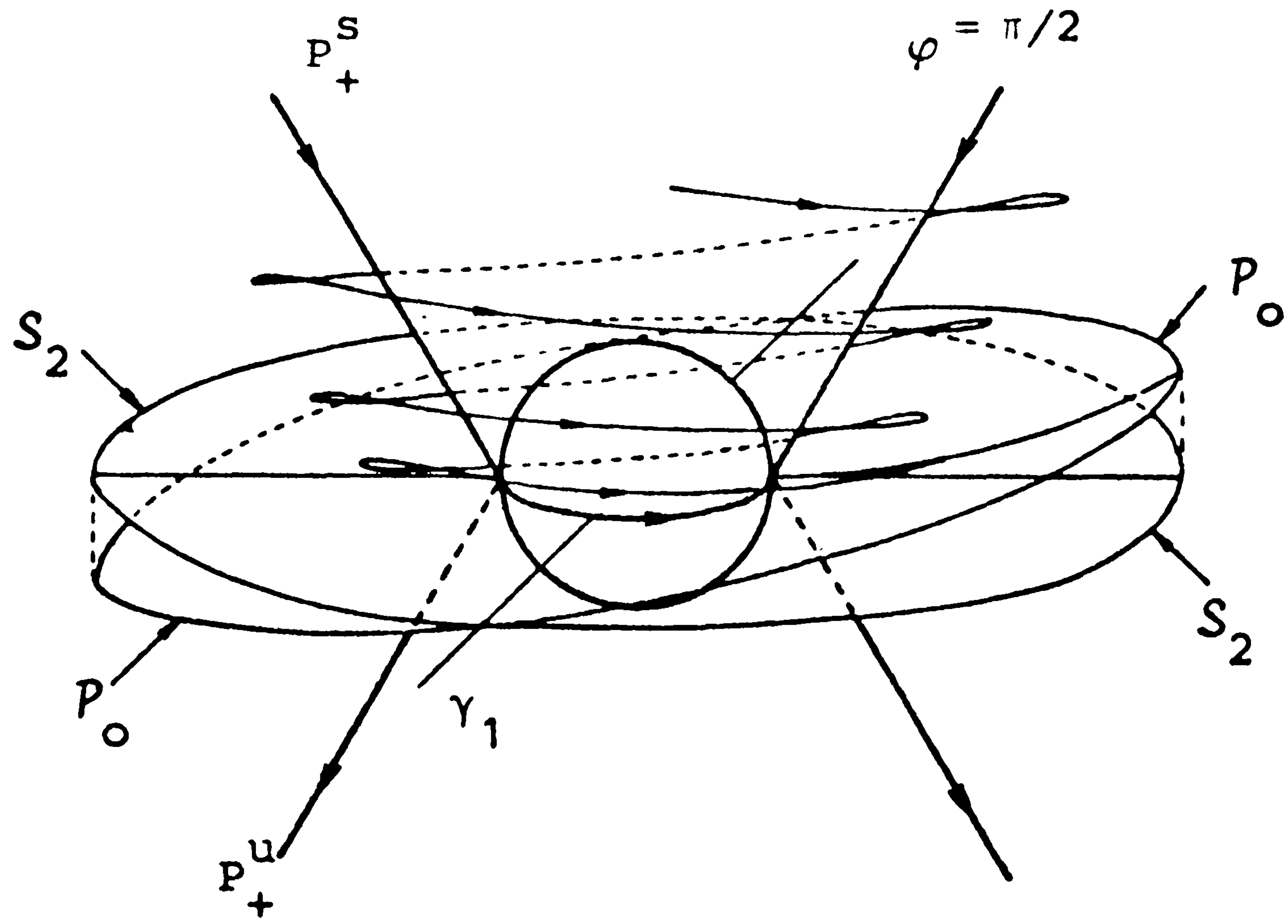

Fig. 7.1.

we see that the first intersection takes place in the semiplane $w > 0$.

Let $f_1(x)$ be a C^∞ function such that $f_1(x) \equiv 1$ if $x \leqslant \alpha_1$ and $f_1(x) \equiv 0$ if $x \geqslant \alpha_2$, where $0 < \alpha_1 < \alpha_2$ are two small real constants. Furthermore we suppose $f'_1(x) < 0$ if $x \in (\alpha_1, \alpha_2)$, $f''_1(\alpha_1 + z) < 0$ if $0 < z < (\alpha_2 - \alpha_1)/2$ and $f_1(\alpha_1 + z) = 1 - f_1(\alpha_2 - z)$ if $0 \leqslant z \leqslant (\alpha_2 - \alpha_1)/2$. We define

$$\bar{\psi}(x, y, \xi, \eta) = y f_1(x) + (1 - f_1(x))v,$$

where v is the function of x, y, ξ, η given by (7.1). The function $\bar{\psi}$ defines a surface

$$S_0 = \{(x, y, \xi, \eta) \in \mathscr{V} \mid \bar{\psi}(x, y, \xi, \eta) = 0\}.$$

We note that if α_1 is sufficiently small, for $x \leqslant \alpha_1$ the flow is transversal to S_0.

LEMMA 7.1. *If α_2 is sufficiently small and satisfies $\alpha_2 \leqslant 2\alpha_1$, for every value of x, $0 < \alpha_1 < x < \alpha_2$, the derivative of $\bar{\psi}$ with respect to the physical time t equals zero at exactly two points $p_1, p_2 \in S_0$. When x decreases to α_1 both points have the same limit.*

Proof. If $\alpha_1 < x < \alpha_2$, we have

$$v = -f_1(1 - f_1)^{-1} y \tag{7.3}$$

on S_0. Then, if we recall that $\mathrm{d}t = \xi^2 \mathrm{d}\kappa$ (see section 2) on this region

$$\frac{\mathrm{d}\bar{\psi}}{\mathrm{d}\kappa} = f_1 \frac{\mathrm{d}y}{\mathrm{d}\kappa} + (1 - f_1)\frac{\mathrm{d}v}{\mathrm{d}\kappa} + y \frac{f'_1}{1 - f_1}\frac{\mathrm{d}x}{\mathrm{d}\kappa}. \tag{7.4}$$

From (7.1) and (7.3)

$$\eta = -\frac{y}{\xi x^2}\left(\frac{f_1}{1 - f_1}\tilde{r}^{1/2} x + \frac{4\varepsilon}{(2 + \varepsilon)^{1/3}}\right), \tag{7.5}$$

where $\tilde{r} = (\xi^4 x^4/2 + 8\varepsilon/(2+\varepsilon)^{1/3})^{1/2}$. Using the energy integral (2.2) and (7.5)

$$y^2 = \frac{(1-f_1)^2}{A_1}\xi^2 x^4(1 - \xi^2 + A_2\xi^2 x^2), \tag{7.6}$$

where $A_1 = \varepsilon(2+\varepsilon)^{-1/3}(1-f_1)^2\xi^4 x^4 + (\tilde{r}^{1/2} f_1 x + 4\varepsilon(2+\varepsilon)^{-1/3}(1-f_1))^2$, $A_2 = \varepsilon(2+\varepsilon)^{-1/3}(1+u^2)^{-1/2}$ and $u = (4(2+\varepsilon)^{1/3})^{-1}\xi^2 x^2$.

We can also compute from (7.5) and (7.6), $dv/d\kappa$ on S_0 when $\alpha_1 < x < \alpha_2$ as a function of ξ, η

$$\frac{\delta v}{d\kappa} = \frac{x}{\tilde{r}^{1/2}} - \frac{2x\xi^2}{\tilde{r}^{1/2}} + \frac{4\varepsilon\xi^2 x^3}{\tilde{r}^{1/2}(\xi^4 x^4 + 16(2+\varepsilon)^{2/3})^{1/2}} - $$
$$-\frac{f_1^2\xi^4 x^7}{2\tilde{r}^{3/2}A_1}(1 - \xi^2 + A_2\xi^2 x^2). \tag{7.7}$$

Inserting (7.7) in (7.4) and using (2.3) we have, after some computations

$$\frac{d\bar{\psi}}{d\kappa} = (1-f_1)\tilde{r}_0^{-1/2}x(1+o(1)) - (2(1-f_1)\tilde{r}_0^{-1/2}x + f_1 x^4/4)\xi^2(1+o(1))$$

where $\tilde{r}_0 = (8\varepsilon(2+\varepsilon)^{-1/3})^{1/2}$.

We look for the solutions of $d\bar{\psi}/d\kappa = 0$ or, equivalently,

$$1 = \xi^2\left(2 + \frac{f_1}{4(1-f_1)}\tilde{r}_0^{1/2}x^3\right)(1+o(1)). \tag{7.8}$$

It is enough to check that the expression $2 + f_1\tilde{r}_0^{1/2}x^3/4(1-f_1)$ decreases monotonically from $+\infty$ to some constant when x goes from α_1 to α_2.

The derivative of $f_1(1-f_1)^{-1}x^3$ is negative if

$$\bar{g}(x) = 3\bar{f}_1(1-\bar{f}_1) - x\bar{f}'_1 < 0,$$

where $\bar{f}_1 = 1 - f_1$. Using the symmetry of $\bar{f}'_1$ with respect to the point $x = (\alpha_1 + \alpha_2)/2$, it is sufficient to prove $\bar{g}(x) < 0$ for $\alpha_1 < x \leqslant (\alpha_1 + \alpha_2)/2$. For these values of x, by the mean value theorem and the hypothesis about f''_1 we have

$$3\bar{f}_1(1-\bar{f}_1) < 3\bar{f}'_1(x)(x - \alpha_1).$$

Then, if $x \leqslant 3\alpha_1/2$, $\bar{g}(x) < 0$. We conclude that if $\alpha_2 \leqslant 2\alpha_1$ the solution ξ^2 of (7.8) increases when x goes from α_1 to α_2. Now we note that when x tends to α_2, $f_1(x)$ tends to 0 and there is only one value of ξ^2 which satisfies (7.8). When x tends to α_1, this value of ξ^2 tends to zero. Therefore if we fix $x = x^*$, $\alpha_1 < x^* < \alpha_2$, $d\bar{\psi}/dt$ has two solutions $\pm\xi^*$. Then if we recover y and η from (7.6) and (7.5), four points given by

$$q_1 = (x^*, \xi^*, y^*, -\eta^*), \qquad q_2 = (x^*, \xi^*, -y^*, \eta^*),$$
$$q_3 = (x^*, -\xi^*, y^*, \eta^*), \qquad q_4 = (x^*, -\xi^*, -y^*, -\eta^*), \tag{7.9}$$

are obtained.

Recall that from (2.1), ξ, η are the Levi–Civita variables, so we must identify q_1

with q_3 and q_2 with q_4. There are two real points in (7.9), one with $\dot{x}_1 > 0$ and $\dot{x}_2 < 0$ in the semiplane $w < 0$, and the other with $\dot{x}_1 < 0$ and $\dot{x}_2 > 0$ in the semiplane $w > 0$.

We note that $d\bar{\psi}/dt = 0$ has the same solutions that $d\bar{\psi}/dk = 0$ if $\alpha_1 < x < \alpha_2$. ■

Following Lemma 7.1 there exists in S_0 a curve ω^* which separates two regions where $d\bar{\psi}/dt > 0$ (the region $\mathscr{M}^*$) and $d\bar{\psi}/dt < 0$ respectively (see Fig. 7.2).

Let $p \in \mathscr{V}$. We define, if they exist

$$t_1(p) = \min\{t > 0 \,|\, \varphi(t,p) \in S_0\},$$
$$t_2(p) = \max\{t < 0 \,|\, \varphi(t,p) \in S_0\}, \tag{7.10}$$

or briefly t_1, t_2 if confusion can not occur.

If $p \in \mathscr{M}^*$ and t_1, t_2 exist we define two maps ψ, Φ by $\psi(p) = \varphi(t_1, p)$ and $\Phi^{-1}(p) = \varphi(t_2, p)$. In this case, the Poincaré map on $\mathscr{M}^*$ is given by $f = \Phi \circ \psi$.

These maps are diffeomorphisms.

We will use S_0 as surface of section. We suppose that the constants α_1 and α_2 which define S_0 satisfy the hypothesis of Lemma 7.1, and they will be such that S_0 does not cut $P^s_+ \cup P^u_+$ at any point of the annulus $\alpha_1 \leqslant x \leqslant \alpha_2$. This is true for small α_1 and α_2. Now we fix the spheres B_+ and B_- as defined in Section 2, contained in $x < \alpha_1$.

Now we are interested in the forward and backward intersections of the parabolic manifold with S_0. For certain values of the parameter ε, we assert that these

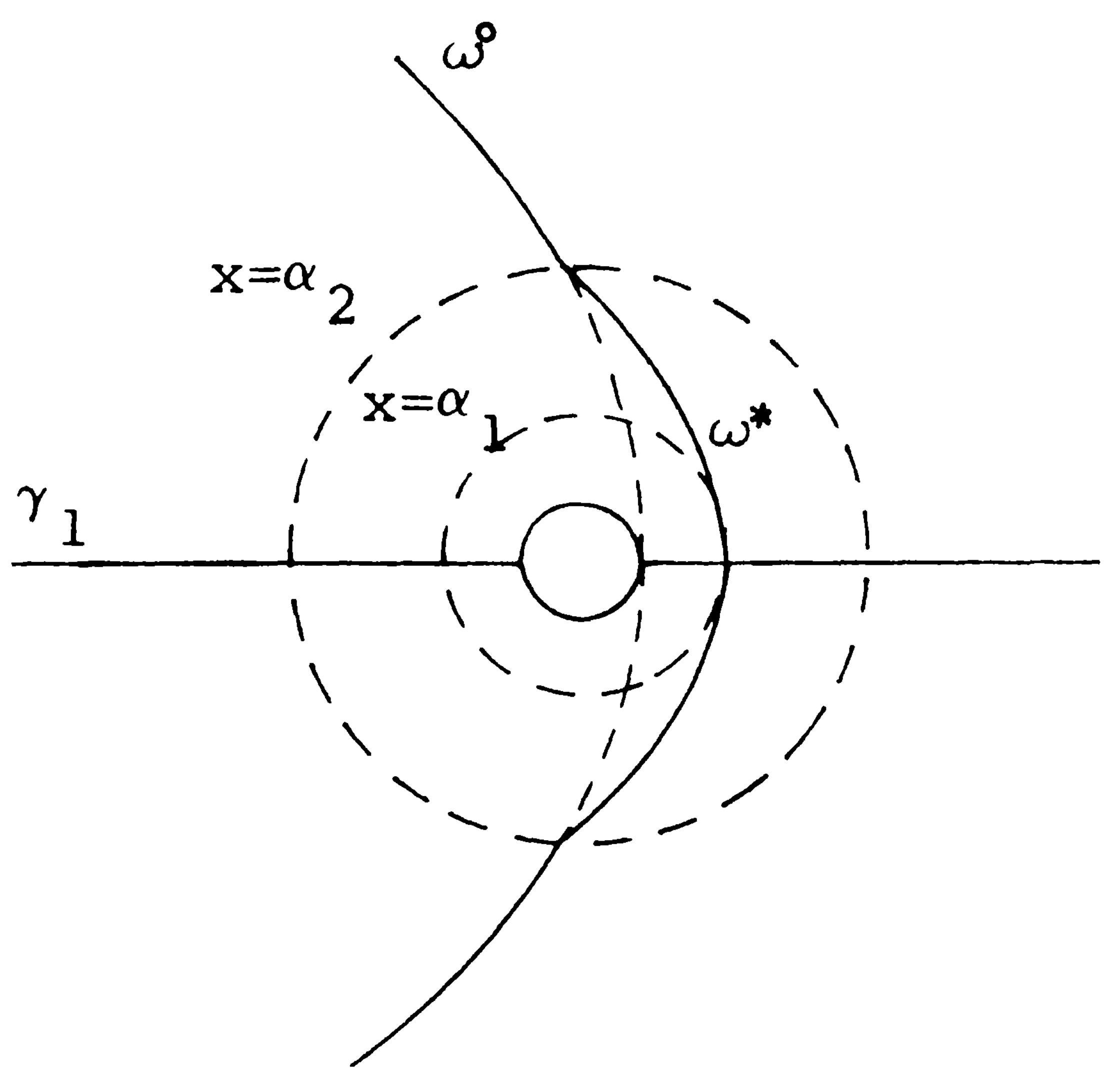

Fig. 7.2.

intersections are continuous curves with two end points on $\mathscr{C}$. Some evidence, analytical and numerical, for that assertion will be given in the next section. The study of orbits passing through ω^0 will be useful to that goal. When the intersections of $P^{u;s}_{+,-}$ with S_0 have been obtained, it will be easy to show the existence of orbits which escape parabolically to infinity for $t \to \pm\infty$. These kind of orbits will be essential to the establishment a theorem of symbolic dynamics.

8. The Manifold of Parabolic Orbits

We look for the first intersections (forward and backward) of S_0 and the manifolds of parabolic orbits.

We define the maps i_1^{-1}, i_2, i_3^{-1}, i_4 on $\mathscr{E}_1$, $\mathscr{E}_2$, $\mathscr{E}_3$ and $\mathscr{E}_4$, respectively, (see Section 2) as follows

$$i_k^{-1}(p) = \varphi(t_2, p) \quad \text{if} \quad k = 1, 3,$$
$$i_k(p) = \varphi(t_1, p) \quad \text{if} \quad k = 2, 4,$$

where t_1, t_2 are given by (7.10).

Orbits of P^s_+ near Ω_1 (see Lemma 5.2) cross a neighbourhood of L^s going back by the flow. They escape from this neighbourhood following $W^{s,1}_{L^s}$ or $W^{s,2}_{L^s}$ depending on the side in P^s_+ where they are with respect to Ω_1. Then, $i_1^{-1}(e_1)$ contains an arc ξ_1 ending in $l^{s,1}$ and $l^{s,2}$. It can exist more than one orbit in $W^{u,1}_{L^s} \cap P^s_+$ as Ω_1. We do not care about this type of orbits if $W^{u,1}_{L^s}$ does not cross P^s_+. They only produce loops which start in $l^{s,1}$ and end in $l^{s,2}$. On the other hand, the number of orbits in $W^{u,1}_{L^s} \cap P^s_+$ where $W^{u,1}_{L^s}$ crosses P^s_+ must be finite (due to analyticity and compactness) and therefore it must be odd. Then $i_1^{-1}(e_1)$ will contain an odd number of arcs between $l^{s,1}$ and $l^{s,2}$. In this case we only consider the arc ξ_1 which is furthest from ω_0. Recall that α_1 and α_2 were selected such that ξ_1 is contained in $\mathscr{M}^\star$.

It is clear that ξ_1 can be discontinuous. In fact, it is so for small values of ε (see Lemma 8.2). It means $\xi_1 \cap \omega^0 \neq \emptyset$. The points of $X_1 \cup X_2$ (see Section 6) correspond to local maxima of $v(t)$ on the orbits. Therefore, in order to prove the continuity of ξ_1 it is enough to look for possible intersections of ξ_1 and $X_3 \cup X_4$. But, using the symmetries, ξ_1 will be continuous if the following assertions are true

Assertion 1. If $p = (\theta, w) \in \omega^0$, $w > 0$, $0 < \theta \leqslant \theta_L$, then there exists $t_0 < 0$ such that $v(t_0) = 0$.

Assertion 2. If $p = (\theta, w) \in \omega^0$, $w > 0$, $\theta_L \leqslant \theta < \pi/2$, then there exists $t_0 > 0$ such that $v(t_0) = 0$.

LEMMA 8.1. *There is a critical value $\varepsilon^* < 0.502$ such that, if $\varepsilon \in (\varepsilon^*, 55/4)$ for every point $p = (\theta, w) \in \omega^0, w > 0$, $\theta_L \leqslant \theta < \pi/2$ there exists $t_0 > 0$ such that $\theta(t_0) = 0$.*

Proof. From the energy integral (1.6), on ω^0 we have $r = -V(\theta)/2$. Then the projection on the position plane of ω^0 is homothetical to the zero velocity curve and given by $V(x_1, x_2) = -2$.

Coordinates $(x_1, x_2, \dot{x}_1, \dot{x}_2)$ of p can be computed as functions of θ:

$$\begin{aligned} x_{1,p} &= \frac{W}{\sqrt{2}}, \\ x_{2,p} &= \sqrt{\frac{2+\varepsilon}{2\varepsilon}}\,\frac{W \sin\theta}{2\cos\theta}, \\ \dot{x}_{1,p} &= -2\sin\theta, \\ \dot{x}_{2,p} &= \sqrt{\frac{2+\varepsilon}{\varepsilon}}\cos\theta. \end{aligned} \tag{8.1}$$

Let us suppose $x_2(t) > 0$ for all $t > 0$. From (1.1)

$$\ddot{x}_2 < -\frac{8(2+\varepsilon)x_2}{(b^2 + 4x_2^2)^{3/2}} \tag{8.2}$$

if b is an upper bound of $x_1(t)$, that is, $x_1(t) < b$ for all $t > 0$. From (8.2) we get

$$\frac{\dot{x}_2^2}{2} < \frac{2(2+\varepsilon)}{(b^2 + 4x_2^2)^{1/2}} + F$$

where

$$F = \frac{\dot{x}_{2,p}^2}{2} - \frac{2(2+\varepsilon)}{(b^2 + 4x_{2,p}^2)^{1/2}}.$$

If $F \leqslant 0$, $x_2(t)$ cannot be arbitrarily large and it must be equal to zero for some $t_0 > 0$. We will determine the values of ε such that $F < 0$. It is easy to see for initial conditions (8.1), that $F < 0$ if and only if the function

$$\tilde{F}(\theta, \varepsilon) = 2\varepsilon b^2 \cos^4\theta + (2+\varepsilon)W^2 \sin^2\theta \cos^2\theta - 32\varepsilon^3$$

is negative.

We take $b = z_1$ where $(z_1, x_{2,p})$ is a point of the zero velocity curve, that is

$$\frac{1}{z_1} + \frac{4\varepsilon}{\left(z_1^2 + \dfrac{(2+\varepsilon)}{2\varepsilon} W^2 \tan^2\theta\right)^{1/2}} = 1. \tag{8.3}$$

Using (8.3) we get $\tilde{F}(\theta, \varepsilon) < 0$ if and only if $z_1 > 1/\sin^2\theta$.

If $\alpha \geqslant 0$ is a constant, the function

$$g(z_1) = \frac{1}{z_1} + \frac{4\varepsilon}{(z_1^2 + \alpha)^{1/2}}$$

given by the zero velocity curve, is a decreasing function of z_1. Then $z_1 > 1/\sin^2\theta$ is equivalent to $g(z_1) < g(1/\sin^2\theta)$, that is

$$G_1(\theta, \varepsilon) = \frac{\cos^4\theta}{\sin^4\theta} + \frac{2+\varepsilon}{2\varepsilon} W^2 \sin^2\theta \cos^2\theta - 16\varepsilon^2 < 0. \tag{8.4}$$

We note that $W(\theta)$ and $\cos^4\theta/\sin^4\theta$ are decreasing functions in the interval $[\theta_L, \pi/2)$. Then we can use $W(\theta_L) = (1+2\varepsilon)2^{-1/2}$ and $\cos^4\theta_L/\sin^4\theta_L$ as upper bounds of these functions. Therefore, if $\theta \in [\theta_L, \pi/2)$

$$G_1(\theta,\varepsilon) \leqslant \left[\frac{2+\varepsilon}{3\varepsilon}\right]^2 + \frac{(2+\varepsilon)(1+2\varepsilon)^2}{16\varepsilon} - 16\varepsilon^2 = G_1(\varepsilon).$$

Now the proof is finished because $G_1(\varepsilon) < 0$ for $\varepsilon > 0.502$. ∎

In particular, Lemma 8.1 implies that points p in the hypotheses of Assertion 2 cannot escape to I_+ without crossing the axis $x_2 = 0$.

In order to give more information about Assertions 1 and 2, we have made some numerical computations for different values of ε in the range $0 < \varepsilon < 55/4$. Before we give these results we will make some comments.

We note that from (8.4) we have for $0 < \varepsilon < 55/4$

$$G_1(\theta,\varepsilon) \leqslant \varepsilon^2\left[\frac{\cos^4\theta}{\varepsilon^2\sin^4\theta} + \left[\frac{1}{\varepsilon}+\frac{1}{2}\right]\left[\frac{1}{\varepsilon\sqrt{2}} + \frac{4\cos\theta}{\sqrt{2+16\sin^2\theta/55}}\right]^2 \cos^2\theta\sin^2\theta - 16\right]$$
$$= \varepsilon^2 G_2(\theta,\varepsilon).$$

For a fixed value of ε, let $p = (\theta, w) \in \omega^0$ be, with $\theta \in [\theta_L(\varepsilon), \pi/2)$, such that $G_2(\theta, \varepsilon) < 0$. Then, as in Lemma 8.1, there exists $t_0 > 0$ such that $\theta(t_0) = 0$.

If we fix $0 < \varepsilon < 55/4$, $G_2(\theta, \varepsilon)$ is a decreasing function of θ if $\theta \in [\pi/4, \pi/2)$. Moreover if we fix θ in that interval and $G_2(\theta, \varepsilon_0) < 0$ for some $\varepsilon_0 > 0$, then $G_2(\theta, \varepsilon) < 0$ for all $\varepsilon_0 \leqslant \varepsilon < 55/4$.

Using the above reasoning and the computation $G_2(0.87, 0.35) < 0$ we have that for all $\varepsilon \geqslant 0.35$ if $p = (\theta, w) \in \omega^0$ with $\theta \in [0.87, \pi/2)$, the orbit $\varphi(t, p)$ cuts the x_1-axis for some positive time. We note that in that range of ε there are values of the parameter in cases I, III and V. We have studied the three cases numerically.

In fact, it is enough to study the behavior of the points $p \in \omega^0$ such that

$$r_p < r_z, \tag{8.5}$$

where $r_z = (1+4\varepsilon)/\sqrt{2}$ is the value of the momentum r at the point of the zero velocity curve with $\theta = 0$, and r_p the momentum at p. If $r_p > r_z$ and the orbit $\varphi(t, p)$ crosses the axis $x_2 = 0$ for some positive time, then $\varphi(t, p)$ would go into the region $r < r_z$ before the crossing. Therefore $\varphi(t, p)$ would have passed through the plane $\mathscr{P}_0$.

It is easy to see that if $\theta > \theta_z(\varepsilon)$, where

$$\theta_z(\varepsilon) = \arccos\left(\frac{\sqrt{2+\varepsilon}}{(2+8\varepsilon)\sqrt{2+\varepsilon} - 4\varepsilon\sqrt{\varepsilon}}\right),$$

then, the point $p = (\theta, w) \in \omega^0$ satisfies (8.5). $\theta_z(\varepsilon)$ is an increasing function of ε and

$\theta_z(0.35) \gtrsim 1.33$. That is, for all $0.35 \leqslant \varepsilon < 55/4$ and all $\theta_z(\varepsilon) \leqslant \theta < \pi/2$, the orbit $\varphi(t, p)$ of the corresponding point $p = (\theta, w) \in \omega^0$ crosses the x_1-axis. So $\varphi(t, p)$ crosses $\mathscr{P}_0$.

Some of the numerical results are given in Tables 8.I, 8.II, 8.III, 8.IV, 8.V and 8.VI. There, θ_0 is the coordinate θ of $p \in \omega^0$, (θ_i, w_i) is the cut number i of $\varphi(t, p)$ with $\mathscr{P}_0$ following the flow for positive time if $i > 0$, and for negative time if $i < 0$.

In Table 8.Ia there is a discontinuity in w_1 between 0.7 and 0.72. This is due to the existence of one point $p = (\theta', w')$ with $0.7 < \theta' < 0.72$ such that the first intersection

TABLE 8.I(a) $\varepsilon = .35$

θ_0	θ_1	w_1
θ_L	1.233732	0.280173
0.6	1.233541	0.279907
0.62	1.232199	0.278033
0.64	1.229658	0.274443
0.66	1.226029	0.269233
0.68	1.221439	0.262503
0.7	1.216021	0.254359
0.72	1.294751	0.477078
0.74	1.271515	0.472045
0.76	1.252599	0.465815
0.78	1.235823	0.458724
0.8	1.220453	0.450939
0.82	1.206164	0.442578
0.84	1.192796	0.433739
0.86	1·180265	0.424511
0.88	1.168536	0.414975
0.9	1.157597	0.405209
0.92	1.147456	0.395288
0.94	1.138135	0.385285
0.96	1.129664	0.375270
0.98	1.122080	0.365310
1.	1.115431	0.355473
1.02	1.109767	0.345823
1.04	1.105146	0.336421
1.06	1.101631	0.327329
1.08	1.109929	0.318603
1.1	1.098199	0.310295
1.12	1.098434	0.302457
1.14	1.100081	0.295131
1.16	1.103229	0.288357
1.18	1.107971	0.282165
1.2	1.114405	0.276578
1.22	1.122630	0.271609
1.24	1.132748	0.267256
1.26	1.144861	0.263503
1.28	1.159066	0.260315
1.3	1.175454	0.257636
1.32	1.194104	0.255379
1.34	1.215076	0.253425
1.36	1.238400	0.251611

TABLE 8.I(b)

θ_0	θ_3	w_3
0.72	1.209908	0.244910
0.74	1.203228	0.234270
0.76	1.196104	0.222558
0.78	1.188650	0.209893
0.8	1.180973	0.196402
0.82	1.173169	0.182212
0.84	1.165332	0.167455
0.86	1.157546	0.152266
0.88	1.149894	0.136782
0.9	1.142453	0.121145
0.92	1.135301	0.105500
0.94	1.128514	0.089996
0.96	1.122169	0.074782
0.98	1.116345	0.060015
1.	1.111122	0.045849
1.02	1.106584	0.032445
1.04	1.102819	0.019962
1.06	1.099917	0.008561
1.08	1.097972	−0.001602
1.1	1.097082	−0.010370
1.12	1.097348	−0.17594
1.14	1.098869	−0.023132
1.16	1.101748	−0.026856
1.18	1.106085	−0.028649
1.2	1.111982	−0.028416
1.22	1.119533	−0.026082
1.24	1.128834	−0.021603
1.26	1.139977	−0.014965
1.28	1.153051	−0.006193
1.3	1.168148	0.004644
1.32	1.185359	0.017424
1.34	1.204775	0.031967
1.36	1.226491	0.048022

TABLE 8.II $\varepsilon = 2$

θ_0	θ_1	w_1
θ_L	0.198417	−0.828670
0.9	0.198643	−0.828650
0.92	0.199819	−0.828539
0.94	0.202124	−0.828301
0.96	0.205706	−0.827895
0.98	0.210732	−0.827270
1.	0.217382	−0.826362
1.02	0.225854	−0.825092
1.04	0.236364	−0.823358
1.06	0.249143	−0.821037
1.08	0.264435	−0.817975
1.1	0.282492	−0.813990
1.12	0.303572	−0.808861
1.14	0.327923	−0.802333
1.16	0.355775	−0.794119
1.18	0.387327	−0.783902
1.2	0.422736	−0.771348
1.22	0.462104	−0.756119
1.24	0.505478	−0.737884
1.26	0.552846	−0.716336
1.28	0.604146	−0.691200
1.3	0.659272	−0.662236
1.32	0.718082	−0.629238
1.34	0.780404	−0.592022
1.36	0.846028	−0.550419
1.38	0.914698	−0.504259
1.4	0.986083	−0.453363
1.42	1.059748	−0.397539
1.44	1.135105	−0.336598
1.46	1.211357	−0.270410
1.48	1.287426	−0.199048
1.5	1.361865	−0.123178

TABLE 8.III $\varepsilon = 5$

θ_0	θ_1	w_1
θ_L	−0.043385	−0.917901
0.98	−0.043283	−0.917911
1.	−0.042192	−0.918009
1.02	−0.039766	−0.918218
1.04	−0.035804	−0.918536
1.06	−0.030073	−0.918956
1.08	−0.022296	−0.919461
1.1	−0.012146	−0.920021
1.12	0.000766	−0.920583
1.14	0.016902	−0.921063
1.16	0.036802	−0.921332
1.18	0.061098	−0.921197
1.2	0.090502	−0.920376
1.22	0.125789	−0.918471
1.24	0.167748	−0.914935
1.26	0.217086	−0.909060
1.28	0.274312	−0.899984
1.3	0.339600	−0.886749
1.32	0.412711	−0.868392
1.34	0.493015	−0.844059
1.36	0.579619	−0.813063
1.38	0.671538	−0.774885
1.4	0.767825	−0.729093
1.42	0.867601	−0.675237
1.44	0.970003	−0.612727
1.46	1.074043	−0.540726
1.48	1.178425	−0.458016
1.5	1.281296	−0.362819
1.52	1.379925	−0.252588
1.54	1.470138	−0.124426
1.56	1.544523	0.012741

of $\varphi(t, p)$ with $\mathscr{P}_0$ is a point on ω^0. To see that, we append the Table 8.Ib. In Tables 8.IV, 8.V and 8.VI there are also discontinuities of the same type.

On the other hand, we have the following result.

LEMMA 8.2. *If* $0 < \varepsilon < \varepsilon_e = 2\sqrt{3}/(16 - \sqrt{3}) \approx 0.242789\ldots$, *there are points of* ω^0 *which escape to infinity without crossing* $\mathscr{P}_0$.

Proof. Let $p = (\theta, w)$ in the hypotheses of Assertion 2.

From (1.1) $\ddot{x}_2 \geqslant -(2+\varepsilon)/x_2^2$, and, by integration, if $\dot{x}_2 \geqslant 0$ then $\dot{x}_2^2/2 - (2+\varepsilon)/x_2 \geqslant F$, where $F = \dot{x}_{2,p}^2/2 - (2+\varepsilon)/x_{2,p}$ is the energy of a 2-body problem. Using (8.1) we can compute F for $\theta = \theta_L$:

$$F = \frac{2+\varepsilon}{1+2\varepsilon}\left[\frac{2+\varepsilon}{4\varepsilon} - \frac{4}{\sqrt{3}}\right].$$

TABLE 8.IV $\varepsilon=0.35$

θ_0	θ_1	w_1
0.05	−0.100467	0.992208
0.1	−0.203714	0.970765
0.12	−0.246405	0.959373
0.14	−0.290171	0.946882
0.16	−0.335233	0.933616
0.18	−0.381867	0.919852
0.2	−0.430456	0.905804
0.22	−0.481570	0.891597
0.24	−0.536152	0.877230
0.26	−0.595958	0.862485
0.28	−0.664960	0.846637
0.3	−0.757255	0.826765
0.32	−1.189098	0.429368
0.34	−1.224086	0.449059
0.36	−1.269140	0.466952
0.38	−1.225481	0.261927
0.4	−1.246669	0.290974
0.41	−1.257390	0.304571
0.45	−1.301675	0.352264
0.47	−1.325439	0.371771
0.5	−1.368039	0.394770
0.52	−1.310158	0.251663
0.55	−1.321476	0.269300
0.58	−1.326895	0.277242

TABLE 8.V $\varepsilon=2$

θ_0	θ_1	w_1
0.005	−0.010000	0.999960
0.1	−0.200182	0.984397
0.15	−0.300583	0.965511
0.2	−0.401296	0.940132
0.25	−0.502376	0.909128
0.3	−0.603944	0.873359
0.35	−0.706375	0.833494
0.4	−0.810730	0.789711
0.45	−0.920037	0.740963
0.5	−1.045568	0.681453
0.55	−0.438186	−0.763271
0.6	−0.457144	−0.749884
0.65	−0.474358	−0.737493
0.7	−0.489412	−0.726511
0.75	−0.501870	−0.717362
0.8	−0.511229	−0.710488
0.85	−0.516871	−0.706376
θ_L	−0.518178	−0.705435

TABLE 8.VI $\varepsilon=5$

θ_0	θ_1	w_1
0.05	−0.099980	0.996881
0.1	−0.199837	0.987588
0.15	−0.299441	0.972312
0.2	−0.398645	0.951348
0.25	−0.497301	0.925060
0.3	−0.595275	0.893840
0.35	−0.692507	0.858036
0.4	−0.789118	0.817847
0.45	−0.885642	0.773143
0.5	−0.983633	0.722978
0.55	−1.087901	0.663868
0.6	−1.229597	0.572026
0.65	−0.298474	−0.892991
0.7	−0.316316	−0.886799
0.75	−0.332675	−0.880988
0.8	−0.347090	−0.875780
0.85	−0.359027	−0.871425
0.9	−0.367824	−0.868211
θ_L	−0.373124	−0.866292

Then $F > 0$ at $\theta = \theta_L$ if $\varepsilon < 2\sqrt{3}/(16 - \sqrt{3})$. ■

Lemma 8.2 proves that ξ_1 is broken for small values of ε.

The numerical computations show the existence of values $\varepsilon^{(1)} \in (0.2847, 0.2848)$ and $\varepsilon^{(2)} \in (0.2733, 0.2734)$ such that the Assertions 1 and 2 are true for $\varepsilon^{(1)} < \varepsilon < 55/4$ and $\varepsilon^{(2)} < \varepsilon < 55/4$, respectively. These numerical results give evidence for formulate the following conjecture.

Conjecture. There exists a critical value $\varepsilon_c \in (0.2847, 0.2848)$ such that the Assertions 1 and 2 are true for all $\varepsilon_c < \varepsilon < 55/4$.

Using the conjecture for $\varepsilon \in (\varepsilon_c, 55/4)$ the intersection between ξ_1 and ω^0 is empty. In the following we will reduce the case I defined by Proposition 1.1, to values of ε, $\varepsilon_c < \varepsilon < \varepsilon_1$.

In the same way, $i_2(e_2)$, $i_3^{-1}(e_3)$ and $i_4(e_4)$ contain arcs ξ_2, ξ_3 and ξ_4, respectively such that $\xi_1 = L^1(\xi_2)$, $\xi_3 = L^2(\xi_2)$ and $\xi_4 = L^1(\xi_3)$. Figure 8.1 shows the evolution of these arcs as a function of ε. In case I, ξ_2 cuts ξ_3 at least in one point. So we have a biparabolic orbit of type PP_{+-} (see Figure 8.2). It means that the orbit comes parabolically from one infinity, I_+ in this case, and goes parabolically to the other I_-. $\xi_1 \cap \xi_4$ gives the symmetrical orbit of type PP_{-+}. In the case III a new type of biparabolic orbits appears coming from, and going to, the same infinity.

We call them PP_{++} (see Figure 8.3) and PP_{--}. In Case V there are only the latter type of biparabolic orbits.

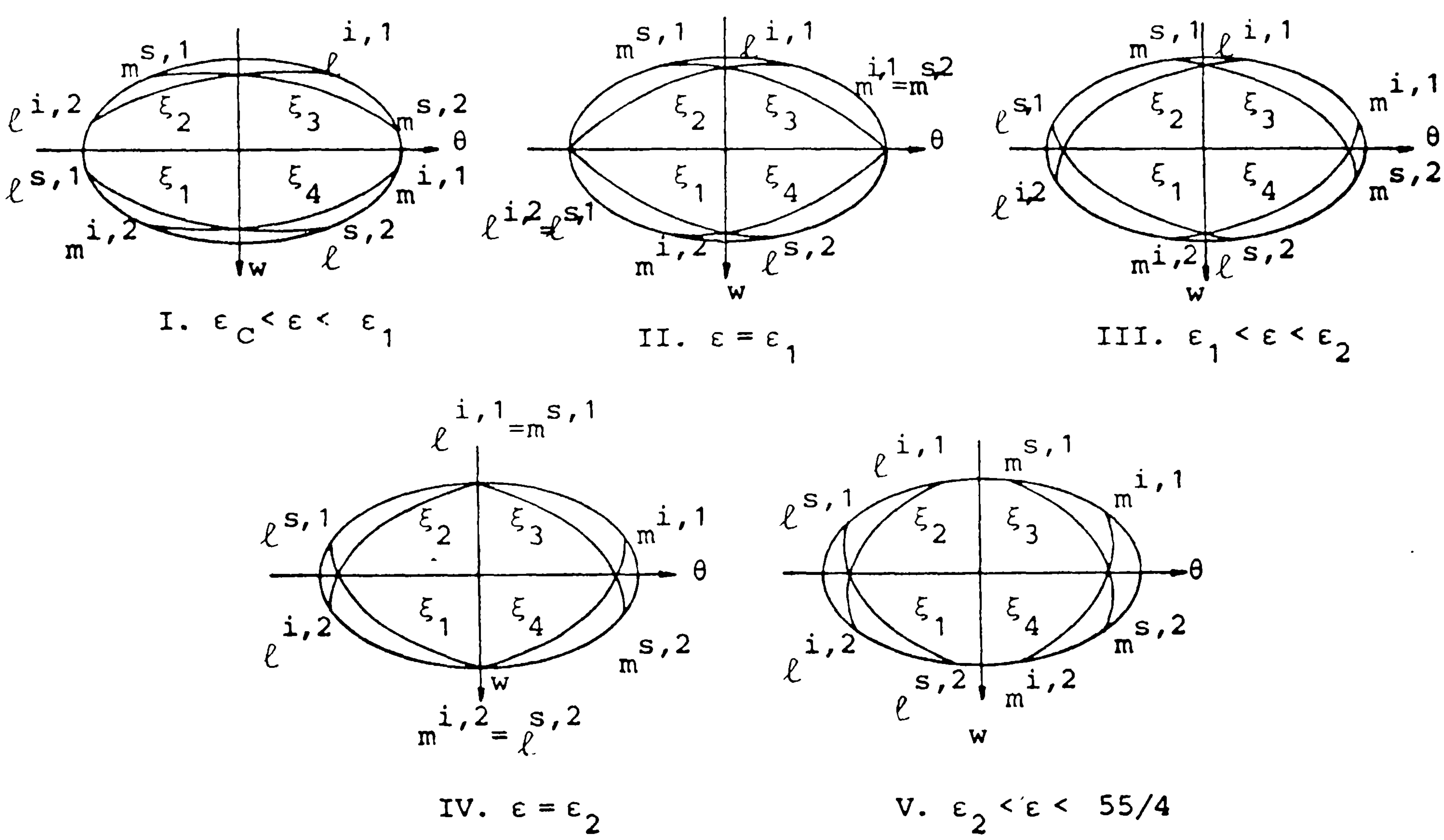

Fig. 8.1.

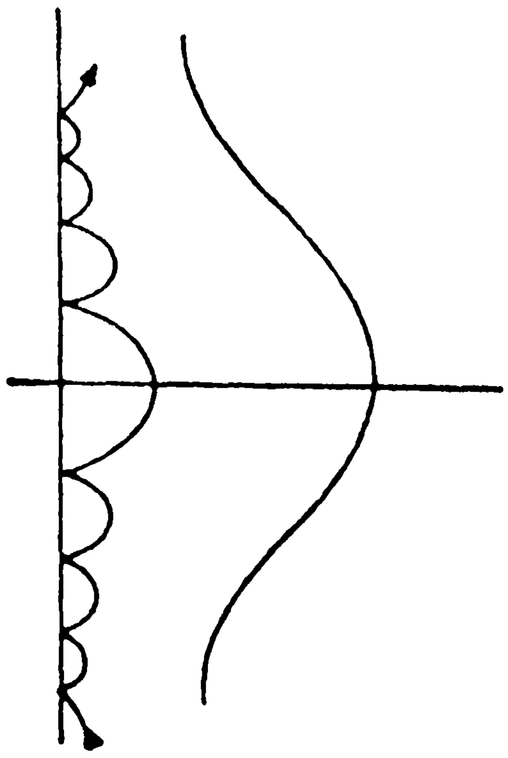

Fig. 8.2.

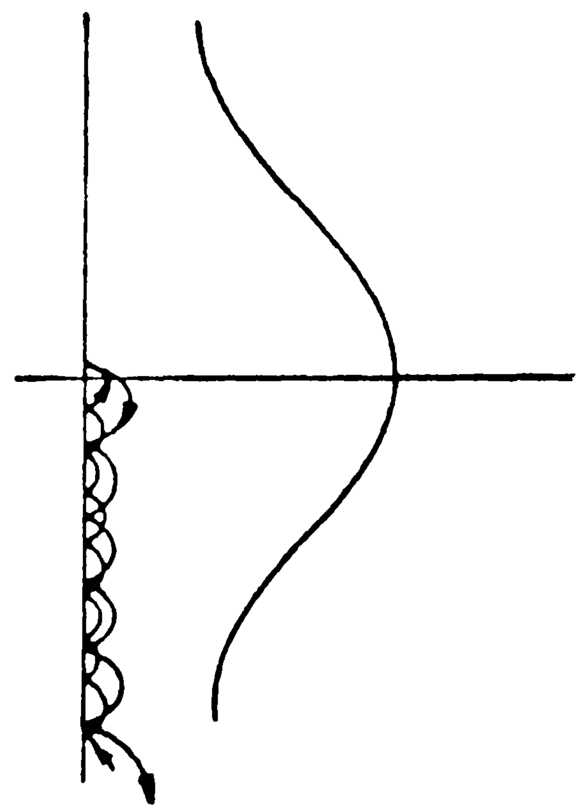

Fig. 8.3.

9. Some Properties of the Poincaré Map

We define $R_1 = \psi^{-1}(D_+)$, $R_2 = \Phi(D'_+)$, $R_3 = \psi^{-1}(D_-)$ and $R_4 = \Phi(D'_-)$. We can suppose $R_i \subset \mathcal{M}$ for $i = 1, 2, 3, 4$ because $\xi_i \subset \mathcal{M}$, for $i = 1, 2, 3, 4$.

LEMMA 9.1. *Let γ be an arc in $\mathcal{M}$.*

(i) *If $\gamma \subset R_1(R_3)$ has an endpoint in $\xi_1(\xi_3)$, then $\psi(\gamma)$ is a spiral in $D_+(D_-)$ which tends to* P.O.$_+$(P.O.$_-$). (See Fig. 6.4.)

(ii) *If $\gamma \subset R_2(R_4)$ has an endpoint in $\xi_2(\xi_4)$, $\Phi^{-1}(\gamma)$ is a spiral in $D'_+(D'_-)$ tending to* P.O.$_+$(P.O.$_-$).

Lemma 9.1 is a consequence of Lemma 2.1.

We consider the family of segments $\{c_j^1\}$ defined in D^1 (see Section 6). Let $m^2 = \min\{j \in \mathbb{N} \mid \Phi(d_j^1)$ is a continuous arc in $S_0\} + 1$. Then $\Phi(P_k^1)$ with $k = 2m^2$ is contained in $\mathcal{M}$ and it does not contain any point of ω^0. The arc of β_0 between $l^{i,1}$ and $m^{i,1}$, and the boundary of $\Phi(P_k^1)$, $k = 2m^2$, determines in $\Phi(D^1)$ a region which contains $\Phi(P_j^1)$ for all $j \geqslant 2m^2$. We denote this region by $\mathcal{U}^1$. For the sake of simplicity we keep the letter D^1 for the region such that $\mathcal{U}^1 = \Phi(D^1)$. In the same way we reduce the sets D^3, D^2, and D^4. We can define in $\mathcal{M}$ the sets

$$\mathcal{U}^3 = \psi^{-1}(D^3), \qquad \mathcal{U}^4 = \psi^{-1}(D^4),$$
$$\mathcal{U}^1 = \Phi(D^1), \qquad \mathcal{U}^2 = \Phi(D^2).$$

It is clear that we can obtain pictures which are qualitatively different for the sets $\mathcal{U}^{1,2,3,4}$ depending on ε.

LEMMA 9.2. *Let $\gamma = \{(\theta, w) \in \mathcal{M} \mid \theta = \theta(\tau), w = w(\tau), 0 < \tau \leqslant 1\}$ such that $\gamma(\tau)$ tends to a point $p \in \beta_0$ when τ tends to 0. If $\gamma(1) \in \psi^{-1}(c_m^2)$ $(\Phi(c_m^2))$ and $\gamma(\tau) \subset \mathcal{U}^3$ $(\mathcal{U}^1)$ for $0 < \tau \leqslant 1$, then, there exists a sequence $\tau_1, \tau_2, \ldots \tau_n, \ldots$ which tends to 0 such that*

$f(\gamma) \supset \bigcup_{j \in \mathbb{N}} \gamma'_j$ $(f^{-1}(\gamma) \supset \bigcup_{j \in \mathbb{N}} \gamma'_j)$ *where*

$$\gamma'_j = \{(\theta, w) \in f(\gamma)\ (f^{-1}(\gamma)) \mid \theta = \theta(\tau),\ w = w(\tau),\ \tau_j < \tau < \tau_{j+1}\}$$

such that, $\gamma'_j \subset \mathcal{U}^1$ $(\mathcal{U}^3)$, $\gamma'_j(\tau)$ *tends to* $m^{i,1}$ $(l^{s,1})$ *when* τ *tends to* τ_j *and* $\gamma'_j(\tau)$ *tends to* $l^{i,1}$ $(m^{s,1})$ *when* τ *tends to* τ_{j+1} *if* j *is odd, and when* j *is even,* $\gamma'_j \subset \mathcal{U}^2(\mathcal{U}^4)$, $\gamma'_j(\tau)$ *tends to* $l^{i,2}$ $(l^{s,2})$ *when* τ *tends to* τ_j *and* $\gamma'_j(\tau)$ *tends to* $m^{i,2}$ $(m^{s,2})$ *when* τ *tends to* τ_{j+1}.

Proof. Let us consider $\gamma(1) \in \psi^{-1}(c_m^2)$ and $\gamma(\tau) \subset \mathcal{U}^3$ (the other case is symmetrical). Then $\psi(\gamma(\tau))$ is a spiral curve in D^3 which tends to $(0, 0)$ when τ tends to 0. Taking $\tau_1, \tau_2, \ldots \tau_n, \ldots$ as the parameter values, in increasing order, at the intersection points between σ^s_+, σ^s_- and $\psi(\gamma(\tau))$ the Lemma 9.1 follows. ■

The intersections of the sets $\mathcal{U}^1$, $\mathcal{U}^3$, $\mathcal{U}^2$, $\mathcal{U}^4$, R_1, R_2, R_3 and R_4 give different connexions between passages near the homothetic Euler solution and near infinity.

In the cases I, III, and V we define the following sets (see Fig. 9.1):

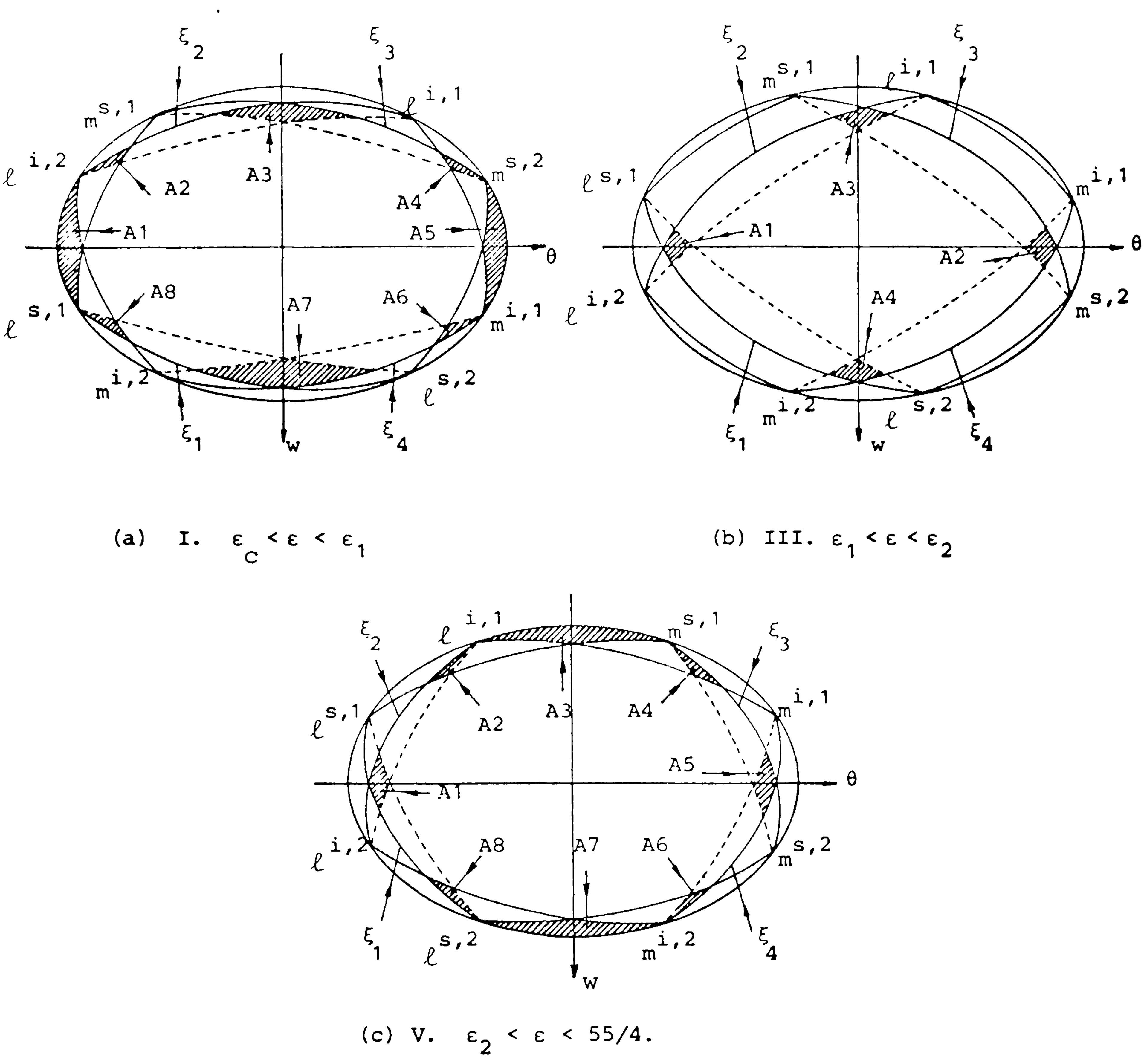

Fig. 9.1.

Case I

$$\begin{aligned} A1 &= \mathcal{U}^3 \cap \mathcal{U}^2, & A5 &= \mathcal{U}^1 \cap \mathcal{U}^4, \\ A2 &= \mathcal{U}^3 \cap R_2, & A6 &= \mathcal{U}^4 \cap R_4, \\ A3 &= R_2 \cap R_3, & A7 &= R_4 \cap R_1, \\ A4 &= R_3 \cap \mathcal{U}^1, & A8 &= R_1 \cap \mathcal{U}^2. \end{aligned} \tag{9.1}$$

Case III

$$\begin{aligned} A1 &= R_1 \cap R_2, & A3 &= R_2 \cap R_3, \\ A2 &= R_3 \cap R_4, & A4 &= R_4 \cap R_1. \end{aligned} \tag{9.2}$$

Case V

$$\begin{aligned} A1 &= R_1 \cap R_2, & A5 &= R_3 \cap R_4, \\ A2 &= R_2 \cap \mathcal{U}^3 & A6 &= R_4 \cap \mathcal{U}^4, \\ A3 &= \mathcal{U}^3 \cap \mathcal{U}^1, & A7 &= \mathcal{U}^4 \cap \mathcal{U}^2, \\ A4 &= \mathcal{U}^1 \cap R_3, & A8 &= \mathcal{U}^2 \cap R_1. \end{aligned} \tag{9.3}$$

Our goal is to characterize the orbits which cross the sets Ai defined above by sequences of symbols. So first we give an abstract theorem of symbolic dynamics. Then we apply this theorem to the cases I, III and V of the isosceles problem.

10. A Theorem of Symbolic Dynamics

We consider in the plane (x, y) n bounded, connected and pairwise disjoint sets that we call $A1$, $A2$, ... An. Let $A = \cup_{i \in I} Ai$ where $I = \{1, 2, \ldots, n]$ and let f be an homeomorphism from A to $f(A) \subset \mathbb{R}^2$. We associate to f an $n \times n$ transition matrix $\mathcal{A}_0 = (\bar{\alpha}_{i,j})$ defined by

$$\bar{\alpha}_{i,j} = \begin{cases} 1 & \text{if } f(Ai) \cap Aj \neq \emptyset, \\ 0 & \text{if } f(Ai) \cap Aj \neq \emptyset, \end{cases} \tag{10.1}$$

Let us consider a set S of special symbols $S = \{\dot{N}, L, M, \dot{n}, l, m]$ (we note that the finite set S can be arbitrary and the full construction is carried away in a similar way). We suppose that it is possible to associate to f a new matrix $\mathcal{A}$ of zeros and ones so that

$$\mathcal{A} = (\alpha_{i,j}) = \begin{bmatrix} \mathcal{A}_0 & \mathcal{A}_1 \\ \mathcal{A}_2 & 0_6 \end{bmatrix} \tag{10.2}$$

We call it the transition matrix with respect to $J = I \cup S$. In (10.2), 0_6 is a 6×6 matrix of zeros. $\mathcal{A}_0$ is given by (10.1). $\mathcal{A}_1$ and $\mathcal{A}_2$ have orders $n \times 6$ and $6 \times n$ respectively and they verify the following properties

(1) $\quad \sum_{i=1}^{n} \alpha_{j,i} \neq 0 \quad \text{if} \quad j \in \{\dot{n}, l, m\},$

$$
\begin{aligned}
&(2) \qquad \sum_{i=1}^{n} \alpha_{i,j} \neq 0 \quad \text{if} \quad j \in \{\dot{N}, L, M\}, \\
&(3) \qquad \sum_{i=1}^{n} \alpha_{j,i} = 0 \quad \text{if} \quad j \in \{\dot{N}, L, M\}, \\
&(4) \qquad \sum_{i=1}^{n} \alpha_{i,j} = 0 \quad \text{if} \quad j \in \{\dot{n}, l, m].
\end{aligned}
\tag{10.3}
$$

Let Σ' be the set of couples of sequences (a', a) of the following types

(a) $(a', a) = ((\ldots a'_{-1}; a'_0, a'_1, \ldots), (\ldots a_{-1}; a_0, a_1, \ldots))$, $a'_i \in I$ and $a_i \in \mathbb{N}$ for all $i \in \mathbb{Z}$,

(b1) $(a', a) = ((a'_k, a'_{k+1}, \ldots), (a_k, a_{k+1}, \ldots))$, $k < 0$, $a'_i \in I$, $a_i \in \mathbb{N}$ for all $i \in \mathbb{Z}$, $k < i$ and $a'_k = \dot{n}, a_k = \infty$,

(b2) $(a', a) = ((a'_k, a'_{k+1}, \ldots), (a_k, a_{k+1}, \ldots))$, $k < 0$, $a'_i \in I$ if $k < i, a'_k \in \{l, m\}$, $a_i \in \mathbb{N}$ for all $i \in \mathbb{Z}$, $k \leqslant i$,

(c1) $(a', a) = ((\ldots a'_{h-1}, a'_h), (\ldots a_{h-2}, a_{h-1}))$, $h > 0$, $a'_{i+1} \in I$, $a_i \in \mathbb{N}$ for all $i \in \mathbb{Z}$ $i < h-1$ and $a'_h = \dot{N}$, $a_{h-1} = \infty$.

(c2) $(a', a) = ((\ldots a'_{h-1}, a'_h), (\ldots a_{h-2}, a_{h-1}))$, $h > 0$, $a'_i \in I$ if $i < h$, $a'_h \in \{L, M\}$, $a_i \in \mathbb{N}$ for all $i \in \mathbb{Z}$, $i \leqslant h-1$,

or some of the 4 types of finite sequences on the left and on the right, which can be obtained joining the types (b) and (c). We call them (d11), (d12), (d21) and (d22), where the first figure means the type of the left ending and the second one the right ending.

We define Σ as the subset of Σ' such that the sequence a' of each couple $(a', a) \in \Sigma$ is admissible with respect to the $\mathscr{A}$ matrix. That means, $\alpha_{u,v} = 1$, where $u = a'_{i-1}$ and $v = a'_i$, *for all* $i \in \mathbb{Z}$ for which a'_{i-1} and a'_i are defined.

For every $i \in I$ we define

$$
\begin{aligned}
I_i &= \{j \in I \mid \alpha_{i,j} = 1\}, & c(i) &= \text{card}(I_i), \\
I'_i &= \{j \in I \mid \alpha_{j,i} = 1\}, & g(i) &= \text{card}(I'_i), \\
\mathbf{S}_i &= \{j \in S \mid \alpha_{i,j} = 1\} \setminus \{\dot{N}, \dot{n}\}, & r(i) &= \text{card}(\mathbf{S}_i), \\
\mathbf{S}'_i &= \{j \in S \mid \alpha_{j,i} = 1\} \setminus \{\dot{N}, \dot{n}\}, & z(i) &= \text{card}(\mathbf{S}'_i).
\end{aligned}
$$

We need some hypotheses about the sets Ai and the behaviour of f on these sets. These hypotheses have a topological character, not metric as in the case of Moser (see [5]).

We fix a set Ai and we define families of curves of the type

$$
\gamma = \{(x, y) \in \mathbb{R}^2 \mid x = x(\tau),\ y = y(\tau),\ 0 \leqslant \tau \leqslant 1\} \tag{10.4}
$$

such that $\gamma(\tau) = (x(\tau), y(\tau)) \in \text{Int}(Ai)$ for all $0 < \tau < 1$, $\gamma(0) \in \partial Ai$ and $\gamma(1) \in \partial Ai$.

Hypothesis 1. There exist in ∂Ai 4 different arcs Γ_1, Γ_2, Γ_3 and Γ_4 such that every curve γ as in (10.4) with $\gamma(0) \in \Gamma_1$ and $\gamma(1) \in \Gamma_2$ cuts at some point $\gamma(\tau)$, $0 < \tau < 1$, to any curve γ' such that $\gamma'(0) \in \Gamma_3$ and $\gamma'(1) \in \Gamma_4$. Then, the arcs Γ_j, $j = 1$, 2, 3, 4, define in Ai, two types of curves that we call horizontals (h.c.) and verticals (v.c.) respectively.

Two h.c. γ and γ' without intersection in a point $\gamma(\tau)$, $0 < \tau < 1$, define a horizontal strip H (h.s.). The diameter of H ($d(H)$), will be the Hausdorff distance between γ and γ'. The vertical strips (v.s.) are defined in the same way.

We say that 2 h.s. (v.s.) are disjoint when the points of intersection, if they exist, are in ∂Ai.

We note that some of the arcs Γ_j can be reduced to a point. From now on we assume that in every Ai the arcs Γ_j, $j = 1, 2, 3, 4$ are fixed.

Hypothesis 2. For all $i \in I$, there exist in Ai g(i) countable families of h.s. $\{\{Hji\}\}_{j \in I_i'}$ pairwise disjoint and $c(i)$ families of v.s. $\{\{Vmi\}\}_{m \in I_i}$ pairwise disjoint satisfying the following properties:

(a) They are ordered and intercalated so that there exists a global numeration $\{Hi(k)\}_{k \in \mathbb{N}}$ of the h.s. such that every $g(i)$ strips, the picture of $\{Hi(k)\}_{k \in \mathbb{N}}$ is like Figure 10.1. There is a similar arrangement $\{Vi(k)\}_{k \in \mathbb{N}}$ for the families of v.s. Furthermore we assume that it is possible to define limit strips as

$$\begin{aligned} Hi(\infty) = \; & \{(x, y) \in \partial Ai \mid \text{there exists a sequence of points } (x, y)_k \in Hi(k) \text{ for} \\ & \text{all } k \in \mathbb{N}, \text{ such that } (x, y)_k \text{ tends to } (x, y) \text{ when } k \text{ tends to } \infty\}, \\ Vi(\infty) = \; & \{(x, y) \in \partial Ai \mid \text{there exists a sequence of points } (x, y)_k \in Vi(k) \text{ for} \\ & \text{all } k \in \mathbb{N}, \text{ such that } (x, y)_k \text{ tends to } (x, y) \text{ when } k \text{ tends to } \infty\}. \end{aligned}$$

(b) f maps homeomorphically v.s. into h.s., that is,

$$f(Vmi(k)) = Him(k). \tag{10.5}$$

The horizontal (vertical) boundaries are mapped into horizontal (vertical) boundaries if f is defined on them.

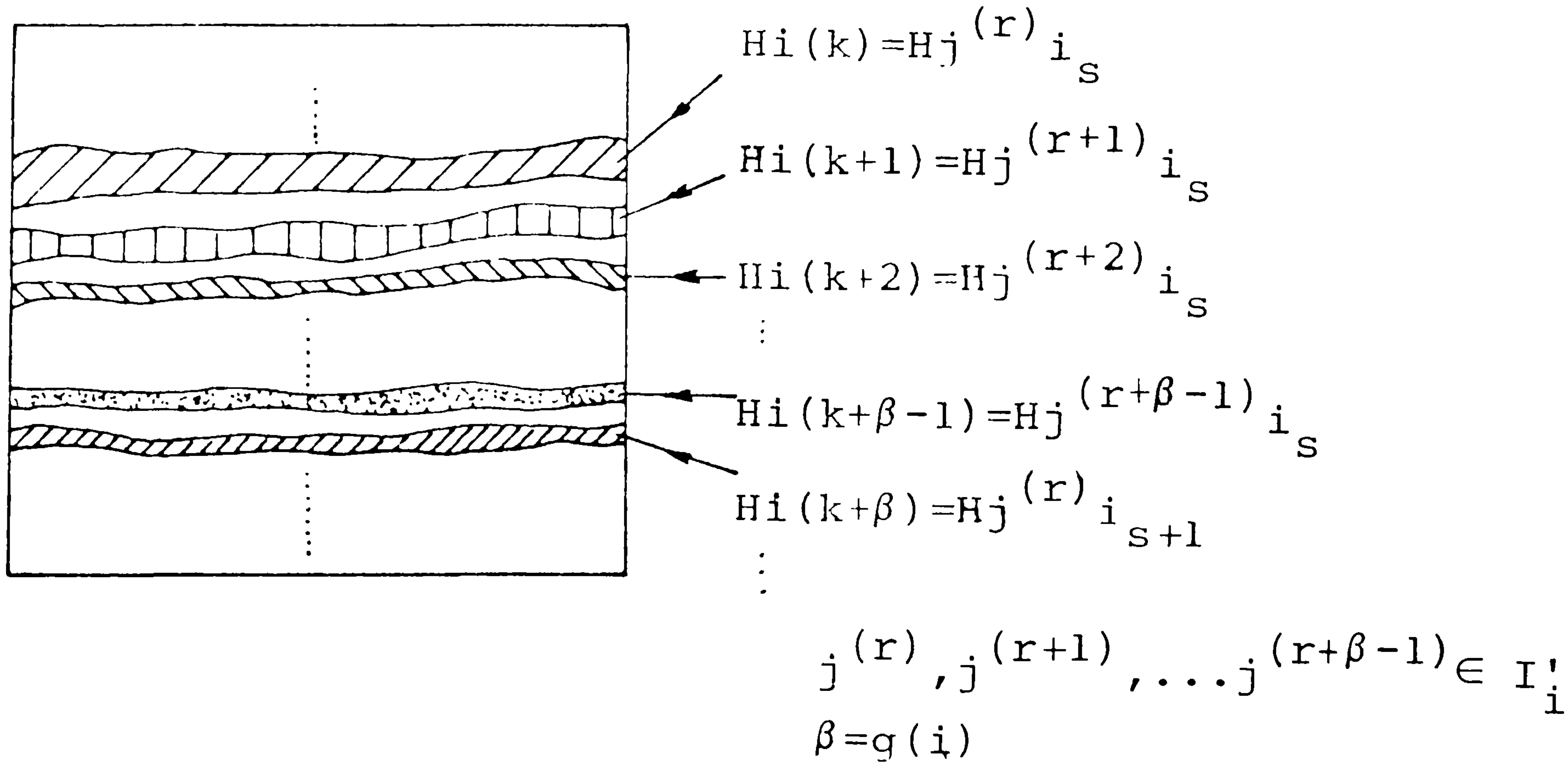

Fig. 10.1.

Hypothesis 3. For all $i \in I$, there exist $z(i)$ families of h.c. $\{\{Eji\}\}_{j \in S_i'}$ and $r(i)$ families of v.s. $\{\{Cji\}\}_{j \in S_i}$ such that

(a) f^{-1} is not defined on the h.c. and f is not defined on the v.c.

(b) Let C be either a v.c. in Ai such that $C \subset Vi(m)$ for some $m \in \mathbb{N}$, or a v.c. in Ai belonging to some of the above families.

Then $f^{-1}(C) \cap Vij(k)$ is a v.c. in Aj for all $j \in I_i'$ and for all $k \in \mathbb{N}$. In a similar way if E is a h.c. in Ai and either $E \subset Hi(m)$ for some $m \in \mathbb{N}$, or E is a h.c. of some of the above families, then $f(E) \cap Hij(k)$ is a h.c. in Aj for all $j \in I_i$ and for all $k \in \mathbb{N}$. Families $\{Eji\}_{j \in S_i'}$ and $\{Cji\}_{j \in S_i}$ can be contained in the families of h.s. and v.s. of the Hypotheses 2. In this case, for every $j \in S_i'$, there exists $m \in I_i$ such that $Eji(k) \subset Hmi(k)$ for all $k \in \mathbb{N}$, and for every $j \in S_i$, there exists $m \in I_i'$ such that $Cji(k) \subset Vmi(k)$ for all $k \in \mathbb{N}$.

We note that for all $k \in \mathbb{N}$ Hypotheses 3 implies $f^{-1}(V) \cap Vij(k)$ is a v.s. for all $j \in I_i'$ and $f(H) \cap Hij(k)$ is a h.s. for all $j \in I_i$.

Let $(a', a) \in \Sigma$. We associate to (a', a) a family of v.s. and a family of h.s. depending on the type of (a', a) as follows:

(a) We define

$$\bar{V}_i = Va'_{i+1}a'_i(a_i) \qquad \text{for all} \quad i \in \mathbb{Z},$$

$$\bar{H}_i = Ha'_{i-1}a'_i(a_{i-1}) \text{ for all} \quad i \in \mathbb{Z}, i \leqslant 0. \tag{10.6}$$

(b) We define $\bar{V}_i$ and $\bar{H}_i$ as in (10.6) if $i > k+1$ and

$$\bar{V}_{k+1} = Va'_{k+2}a'_{k+1}(a_{k+1}) \cap Ha'_{k+1}(\infty), \tag{10.7a}$$

$$\bar{H}_{k+1} = Ha'_{k+1}(\infty),$$

if (a', a) is of type (b1), and

$$\bar{V}_{k+1} = Va'_{k+2}\, a'_{k+1}(a_{k+1}) \cap Ea'_k\, a'_{k+1}(a_k),$$

$$\bar{H}_{k+1} = Ea'_k a'_{k+1}(a_k), \tag{10.7b}$$

if (a', a) is of type (b2).

(c) $\bar{V}_i$ and $\bar{H}_i$ will be given by (10.6) if $i < h-1$ and

$$\bar{V}_{h-1} = Va'_{h-1}(\infty), \tag{10.8a}$$

for sequences of type (cl), and

$$\bar{V}_{h-1} = Ca'_h\, a'_{h-1}(a_{h-1}) \tag{10.8b}$$

for type (c2).

If (a', a) is of type (d) we will define $\bar{V}_i$ and $\bar{H}_i$ as in (10.6) for $k+1 < i < h-1$ and $\bar{V}_{k+1}$, $\bar{H}_{k+1}$, and $\bar{V}_{h-1}$ as in cases (b) or (c) depending on the type of (a', a).

We say that a point $p \in A$ fulfills the couple $(a', a) \in \Sigma$ if $f^m(p) \in \bar{V}_m$ for all $m \in \mathbb{Z}$ for which $\bar{V}_m$ is defined.

THEOREM 10.1. *Let $A = \bigcup_{i \in I} Ai$, $I = \{1, 2, \dots n\}$, where for every $i \in I$, Ai is a bounded and connected set in the plane. Let f be a homeomorphism from A to $f(A)$ with a transition matrix $\mathscr{A}$ as in* (10.2) *satisfying the Hypotheses* 1, 2, 3. *Then for every pair of sequences $(a', a) \in \Sigma$, there exists a point p which fulfils it.*

Proof. We suppose that $(a', a) \in \Sigma$ is an (a) type couple.

Let

$$B_1 = \{p \in A \mid f^m(p) \in \bar{V}_m,\ m = 0, 1, 2, \dots\}, \quad \text{and}$$

$$B_2 = \{p \in A \mid f^{-m}(p) \in \bar{V}_{-m},\ m = 1, 2, \dots\}.$$

We define in a recursive way

$$\begin{aligned}\bar{V}_{0,1,2,\dots n} &= \{p \in A \mid f^m(p) \in \bar{V}_m,\ m = 0, 1, 2, \dots n\}\\ &= \bar{V}_0 \cap f^{-1}(\bar{V}_1 \cap f^{-1}(\dots \bar{V}_{n-1} \cap f^{-1}(\bar{V}_n)) \dots).\end{aligned}$$

The Hypothesis 3 implies $\bar{V}_{n-1} \cap f^{-1}(\bar{V}_n)$ is a v.s. in Aa'_{n-1}. By recursion $\bar{V}_{0,1,2,\dots n}$ is a v.s. in Aa'_0.

By definition $\bar{V}_{0,1,2,\dots n+1} \subset \bar{V}_{0,1,2,\dots n}$ are compact sets for all $n \in \mathbb{N}$. Then $B_1 = \bigcap_{n \geqslant 0} \bar{V}_{0,1,2,\dots n} \neq \emptyset$ is a v.s. (possibly a v.c.).

From (10.5), $\bar{H}_{-m+1} = f(\bar{V}_{-m})$. Therefore

$$B_2 = \{p \in A \mid f^{-m}(p) \in \bar{H}_{-m},\ m = 0, 1, 2, \dots\}.$$

We define

$$\begin{aligned}\bar{H}_{0,-1,-2,\dots -n} &= \{p \in A \mid f^{-m}(p) \in \bar{H}_{-m},\ m = 0, 1, 2, \dots n\}\\ &= \bar{H}_0 \cap f(\bar{H}_{-1} \cap \dots \bar{H}_{-n+1} \cap f(\bar{H}_{-n})) \dots).\end{aligned}$$

Using the same argument as above $B_2 = \bigcap_{n \geqslant 0} \bar{H}_{0,-1,\dots -n}$ is a h.s. (possibly a h.c.) in Aa'_0.

Hypothesis 1 implies $B_1 \cap B_2 \neq \emptyset$.

Let us suppose that $(a', a) \in \Sigma$ is a (b1) or (b2) type couple. We define a v.s. B_1 as in the case (a). Let

$$B_2 = \{p \in A \mid f^{-m}(p) \in \bar{V}_{-m},\ m = 1, 2, \dots -(k+1)\}.$$

From (10.5), $\bar{H}_{-m+1} = f(\bar{V}_{-m})$ if $m < -(k+1)$. Moreover by using (10.7) and (10.5) if $f^{k+1}(p) \in \bar{V}_{k+1}$ then $f^{k+1}(p) \in \bar{H}_{k+1}$ and $f^{k+2}(p) \in \bar{H}_{k+2}$. Therefore

$$\begin{aligned}B_2 &= \{p \in A \mid f^{-m}(p) \in \bar{H}_{-m},\ m = 0, 1, 2, \dots -(k+1)\}\\ &= \bar{H}_0 \cap f(\bar{H}_{-1} \cap \cdots \cap f(\bar{H}_{k+2} \cap f(\bar{H}_{k+1})) \dots).\end{aligned}$$

As above, $\bar{H}_{k+2} \cap f(\bar{H}_{k+1})$ is a h.c. in $\bar{H}_{k+2}$. By recurrence B_2 is a h.c. in $\bar{H}_0$. Then $B_1 \cap B_2 \neq \emptyset$.

The Theorem is proved in the same way when (a', a) is a (c) or (d) type couple. ■

Let us suppose that the curves and strips from the Hypotheses 2 and 3 verify the following properties:

(a) Every h.c. in Ai cuts each v.c. in Ai only at one point.
(b) If V is a v.s. $V \subset Vi_m$ for some $m \in \mathbb{N}$, then there exists a v, $0 < v < 1$ such that

$$d(f^{-1}(V) \cap Vij(k)) \leqslant vd(V)$$

for all $j \in I'_i$ and for all $k \in \mathbb{N}$. In the same way, if H is a h.s. $H \subset Hi_m$ for some $m \in \mathbb{N}$, then

$$d(f(H) \cap Hij(k)) \leqslant vd(H)$$

for all $j \in I_i$ and for all $k \in \mathbb{N}$.

Then it is clear that the point p given by the Theorem 10.1 is unique.

11. Symbolic Dynamics in the Isosceles Problem

Theorem 10.1 will give different types of behaviours in the isosceles problem. We will prove Hypotheses 1, 2, and 3 for the case V. In the cases I and III only the results will be given.

In the case V we take $A = \bigcup_{i \in I} Ai$, $I = \{1,2,3,4,5,6,7,8\}$ where Ai sets are defined in (9.3). The Table II.I shows in each Ai, how the arcs Γ_j, $j = 1,2,3,4$ are selected in order to satisfy Hypothesis 1. It can be seen that Γ_j is reduced to one point on β_0 in some cases. (*) means the points of ∂Ai which are not contained in any of the defined arcs Γ_j

TABLE 11.I

	$A1$	$A2$	$A3$	$A4$	$A5$	$A6$	$A7$	$A8$
Γ_1	ξ_1	$l^{i,1}$	$l^{i,1}$	ξ_3	ξ_3	$m^{i,2}$	$m^{i,2}$	ξ_1
Γ_2	$\partial R_1 \setminus \xi_1$	$\partial \mathcal{U}^3 \setminus \beta_0$	$\partial \mathcal{U}^3 \setminus \beta_0$	(*)	$\partial R_3 \setminus \xi_3$	$\partial \mathcal{U}^4 \setminus \beta_0$	$\partial \mathcal{U}^4 \setminus \beta_0$	(*)
Γ_3	ξ_2	ξ_2	$m^{s,1}$	$m^{s,1}$	ξ_4	ξ_4	$l^{s,2}$	$l^{s,2}$
Γ_4	$\partial R_2 \setminus \xi_2$	(*)	$\partial \mathcal{U}^1 \setminus \beta_0$	$\partial \mathcal{U}^1 \setminus \beta_0$	$\partial R_4 \setminus \xi_4$	(*)	$\partial \mathcal{U}^2 \setminus \beta_0$	$\partial \mathcal{U}^2 \setminus \beta_0$

For every Ai, an arc γ as in (10.4) will be a h.c. if $\gamma(0) \in \Gamma_1$ and $\gamma(1) \in \Gamma_2$. It will be a v.c. if $\gamma(0) \in \Gamma_3$ and $\gamma(1) \in \Gamma_4$.

Using Lemmas 9.1 and 9.2 we will define some families of horizontal and vertical curves and strips. $\psi(A1)$ and $\psi(A8)$ are two spiral strips as in Figure 11.1. There is a symmetrical picture in D_- for $\psi(A4)$ and $\psi(A5)$. Moreover $\psi(A2)$, $\psi(A3)$, $\psi(A6)$ and $\psi(A7)$ are spiral strips in $D^3 \cup D^4$ as Figure 11.2 shows. Then we can define the following families of horizontal strips and curves

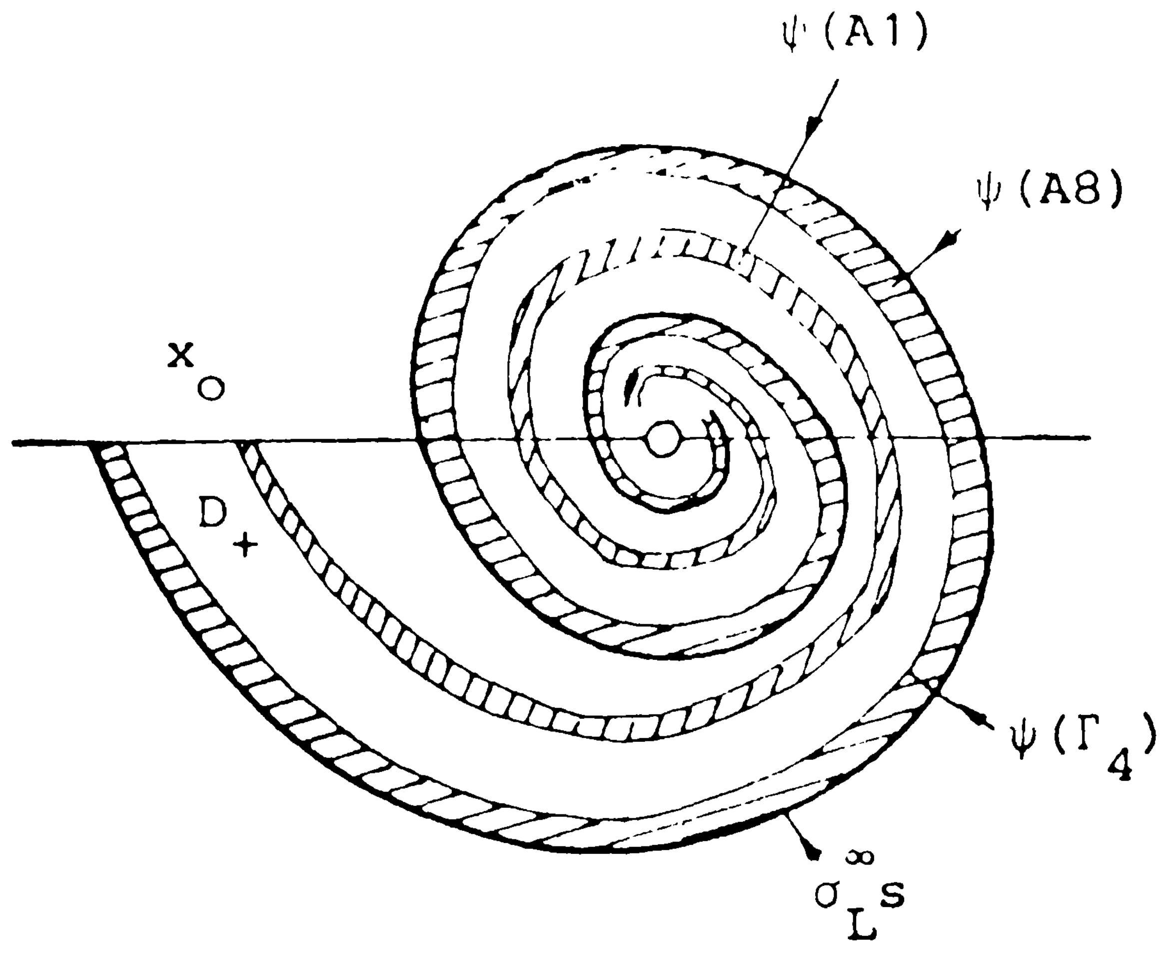

Fig. 11.1.

$$\begin{aligned}
&Hij(k) = \Phi(\mathrm{cl}(\psi(Ai)) \cap Q_k^+) \cap Aj && i=1,8 \quad j=1,2,\\
&Hij(k) = \Phi(\mathrm{cl}(\psi(Ai)) \cap Q_k^-) \cap Aj && i=4,5 \quad j=5,6,\\
&Hij(k) = \Phi(\mathrm{cl}(\psi(Ai)) \cap P_{2k+1}^1) \cap Aj && i=2,3 \quad j=3,4,\\
&Hij(k) = \Phi(\mathrm{cl}(\psi(Ai)) \cap P_{2k}^1) \cap Aj && i=6,7 \quad j=3,4,\\
&Hij(k) = \Phi(\mathrm{cl}(\psi(Ai)) \cap P_{2k}^2) \cap Aj && i=2,3 \quad j=7,8,\\
&Hij(k) = \Phi(\mathrm{cl}(\psi(Ai)) \cap P_{2k+1}^2) \cap Aj && i=6,7 \quad j=7,8,
\end{aligned} \tag{11.1a}$$

for $k > m^1$ if $i = 1, 4, 5$ or 8 and for $k > m^2$ if $i = 2, 3, 6$ or 7, and

$$\begin{aligned}
&Eli(k) = H8i(k) \cap \Phi(\sigma_{L^s}^{\infty}), && i=1,2,\\
&Emi(k) = H4i(k) \cap \Phi(\sigma_{M^s}^{\infty}), && i=5,6,\\
&Eli(k) = H7i(k) \cap \Phi(\sigma_-^u), && i=3,4,7,8,\\
&Emi(k) = H3i(k) \cap \Phi(\sigma_+^u), && i=3,4,7,8,
\end{aligned} \tag{11.1b}$$

for $k > m^1$ if $i = 1, 2, 5$, or 6 and for $k > m^2$ if $i = 3, 4, 7$ or 8.

If $p \in Eli(k)(Emi(k))$ for some k and some i, then $f^{-1}(p)$ is not defined and $\varphi(t, p)$ is an ejection orbit such that $\varphi(t, p)$ tends to $L^s(M^s)$ when t tends to $-\infty$.

Using similar reasoning we can define the following vertical strips and curves

$$\begin{aligned}
&Vij(k) = \psi^{-1}(\mathrm{cl}(\Phi^{-1}(Ai)) \cap Q_k^+) \cap Aj, && i=1,2, \quad j=1,8,\\
&Vij(k) = \psi^{-1}(\mathrm{cl}(\Phi^{-1}(Ai)) \cap Q_k^-) \cap Aj, && i=5,6, \quad j=4,5,\\
&Vij(k) = \psi^{-1}(\mathrm{cl}(\Phi^{-1}(Ai)) \cap P_{2k+1}^1) \cap Aj, && i=3,4, \quad j=2,3,\\
&Vij(k) = \psi^{-1}(\mathrm{cl}(\Phi^{-1}(Ai)) \cap P_{2k}^2) \cap Aj, && i=7,8, \quad j=2,3,
\end{aligned}$$

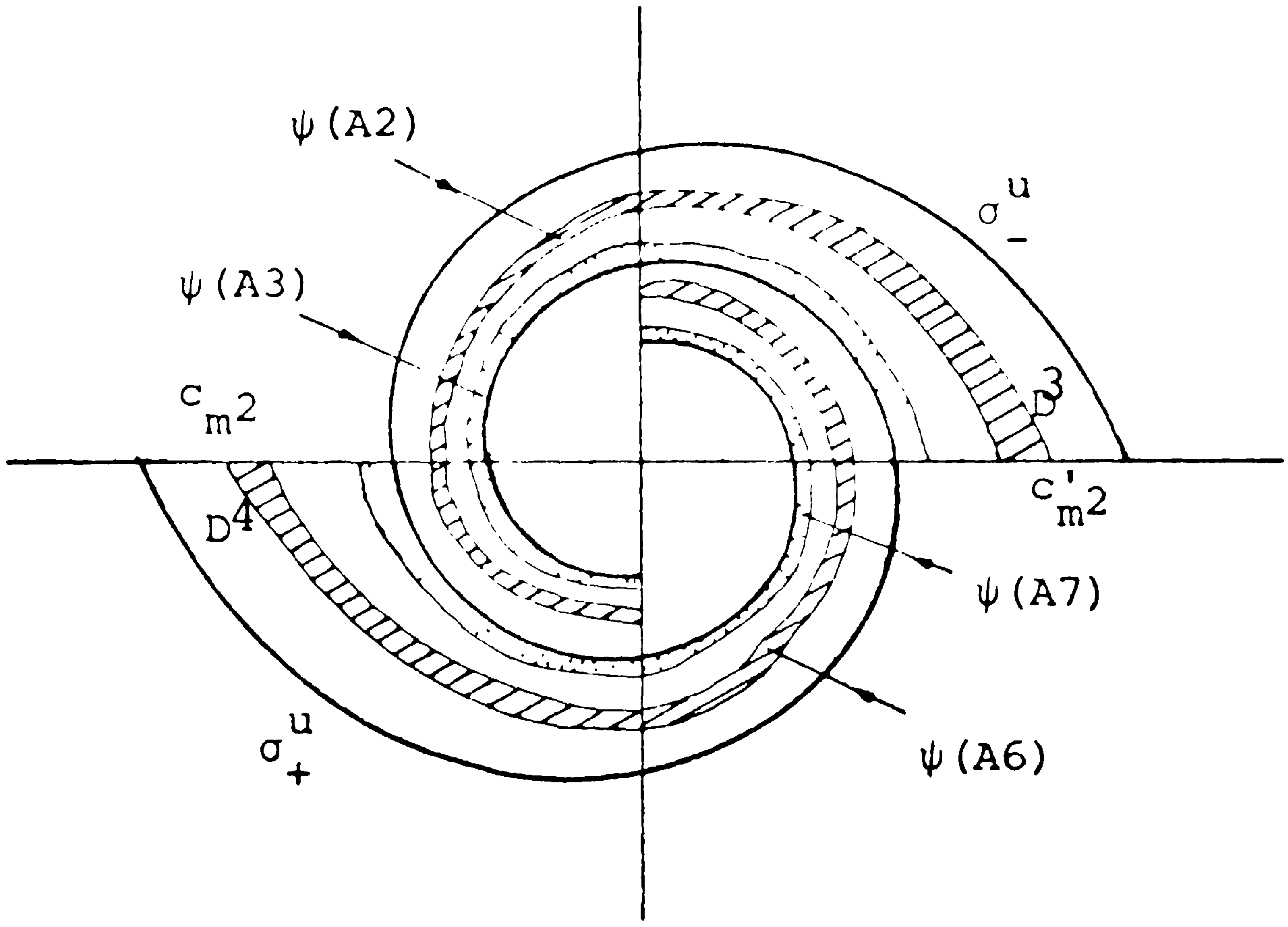

Fig. 11.2.

$$\begin{aligned} Vij(k) &= \psi^{-1}(\mathrm{cl}(\Phi^{-1}(Ai)) \cap P^1_{2k}) \cap Aj, \qquad i=3,4, \quad j=6,7, \\ Vij(k) &= \psi^{-1}(\mathrm{cl}(\Phi^{-1}(Ai)) \cap P^2_{2k+1}) \cap Aj, \qquad i=7,8, \quad j=6,7, \end{aligned} \tag{11.2a}$$

for $k > m^1$ if $i = 1, 2, 5$ or 6 and for $k > m^2$ if $i = 3, 4, 7$ or 8 and

$$\begin{aligned} CLi(k) &= V2i(k) \cap \psi^{-1}(\sigma^{\infty}_{L'}), \qquad i=1,8, \\ CMi(k) &= V6i(k) \cap \psi^{-1}(\sigma^{\infty}_{M'}), \qquad i=4,5, \\ CLi(k) &= V3i(k) \cap \psi^{-1}(\sigma^{s}_{-}), \qquad i=2,3,6,7, \\ CMi(k) &= V7i(k) \cap \psi^{-1}(\sigma^{s}_{+}), \qquad i=2,3,6,7, \end{aligned} \tag{11.2b}$$

for $k > m^1$ if $i = 1, 4, 5$ or 8 and for $k > m^2$ if $i = 2, 3, 6$ or 7.

The Poincaré map f is not defined on the vertical curves. The orbits $\varphi(t, p)$ with $p \in CLi(k)(CMi(k))$ for some k, i, are collision orbits, that is, $\varphi(t, p)$ tends to $L^i(M^i)$ when t tends to $+\infty$.

The limit strips will be the following

$$\begin{aligned} H1(\infty) &= \xi_2 \cap \partial A1, \qquad & V1(\infty) &= \xi_1 \cap \partial A1, \\ H2(\infty) &= \xi_2 \cap \partial A2, & V2(\infty) &= \{l^{i,1}\}, \\ H4(\infty) &= \{m^{s,1}\}, & V4(\infty) &= \xi_3 \cap \partial A4, \\ H5(\infty) &= \xi_4 \cap \partial A5, & V5(\infty) &= \xi_3 \cap \partial A5, \\ H6(\infty) &= \xi_4 \cap \partial A6, & V6(\infty) &= \{m^{i,2}\}, \\ H8(\infty) &= \{l^{s,2}\}, & V8(\infty) &= \xi_1 \cap \partial A8, \end{aligned} \tag{11.3}$$

$H3(\infty)=V3(\infty)$ will be the arc of β_0 between $l^{i,1}$ and $m^{i,1}$, and $H7(\infty)=V7(\infty)$ the arc of β_0 between $l^{s,2}$ and $m^{s,2}$.

The transition matrix $\mathscr{A}_0$ associated to f according to (10.1) is

$$\mathscr{A}_0 = \begin{bmatrix} 1 & 1 & 0 & 0 & 0 & 0 & 0 & 0 \\ 0 & 0 & 1 & 1 & 0 & 0 & 1 & 1 \\ 0 & 0 & 1 & 1 & 0 & 0 & 1 & 1 \\ 0 & 0 & 0 & 0 & 1 & 1 & 0 & 0 \\ 0 & 0 & 0 & 0 & 1 & 1 & 0 & 0 \\ 0 & 0 & 1 & 1 & 0 & 0 & 1 & 1 \\ 0 & 0 & 1 & 1 & 0 & 0 & 1 & 1 \\ 1 & 1 & 0 & 0 & 0 & 0 & 0 & 0 \end{bmatrix} \tag{11.4}$$

We extend $\mathscr{A}_0$ to a matrix $\mathscr{A}$ with respect to $I \cup S$ as in (10.2). S will be the set of special symbols defined in section 10. Let $i \in I$, we define

(i) $\alpha_{i,\dot{N}}(\alpha_{\dot{n},i})=1$, if there exists $p \in \mathrm{cl}(Ai)$ such that $f(p)(f^{-1}(p))$ is not defined and $\varphi(t,p)$ escapes to infinity when t tends to $+\infty(-\infty)$.

(ii) $\alpha_{i,L}(\alpha_{l,i})=1$, if there exists $p \in Ai$ such that $f(p)(f^{-1}(p))$ is not defined and $\varphi(t,p)$ tends to $L^i(L^s)$ when t tends to $+\infty(-\infty)$.

(iii) $\alpha_{i,M}(\alpha_{m,i})=1$, if there exists $p \in Ai$ such that $f(p)(f^{-1}(p))$ is not defined and $\varphi(t,p)$ tends to $M^i(M^s)$ when t tends to $+\infty(-\infty)$.

(iv) $\alpha_{i,j}=0$ in other cases.

Therefore we can write

$$\mathscr{A}_1 = \left[\begin{array}{ccc|c} 1 & 1 & 0 & \\ 0 & 1 & 1 & \\ 0 & 1 & 1 & \\ 1 & 0 & 1 & \\ 1 & 0 & 1 & 0_{8\times 3} \\ 0 & 1 & 1 & \\ 0 & 1 & 1 & \\ 1 & 1 & 0 & \end{array}\right] \tag{11.5}$$

$$\mathscr{A}_2 = \left[\begin{array}{cccccccc} \multicolumn{8}{c}{0_{3\times 8}} \\ \hline 1 & 1 & 0 & 0 & 1 & 1 & 0 & 0 \\ 1 & 1 & 1 & 1 & 0 & 0 & 1 & 1 \\ 0 & 0 & 1 & 1 & 1 & 1 & 1 & 1 \end{array}\right] \tag{11.6}$$

where $0_{8\times 3}(0_{3\times 8})$ is the 8×3 (3×8) matrix of zeros. There is a set Σ associated with $\mathscr{A}$ as given in section 10 whose elements are couples of sequences.

The families of curves and strips defined by (11.1), (11.2) and (11.3) verify part (a) of Hypothesis 2. For part (b), let us consider, for example, the v.s. $V18(k)$ for some $k>m^1$. Using definition (11.2a)

$$f(V18(k)) = \Phi[\Phi^{-1}(A1)\cap Q_k^+ \cap \mathrm{cl}(\psi(A8))]$$
$$= A1\cap\Phi[Q_k^+\cap\mathrm{cl}(\psi(A8))] = H81(k)$$

and (10.5) follows for $m=1$ and $i=8$. We denote by v_1 and v_2 (h_1 and h_2) the vertical (horizontal) boundaries of $V18(k)$ as in Figure 11.3. In this case, h_2 is reduced to $l^{s,2}$ and so f is not defined on it. From Figure 11.4 it is easy to see that f preserves the boundaries v_1, v_2 and h_1. We can prove part (b) of Hypothesis 2 for the rest of the strips in the same way.

LEMMA 11.1. *Let $E(V)$ be a* h.c.(v.c) *in Ai such that $E\subset Hi(m)$ $(V\subset Vi(m))$ for some $m\in\mathbb{N}$. Then $f(E)\cap Hij(k)(f^{-1}(V)\cap Vij(k))$ is a* h.c.(v.c) *in Aj for all $j\in I_i(j\in I_i')$ and for some k for which $Hij(k)(Vij(k))$ is defined.*

Proof. $\psi(E)$ is a spiral curve in $\psi(Ai)$ contained in D_+ if $i=1,8$, in D_- if $i=4,5$, in D^3 if $i=2,3$, and in D^4 if $i=6,7$. So, $\psi(E)$ cuts at infinite points to $\sigma^{\infty}_{L'}$, $\sigma^{\infty}_{M'}$ if $i=1,8$ and $i=4,5$, respectively. $\psi(E)$ cuts σ^s_+ and σ^s_- in other cases. Then, for all $j\in I_i$ and for all $k\in\mathbb{N}$ such that $Hij(k)$ is defined, $\psi(E)\cap\Phi^{-1}(Hij(k))\neq\emptyset$. The proof is similar for v.c. ∎

We have proved Hypotheses 1, 2, and 3. Then we conclude with the following theorem.

THEOREM 11.1 *Let $\varepsilon_2<\varepsilon<55/4$, and let Σ be the set formed by the couples of sequences of elements belonging to $I\cup S=\{1,2,3,4,5,6,7,8\}\cup\{\dot N, L, M, \dot n, l, m\}$ which are of some of the types* (a), (bi), c*i*), (d*ij*), $i=1,2, j=1,2$, *with respect to the*

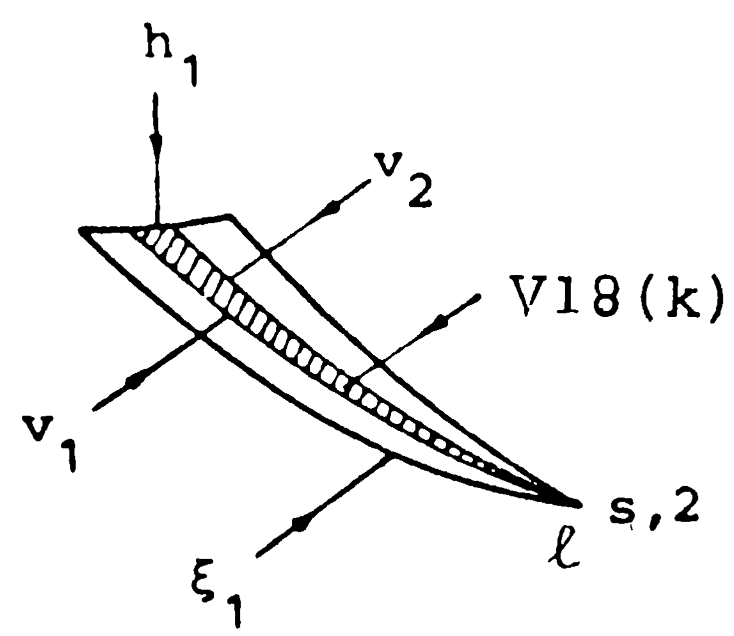

Fig. 11.3.

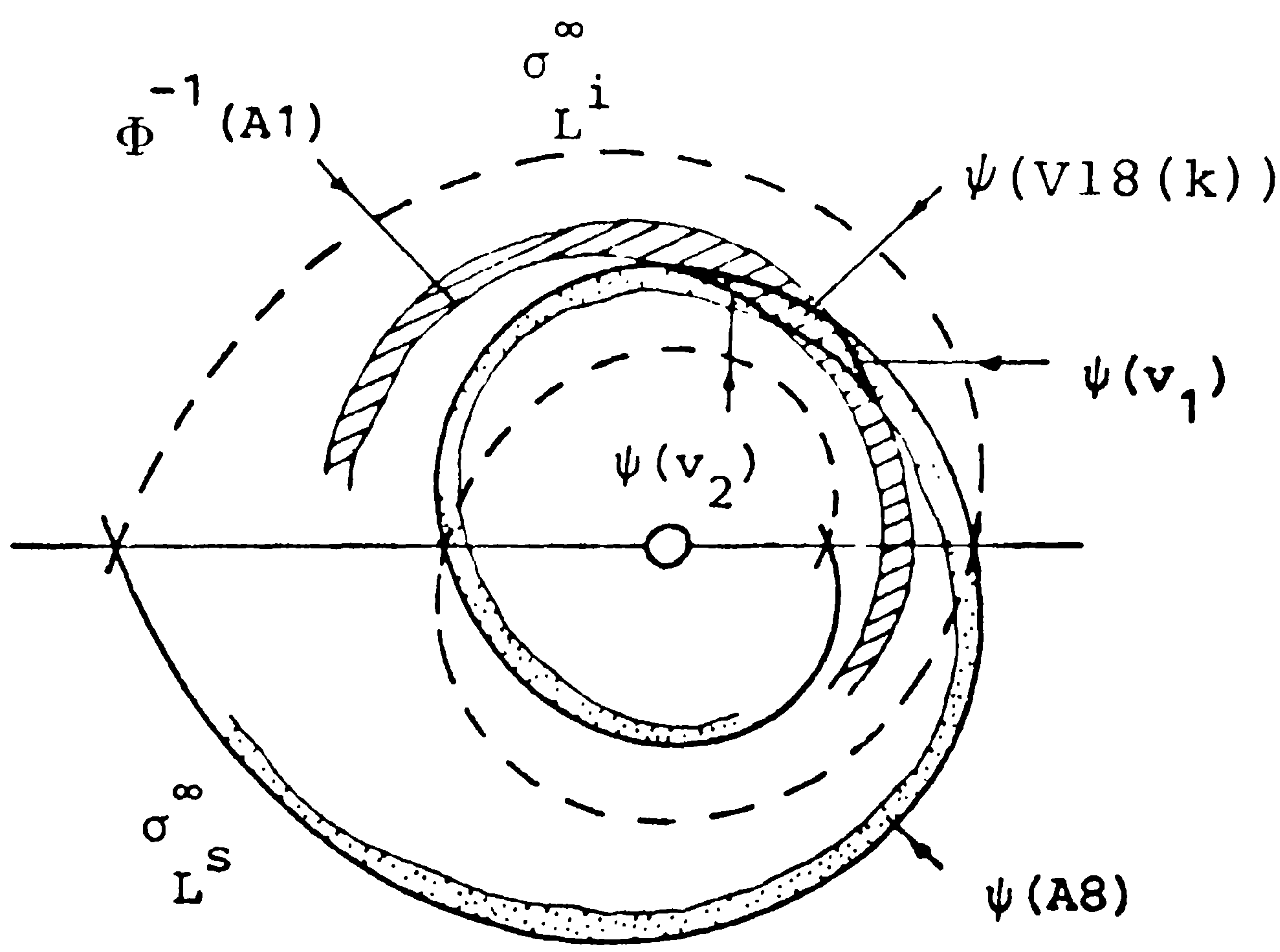

Fig. 11.4

transition matrix

$$\mathscr{A} = \begin{pmatrix} \mathscr{A}_0 & \mathscr{A}_1 \\ \mathscr{A}_2 & 0_6 \end{pmatrix}$$

given by (11.4), (11.5) *and* (11.6).

Then for all couple $(a', a) \in \Sigma$ *such that* $a_j > m^*(\varepsilon) = \max(m^1, m^2)$, *there exists a point* $p \in Aa'_0$ *which fulfils it.*

The geometrical interpretation of the orbits given by Theorem 11.1 needs some comments.

Let $p \in A$ the point that fulfils $(a', a) \in \Sigma$.

If (a', a) is of (a) type, $\varphi(t, p)$ crosses S_0 infinite times for positive and negative time. The sequence a' gives the successive sets Ai which are visited by $\varphi(t, p)$ in each passage by S_0.

Let us suppose that (a', a) is of (b1) type. Then, by the definition (10.7a),

$$f^{k+1}(p) \in \bar{V}_{k+1} = Va'_{k+2}a'_{k+1}(a_{k+1}) \cap Ha'_{k+1}(\infty)$$

for some $k < 0$. From $\mathscr{A}_2$ a'_{k+1} must be equal to 1, 2, 5 or 6. Then, $Ha'_{k+1}(\infty) \subset \xi_2 \cup \xi_4$ and $\varphi(t, p)$ comes parabolically from infinity. For a (b2) couple $(a', a) \in \Sigma$, $f^{k+1}(p) \in Ea'_k a'_{k+1}(a_k)$ for some $k < 0$. Then $\varphi(t, p)$ is an ejection orbit from L^s if $a'_k = l$ and from M^s when $a'_k = m$. Using same reasonings the (cl) couples correspond to orbits which escape parabolically to infinity. The (c2) couples give collision orbits at L^i if $a'_h = L$ and at M^i if $a'_h = M$. The couples of (d) type are the combination of parabolic, ejection and collision orbits. The Table 11.II summarizes the behaviour of the orbits corresponding to the different types of couples. In this Table we use P for parabolic orbits and E and C for ejection and collision respectively.

TABLE 11.II

(a', a)	(b1)	(b2)	(cl)	(c2)	(d11)	(d12)	(d21)	(d22)
$t<0$	P	E			P	P	E	E
$t>0$			P	C	P	C	P	C

In order to represent, on the position plane, the orbits which pass through A we remark some facts.

Let $p \in A2 \cup A3$ and suppose that $f(p)$ exists. We denote by $\bar{\gamma}$ the arc of $\varphi(t, p)$ between p and $f(p)$. There exist t_1, t_2 and t_3 such that $\varphi(t_1, p) \in S^-$, $\varphi(t_2, p) \in D^3$, $\varphi(t_3, p) \in S^- \cup S^+$ and there is not any $t \in (0, t_1) \cup (t_1, t_2) \cup (t_2, t_3)$ such that $\varphi(t, p) \in S^- \cup S^+$. Moreover if $f(p) \in A3 \cup A4$ then $\varphi(t_3, p) \in S^+$ and $\varphi(t_3, p) \in S^-$ if $f(p) \in A7 \cup A8$. When $p \in A6 \cup A7 \subset \mathcal{U}^4$ the result is the same but $\varphi(t_1, p) \in S^+$.

We consider $p \in A8$. $\varphi(t, p)$ goes to S^+ near ξ_1. If $f(p) \in A2$, $\bar{\gamma}$ has only binary collision with $\theta = \pi/2$. These binary collisions will be counted in the passage of $\bar{\gamma}$ by D_+. If $f(p) \in A1$, there is one passage by S^- near $f(p)$ but this passage will be considered when the orbit went out of $A1$.

We have summarized the behaviours of the orbits which pass by A in Table 11.III. The row t_1 tells us if the arc $\bar{\gamma}$ has a first passage by $S^+ \cup S^-$ or not. Row t_3 refers to

TABLE 11.III

P		t_1	t_2	t_3	$f(p)$	
$\mathcal{U}^3$	$A2$	S^-	S_1	S^+	$A3, A4$	$\mathcal{U}^1$
	$A3$			S^-	$A7, A8$	$\mathcal{U}^2$
$\mathcal{U}^4$	$A6$	S^+	S_1	S^+	$A3, A4$	$\mathcal{U}^1$
	$A7$			S^-	$A7, A8$	$\mathcal{U}^2$
R_1	$A1$	S^-	S^+		$A1, A2$	R_2
	$A8$					
R_2	$A4$		S^-		$A5, A6$	R_4
	$A5$	S^+				

a possible last crossing by $S^+ \cup S^-$ immediately before $f(p)$. The central row says whether $\bar{\gamma}$ passes near the Euler homothetic solution or near I_+ or I_-. An element a_n of the sequence a will denote the number of binary collisions at $\theta = \pi/2$ (S^+) or $\theta = -\pi/2$ (S^-) or the number of complete revolutions around the Euler homothetic solution depending on a'_n and a'_{n+1}. Recall that every one of these revolutions is one oscillation of m_3 around the axis $x_2 = 0$ on the position plane.

We give three examples

$$(a', a) = ((\ldots 4, 6; 3, 7, 8, 1, 1, \ldots), (\ldots a_{-2}, a_{-1}; a_0, a_1, a_2, \ldots)), \tag{1}$$

$$(a', a) = ((l, 1; 2, 4, \dot{N}), (a_{-2}, a_{-1}; a_0, \infty)), \tag{2}$$

$$(a', a) = ((m, 3; 4, 6, 7, L), (a_{-2}, a_{-1}; a_0, a_1, a_2)). \tag{3}$$

The Figures 11.5, 11.6 and 11.7 display the evolution of the corresponding orbits on the position plane. In every case we assume that (a', a) is in the hypotheses of Theorem 11.1 but to clarify the pictures we represent the orbits for small values of the elements a_n.

In the case I, that is $\varepsilon_c < \varepsilon < \varepsilon_1$ we take $A = \bigcup_{i \in I} Ai$, $I = \{1, 2, 3, 4, 5, 6, 7, 8\}$, where the sets Ai are defined in (9.1). The transition matrix associated to f respect to $I \cup S$ is given in the form (10.2) where

$$\mathscr{A}_0 = \begin{bmatrix} 1 & 0 & 0 & 1 & 1 & 0 & 0 & 1 \\ 1 & 0 & 0 & 1 & 1 & 0 & 0 & 1 \\ 0 & 0 & 0 & 0 & 0 & 1 & 1 & 0 \\ 0 & 0 & 0 & 0 & 0 & 1 & 1 & 0 \\ 1 & 0 & 0 & 1 & 1 & 0 & 0 & 1 \\ 1 & 0 & 0 & 1 & 1 & 0 & 0 & 1 \\ 0 & 1 & 1 & 0 & 0 & 0 & 0 & 0 \\ 0 & 1 & 1 & 0 & 0 & 0 & 0 & 0 \end{bmatrix}, \tag{11.7}$$

$$\mathscr{A}_1 = \begin{bmatrix} 0 & 1 & 1 & 0 & 0 & 0 \\ 0 & 1 & 1 & 0 & 0 & 0 \\ 1 & 0 & 1 & 0 & 0 & 0 \\ 1 & 0 & 1 & 0 & 0 & 0 \\ 0 & 1 & 1 & 0 & 0 & 0 \\ 0 & 1 & 1 & 0 & 0 & 0 \\ 1 & 1 & 0 & 0 & 0 & 0 \\ 1 & 1 & 0 & 0 & 0 & 0 \end{bmatrix}, \quad \mathscr{A}_2 = \begin{bmatrix} 0 & 0 & 0 & 0 & 0 & 0 & 0 & 0 \\ 0 & 0 & 0 & 0 & 0 & 0 & 0 & 0 \\ 0 & 0 & 0 & 0 & 0 & 0 & 0 & 0 \\ 0 & 1 & 1 & 0 & 0 & 1 & 1 & 0 \\ 1 & 1 & 1 & 1 & 1 & 0 & 0 & 1 \\ 1 & 0 & 0 & 1 & 1 & 1 & 1 & 1 \end{bmatrix}.$$

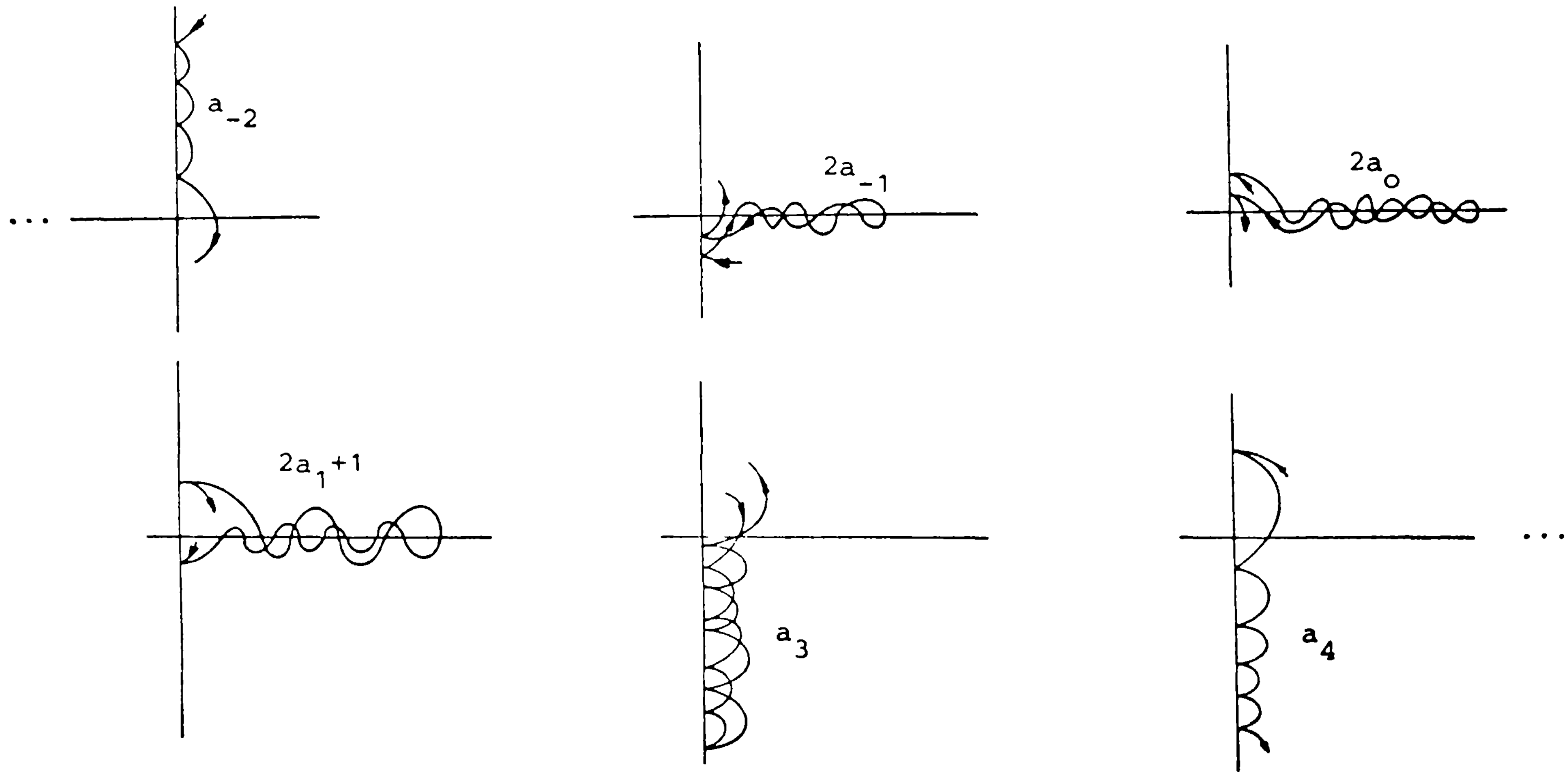

Fig. 11.5.

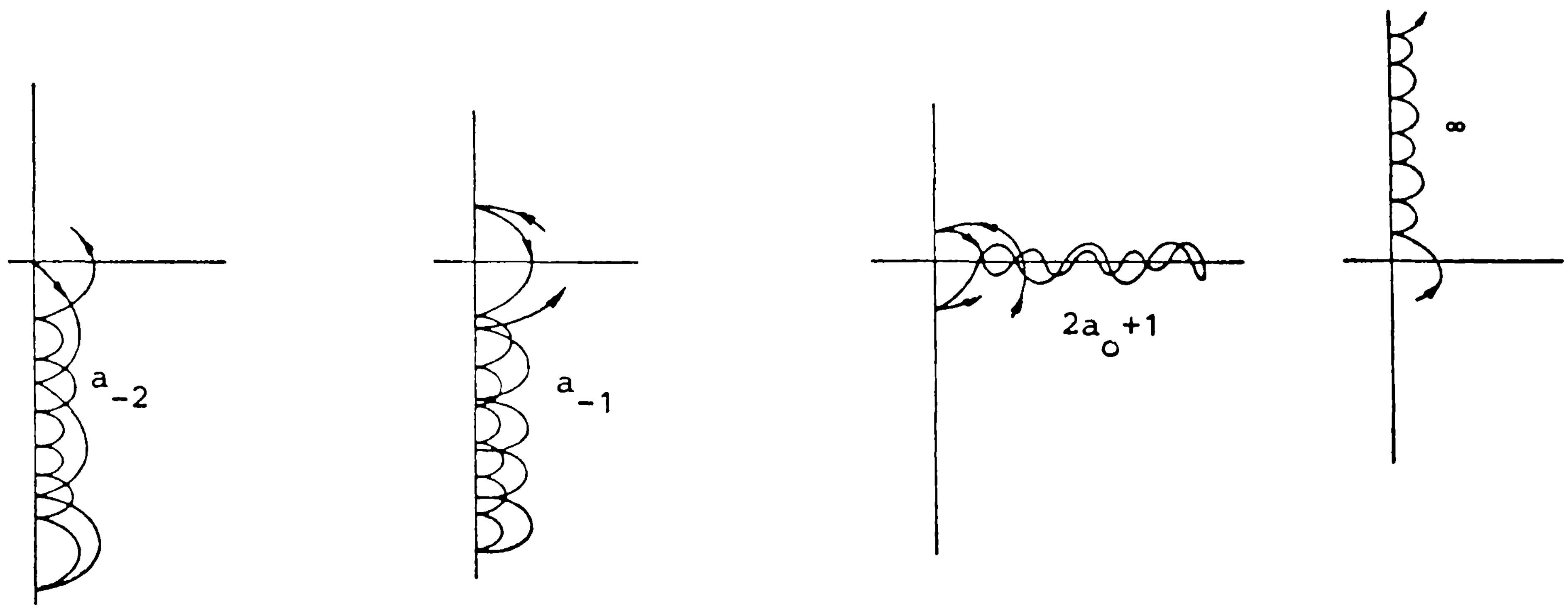

Fig. 11.6.

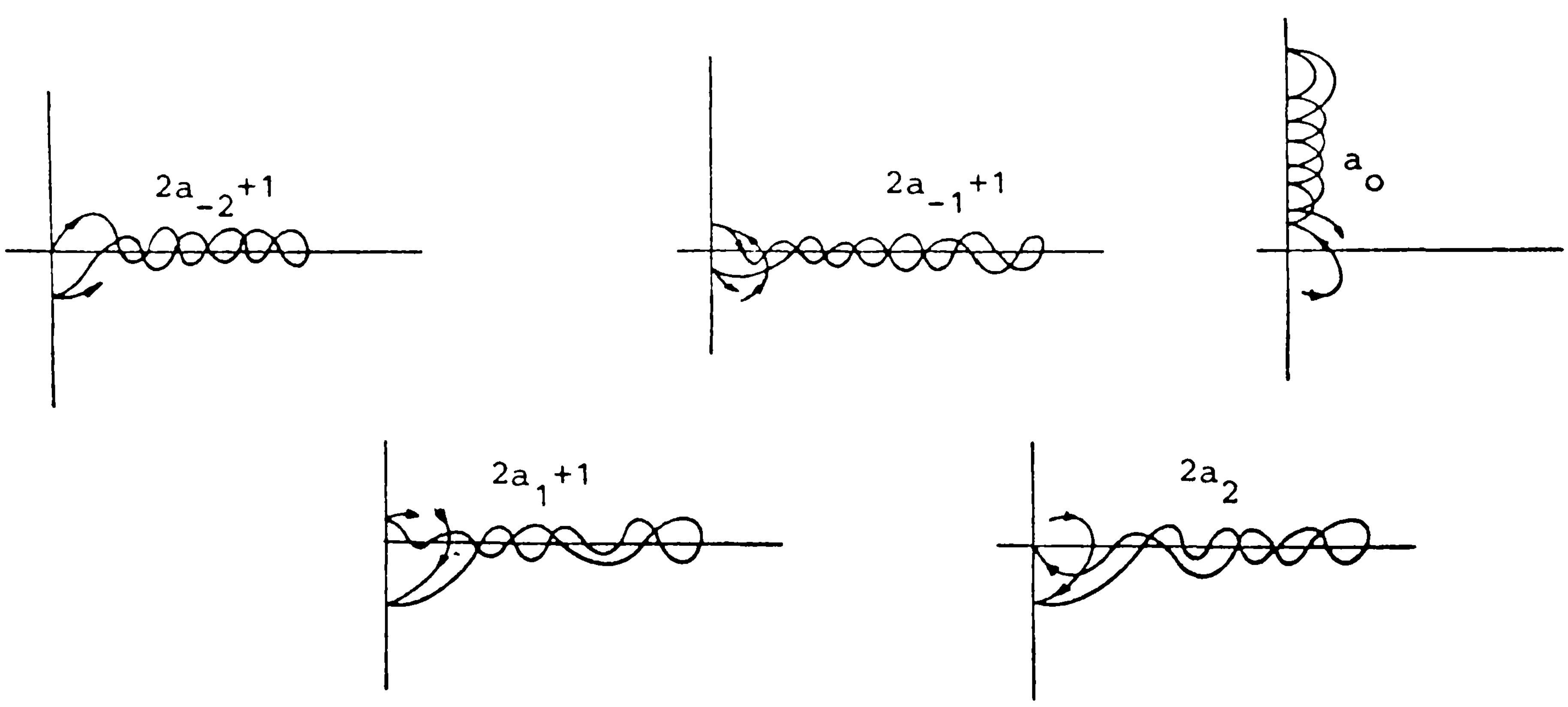

Fig. 11.7.

Now Σ will be the set of couples of sequences with respect to the transition matrix given by (11.7).

A similar study to case V can be done for $\varepsilon_c < \varepsilon < \varepsilon_1$. We obtain for all couples $(a', a) \in \Sigma$ such that $a_j > m^*(\varepsilon)$, a point $p \in Aa'_0$ which fulfils it.

We only note that in this case appears a new type of transitions. For example, we consider (a', a) of (a) type with $a'_n = 5$ for all $n \in \mathbb{Z}$. The corresponding orbit passes infinite times by a neighbourhood of the Euler homothetic solution. It only has binary collisions with $\theta = \pi/2$. This kind of behaviour is not possible for $\varepsilon_2 < \varepsilon < 55/4$.

In the case III, the set A is the union of the four sets defined by (9.2); the transition matrix in this case is the following

$$\mathscr{A} = \left[\begin{array}{cccc|cccccc} 1 & 0 & 1 & 0 & 1 & 1 & 0 & 0 & 0 & 0 \\ 0 & 1 & 0 & 1 & 1 & 0 & 1 & 0 & 0 & 0 \\ 0 & 1 & 0 & 1 & 1 & 0 & 1 & 0 & 0 & 0 \\ 1 & 0 & 1 & 0 & 1 & 1 & 0 & 0 & 0 & 0 \\ \hline 0 & 0 & 0 & 0 & & & & & & \\ 0 & 0 & 0 & 0 & & & & & & \\ 0 & 0 & 0 & 0 & & & 0 & & & \\ 1 & 1 & 1 & 1 & & & & & & \\ 1 & 0 & 1 & 0 & & & & & & \\ 0 & 1 & 0 & 1 & & & & & & \end{array}\right]$$

We note that in this case, we can not assure the existence of orbits which have a large number of oscillations around the x_1-axis without escape to infinity. In fact, if that number is sufficiently large then, the orbit escapes.

12. Some Families of Symmetrical Periodic Orbits

In this section we classify some of the families of symmetrical periodic orbits. All these families are included in the set of orbits given by the Theorem 10.1 in the isosceles problem. To obtain these orbits we use the reversibility of the system (1.5) respect to the symmetries L^1 and L^2. We denote by $\mathrm{Fix}(L^1)$ ($\mathrm{Fix}(L^2)$) the set of points which remain fixed by L^1 (L^2). It is known (see [3]) that if $p \in \mathrm{Fix}(L^1)$, for example, and $\tau = \min \{t > 0 \,|\, \varphi(t,p) \in \mathrm{Fix}(L^1) \cup \mathrm{Fix}(L^2)\}$ is different of zero, then $\varphi(t,p)$ is a symmetrical periodic orbit. In fact, $\varphi(t,p)$ is symmetrical with respect to L^1 and 2τ-periodic if $\varphi(\tau,p) \in \mathrm{Fix}(L^1)$ and it is symmetrical with respect to L^1 and to L^2 with period equal to 4τ if $\varphi(\tau, p) \in \mathrm{Fix}(L^2)$.

In the isosceles problem we have $\mathrm{Fix}(L^1) = \gamma_1 \cup \gamma_+ \cup \gamma_-$ and $\mathrm{Fix}(L^2) = \gamma_2$. Recall the segments γ_+ and γ_- defined by (4.1) correspond to points of binary collision such that the momentum r has a local minimum. In order to obtain the symmetrical periodic orbits, we will follow γ_1, γ_2, γ_+ and γ_- forward and backward by the flow and we will look for the intersections of the obtained curves.

We consider the families of segments $\{x_j\}$, $\{x'_j\}$ defined in $D_+ \cup D'_+$ and $\{y_j\}$, $\{y'_j\}$ defined in $D_- \cup D'_-$. Then, $\{\Phi(x_j)\}$, $(\{\Phi(x'_j)\})$, $\{\psi^{-1}(x_j)\}$ $(\{\psi^{-1}(x'_j)\})$. $\{\Phi(y_j)\}$ $(\{\Phi(y'_j)\})$, $\{\psi^{-1}(y_j)\}$ $(\{\psi^{-1}(y'_j)\})$, are families of arcs in $\mathcal{M}$ between the points $l^{i,1}$ and $l^{i,2}$, $l^{s,1}$ and $l^{s,2}$, $m^{i,1}$ and $m^{i,2}$, and $m^{s,1}$ and $m^{s,2}$, respectively. In a similar way $\{c_j^1\}$, $\{c_j^2\}$, $\{d_j^1\}$ and $\{d_j^2\}$ for $j \geqslant m^2$ give in $\mathcal{M}$ the following families of arcs, $\{\Phi(c_j^1)\}$, $\{\Phi(c_j^2)\}$, $\{\Phi(d_j^1)\}$, $\{\Phi(d_j^2)\}$, $\{\psi^{-1}(c_j^1)\}$, $\{\psi^{-1}(c_j^2)\}$, $\{\psi^{-1}(d_j^1)\}$ and $\{\psi^{-1}(d_j^2)\}$. The elements of these families are arcs which end in two points of β_0.

PROPOSITION 12.1. *Let* $\varepsilon_c < \varepsilon < \varepsilon_2$. *For all couples of positive integers n, m, sufficiently large, there exists a periodic orbit symmetrical with respect to* L^1 *(see Fig.* 12.1) *such that it has n binary collisions with* $x_2 > 0$, *m with* $x_2 < 0$ *and two passages by the axis* $x_2 = 0$ *in one period. The curves represented in Figure* 12.1 *are travelled twice in one period.*

Proof. The intersections $\Phi(x_j) \cap \psi^{-1}(y_k)$, $j, k \geqslant 0$ give the periodic orbits when n and m are even. For odd values of n and m, the orbits are obtained from $\Phi(x'_j) \cap \psi^{-1}(y'_k)$, $j, k > 0$. The intersections $\Phi(x_j) \cap \psi^{-1}(y'_k)$ and $\Phi(x'_k) \cap \psi^{-1}(y_j)$, $j \geqslant 0$, $k \geqslant 1$ give the other orbits.

Moreover if $n = m$, the orbit is symmetrical with respect to L^2. Then the projection on the position plane is symmetrical with respect to the x_1-axis (see Fig. 12.1c). ■

In order to clarify the following pictures as Fig. 12.1 we represent the orbits for small values of n and m.

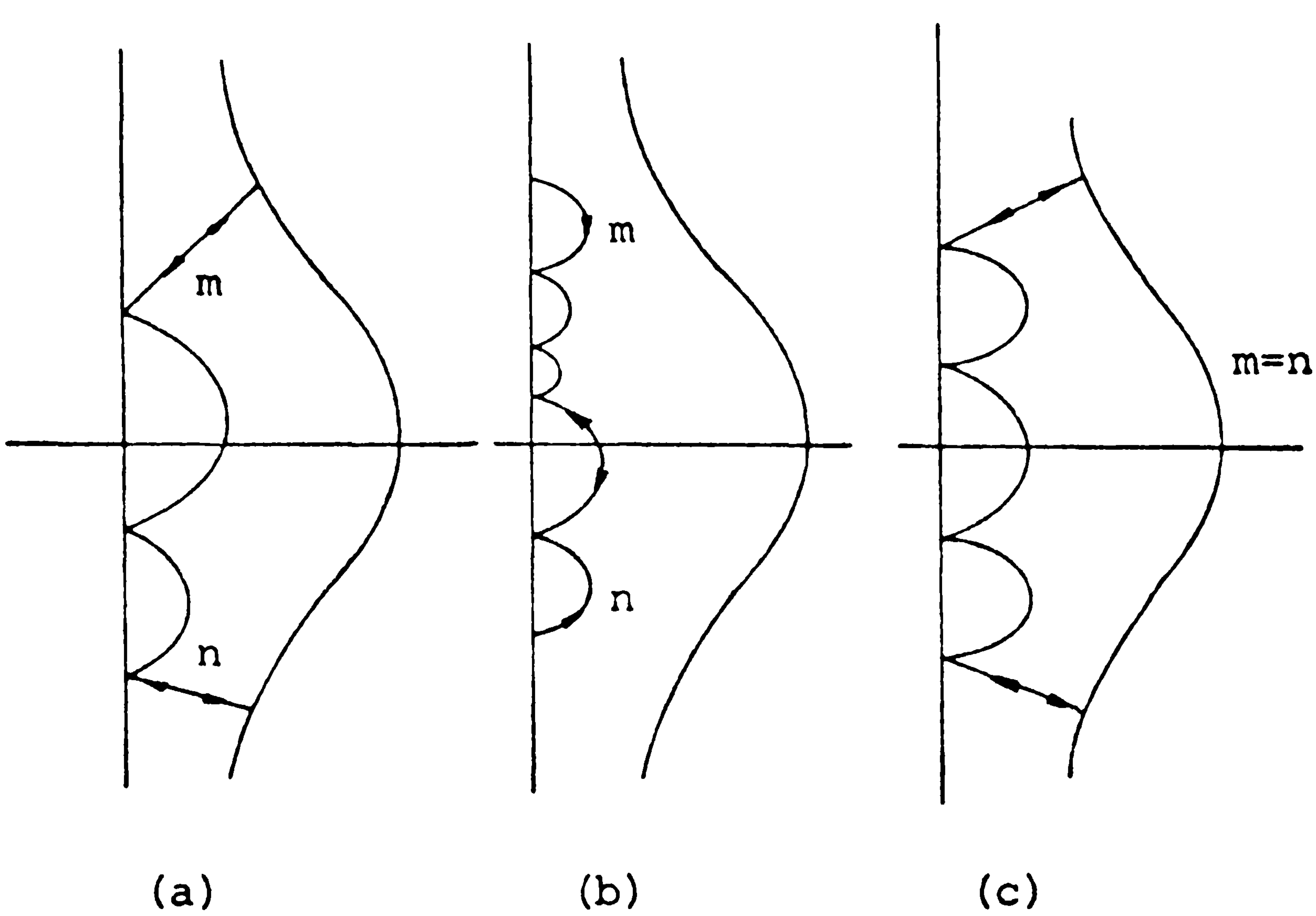

Fig. 12.1.

PROPOSITION 12.2. *Let $\varepsilon_1 < \varepsilon < 55/4$ and let n, m be two large positive integers. If $n \neq m$, there exist two periodic orbits symmetrical with respect to L^1 such that they have $n+m$ binary collisions with constant sgn(x_2) and exactly one collision with the opposite sign of x_2, as in Figures 12.2a and 12.2b. If $n = m$ they complete one period after n binary collisions (see Figure 12.2c).*

Proof. The intersections $\Phi(x_j) \cap \psi^{-1}(x_k)$ give the periodic orbits which have the $n+m$ binary collisions with $x_2 > 0$ if n and m are even. For odd values of n and m the orbits are obtained from $\Phi(x'_j) \cap \psi^{-1}(x'_k)$, and from $\Phi(x_j) \cap \psi^{-1}(x'_k)$ in other cases. The orbits with binary collisions in the semiplane $x_2 < 0$ are symmetrical of these. ■

PROPOSITION 12.3. *Let $\varepsilon < \varepsilon_1$ or $\varepsilon_2 < \varepsilon < 55/4$ and n, m positive integers sufficiently large.*

(i) *There exist two periodic orbits symmetrical with respect to L^1 such that during one period of time, m_3 crosses $n+m$ times the axis $x_2 = 0$ as in Figure 12.3a if $\varepsilon < \varepsilon_1$ and as in Figure 12.3b if $\varepsilon_2 < \varepsilon < 55/4$. If $n = m$ and $\varepsilon < \varepsilon_1$, then the orbit completes one period after n crossings of the axis $x_2 = 0$ (see Figure 12.3c).*
(ii) *There exist two periodic orbits symmetrical with respect to L^1 such that m_3 crosses m times the axis $x_2 = 0$ and n binary collisions take place with constant* sgn(x_2) *in one period (see Figure 12.4).*

Proof. The orbits of (i) are given by $\Phi(c_j^1) \cap \psi^{-1}(c_k^1)$ and $\Phi(c_j^2) \cap \psi^{-1}(c_k^2)$ if $\varepsilon < \varepsilon_1$, and by $\Phi(c_j^1) \cap \psi^{-1}(c_k^2)$ and $\Phi(c_j^2) \cap \psi^{-1}(c_k^1)$ if $\varepsilon_2 < \varepsilon < 55/4$. The part (ii) is obtained from $\Phi(x_j) \cap \psi^{-1}(c_k^2)$ and $\Phi(y_j) \cap \psi^{-1}(c_k^1)$ for every value of ε in the hypotheses. ■

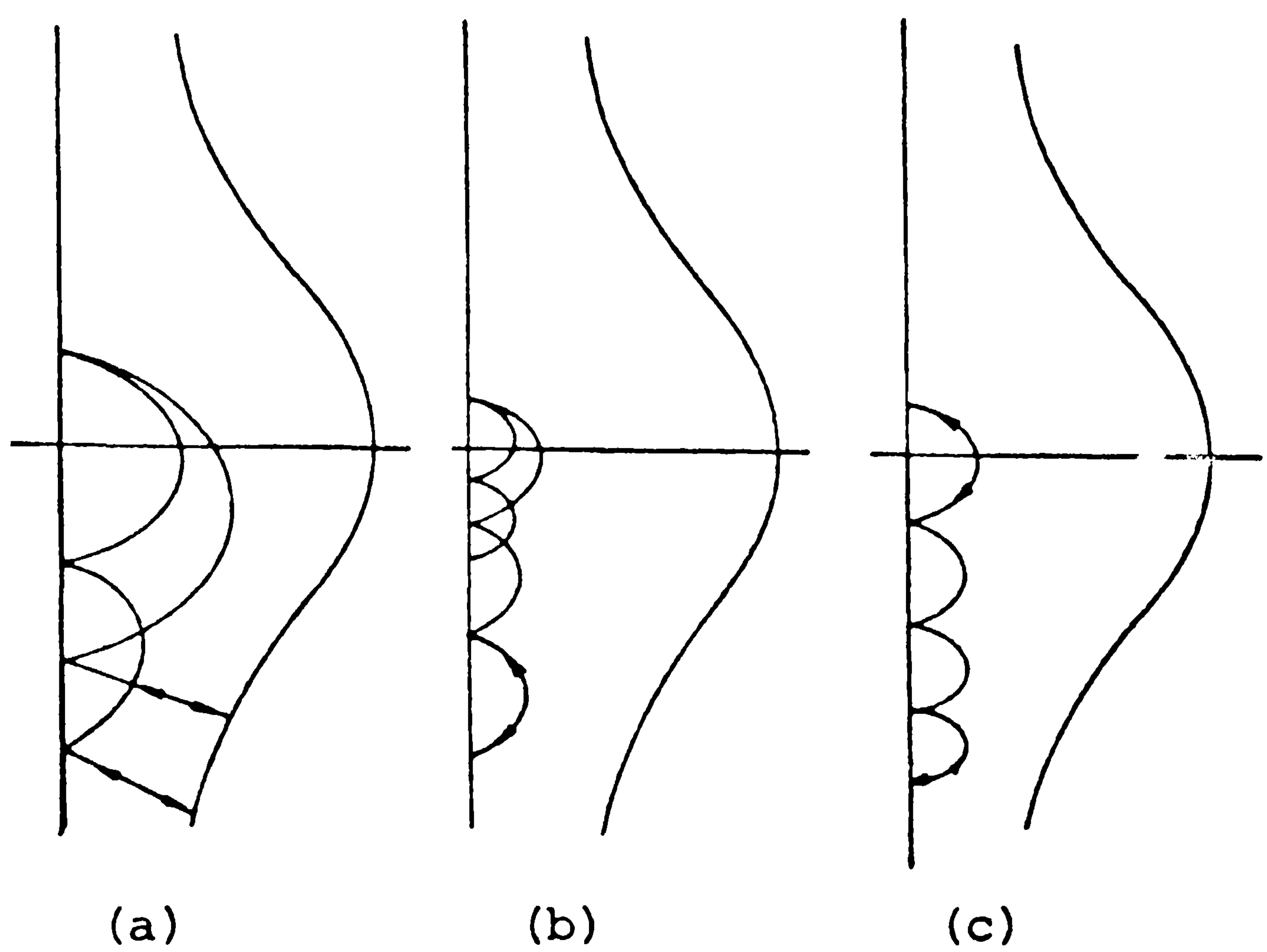

Fig. 12.2.

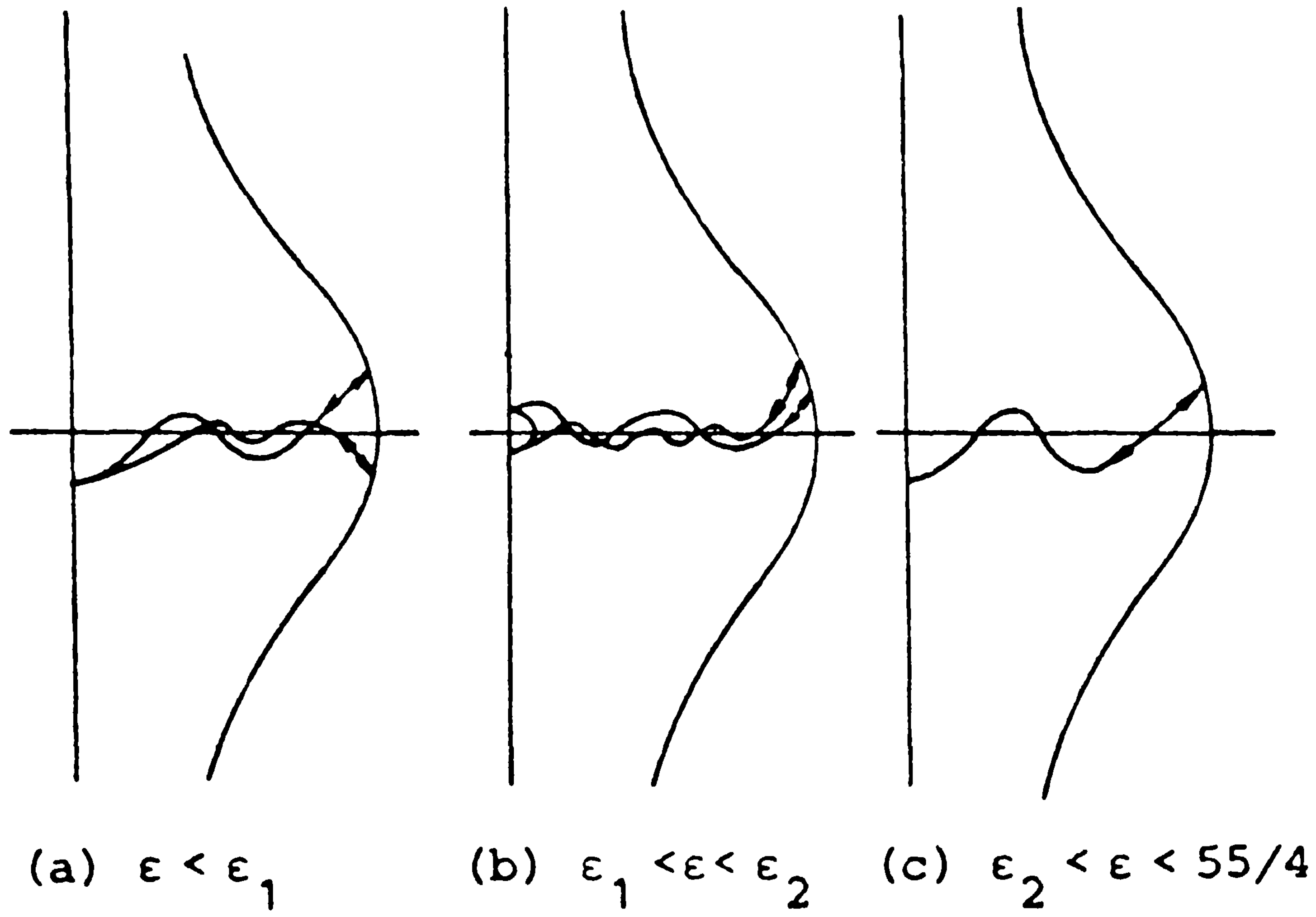

Fig. 12.3.

PROPOSITION 12.4. *Let* $\varepsilon < \varepsilon_1$ *or* $\varepsilon_2 < \varepsilon < 55/4$ *and* n, m *odd positive integers, sufficiently large.*

(i) *There exists a periodic orbit symmetrical with respect to* L^2 *such that during a period,* m_3 *crosses* $n + m$ *times the axis* $x_2 = 0$ *as in Figure 12.5a if* $\varepsilon < \varepsilon_1$, *and* $n + m + 1$ *times as in Figure 12.5b if* $\varepsilon_2 < \varepsilon < 55/4$. *In the last case there are only* $n + 1$ *crossings in one period, when* $n = m$ *(see Figure 12.5d).*

(ii) *There exists a periodic orbit symmetrical with respect to* L^2 *such that, in one*

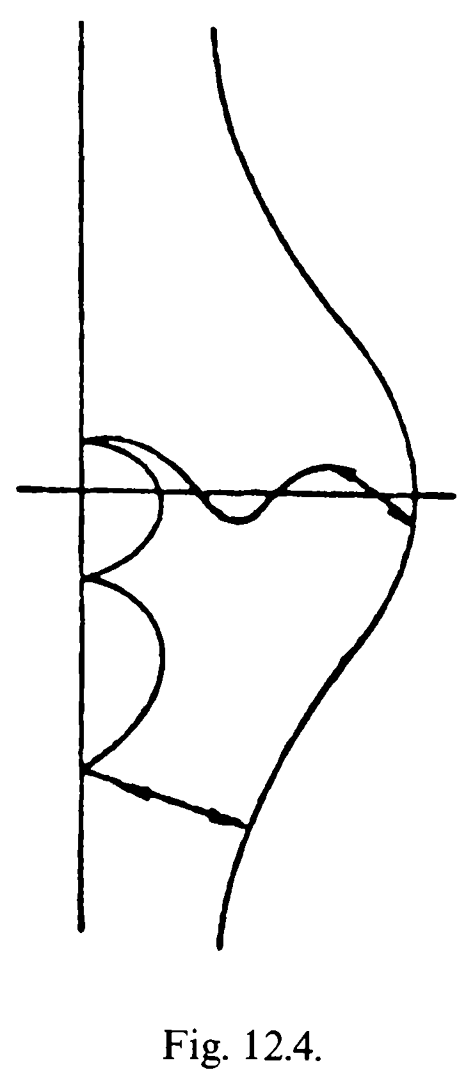

Fig. 12.4.

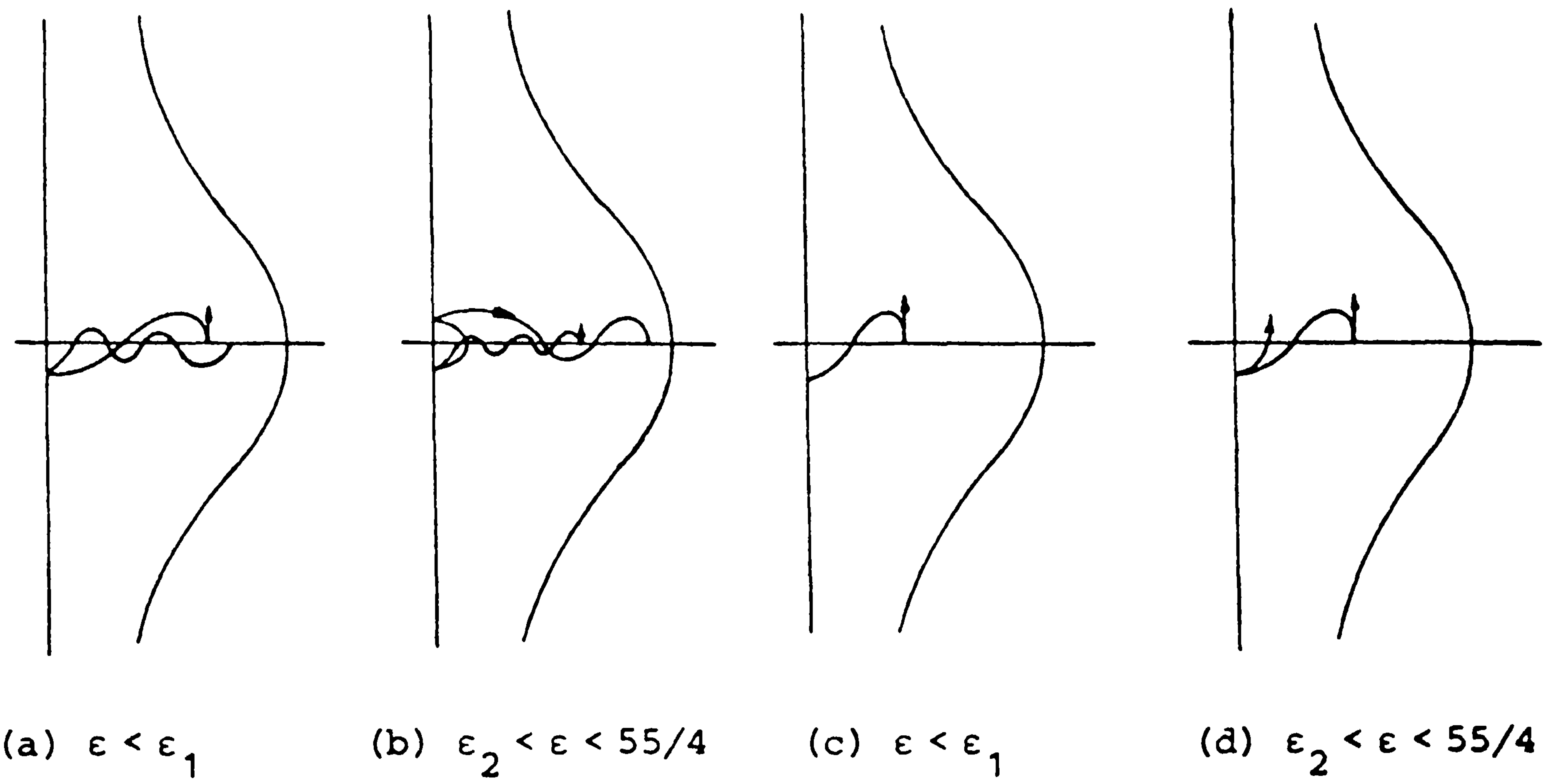

Fig. 12.5.

period, m_3 crosses 2m times the axis $x_2 = 0$ and it has n binary collisions with $x_2 > 0$ and n with $x_2 < 0$ (see Figure 12.6).

Proof. Use $\Phi(d_j^1) \cap \psi^{-1}(d_k^2)$ if $\varepsilon < \varepsilon_1$ and $\Phi(d_j^1) \cap \psi^{-1}(d_k^1)$ for $\varepsilon_2 < \varepsilon < 55/4$ in (i). For the orbits of (ii) consider $\Phi(x_j') \cap \psi^{-1}(d_k^1)$. ■

PROPOSITION 12.5. *Let $\varepsilon < \varepsilon_1$ or $\varepsilon_2 < \varepsilon < 55/4$ and n, m positive integers with different parity.*

(i) *There exists a periodic orbit symmetrical with respect to L^1 and to L^2 such that during one period, m_3 crosses $2(n+m)$ times the axis $x_2 = 0$ as in Figure 12.7a if $\varepsilon < \varepsilon_1$ and as in Figure 12.7b in the other case.*

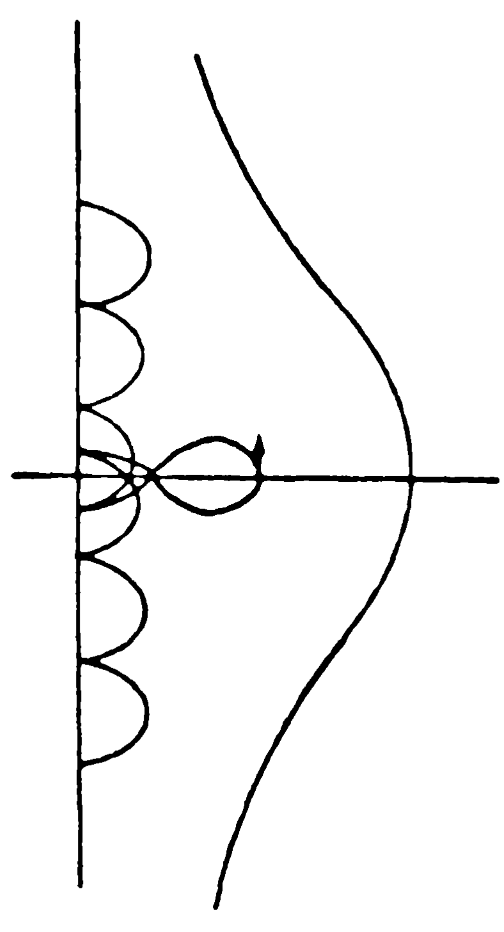

Fig. 12.6.

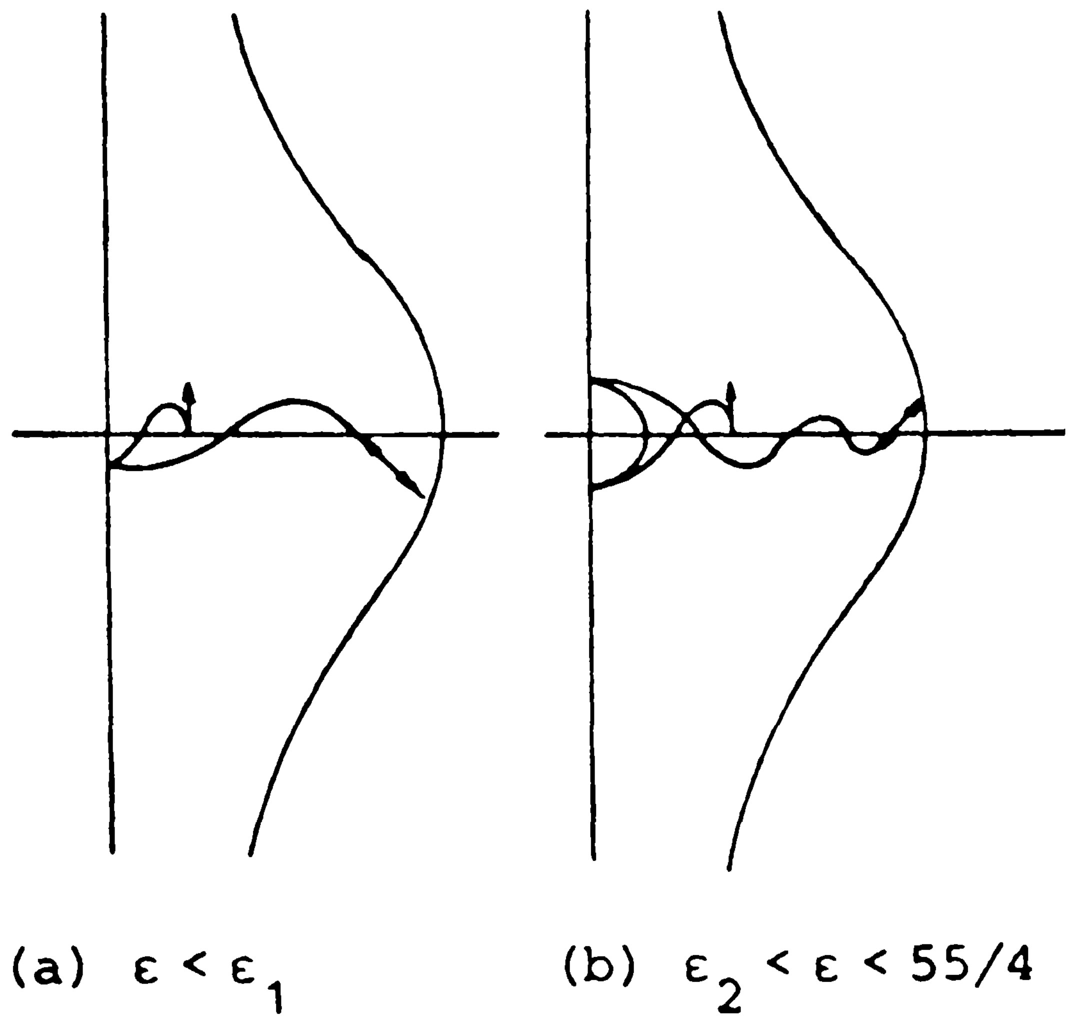

Fig. 12.7.

(ii) *There exist two periodic orbits symmetrical with respect to* L^1 *and to* L^2 *such that* m_3 *crosses m times the axis* $x_2 = 0$ *and n binary collisions with constant* $\operatorname{sgn}(x_2)$ *take place in one period (see Figure 12.8).*

Proof. The orbit of (i) is obtained from $\Phi(c_j^1) \cap \psi^{-1}(d_k^2)$ for $\varepsilon < \varepsilon_1$ and $\Phi(d_j^1) \cap \psi^{-1}(c_k^2)$ for $\varepsilon_2 < \varepsilon < 55/4$. To get the orbits of (ii) it is necessary to consider $\Phi(c_j^2) \cap \psi^{-1}(x'_k)$ and $\Phi(c_j^1) \cap \psi^{-1}(y'_k)$. ∎

Some of these periodic orbits were obtained before this work. The existence of the orbits of (i) in Propositions 12.3 and 12.4 is proved in [10].

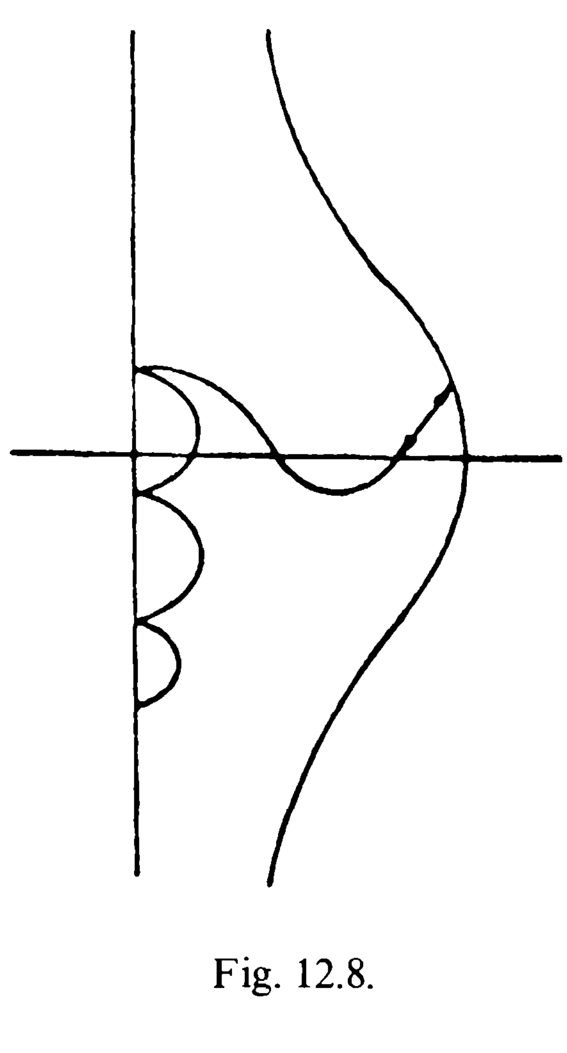

Fig. 12.8.

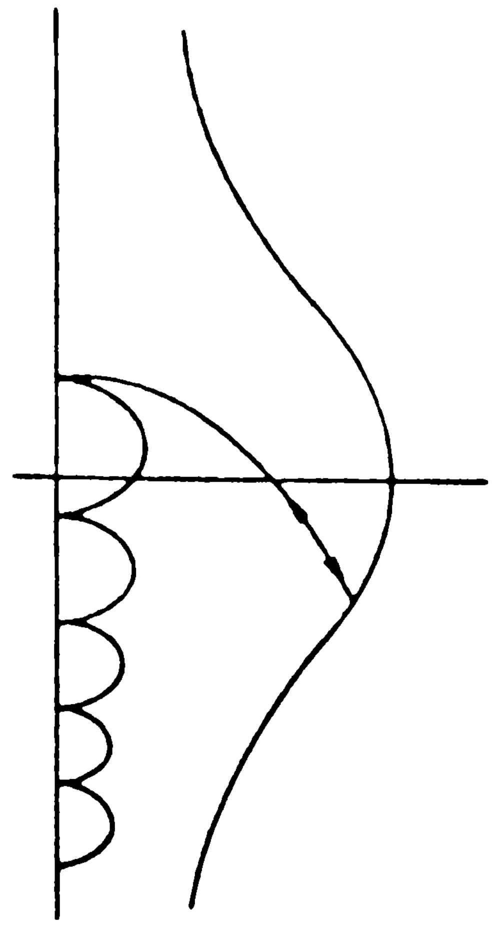

Fig. 12.9.

Finally we remark in the case $\varepsilon_1 < \varepsilon < \varepsilon_2$, the orbits which pass closely to the Euler homothetic solution escape to infinity. It means that for k sufficiently large, $\psi^{-1}(c_k^1)$ for example, is contained in the possible hyperbolic zone determined by ξ_1 (see Figure 9.1b). It is possible that for small k, $\psi^{-1}(c_k^1)$ cuts ξ_1. Let us suppose it is true for $k = 1$. In this case, $\psi^{-1}(c_1^1)$ cuts the arcs of the family $\{\Phi(x_j)\}$. This intersection gives a family of symmetrical periodic orbits as in Figure 12.9. In the same way, if $\psi^{-1}(d_k^2)$ cuts the arcs of $\{\Phi(x_j)\}$ we will obtain a new family of symmetrical periodic orbits. Broucke ([1]) computed some orbits of the last family for small number of binary collisions. This implies the existence of the family corresponding to $\psi^{-1}(c_1^1) \cap \Phi(x_j)$ for all number of binary collisions.

Acknowledgements

The authors wish to express their gratituted to Dr. Jaume Llibre for his advise concerning the last three sections in a preliminary version of this paper. The work was partly supported by CAICYT Grant number 3534/83C3 (Spain).

Appendix A: Some Numerical Computations Concerning Invariant Manifolds of the Isosceles Problem

Some dynamical results given in the work rely on the relative position of curves which are the intersection of the planes $v = 0$ or $y = 0$ (or some other suitable planes) with several invariant manifolds of equilibrium points or periodic orbits. The results, some of them known by other authors, which have been proved analytically have a partial character and say nothing about the good spiraling properties of the curves.

To give evidence enough about the nice global behaviour of several curves we have done several numerical computations. In what follows we summarize the results and we give a sample of pictures. First of all we have computed the intersection $W^{u,1}_{L^s}$ with the plane $\{y=0.5\}$. In $W^{u,1}_{L^s}$ the motion going down is faster than the motion along the triple collision manifold (compare the eigenvalues at L^s). Hence, we have computed first the intersection of $W^{u,1}_{L^s}$ with the triple collision manifold (i.e., an orbit on $r=0$), and the variational solution associated to this orbit such that the starting conditions are contained in (a linear approximation to) $W^{u,1}_{L^s}$ near L^s. In this way we obtain a narrow strip: If $P \in W^{u,1}_{L^s} \cap \{r=0\}$ and Q is the corresponding variational solution at this point we consider the segment $\overline{PR}$ where $R = P + \rho_0 Q$, ρ_0 small. When P changes, the segment generates the strip. Then, starting at points as R, forwards integration produces orbits which generate the full $W^{u,1}_{L^s}$. Checks with different values of ρ_0 are done to obtain an accurate enough description of $W^{u,1}_{L^s}$.

Now we are interested in the spiraling behavior of the curve obtained cutting $W^{u,1}_{L^s}$ with some plane $y=y_0, y_0>0$, and also in how this curve intersects the curve obtained cutting P^s_+ with the same plane. This last curve has been computed in a similar way: Starting at $y=y_1$, y_1 small, an approximation of P^s_+, restriced to $y=y_1$, can be obtained from the analytical expansion of the manifold. Then, backwards integration allows to obtain the intersection with $y=y_0$. Of course, we have done checks, as before, using several values of y_1. Usually the value $y_0=0.5$ has been used.

Figure A1 shows a sample of results for $\varepsilon=1$ and $\varepsilon=30$. In the range [0.1, 30], covered by our computations, the qualitative behavior is the same: The curves show

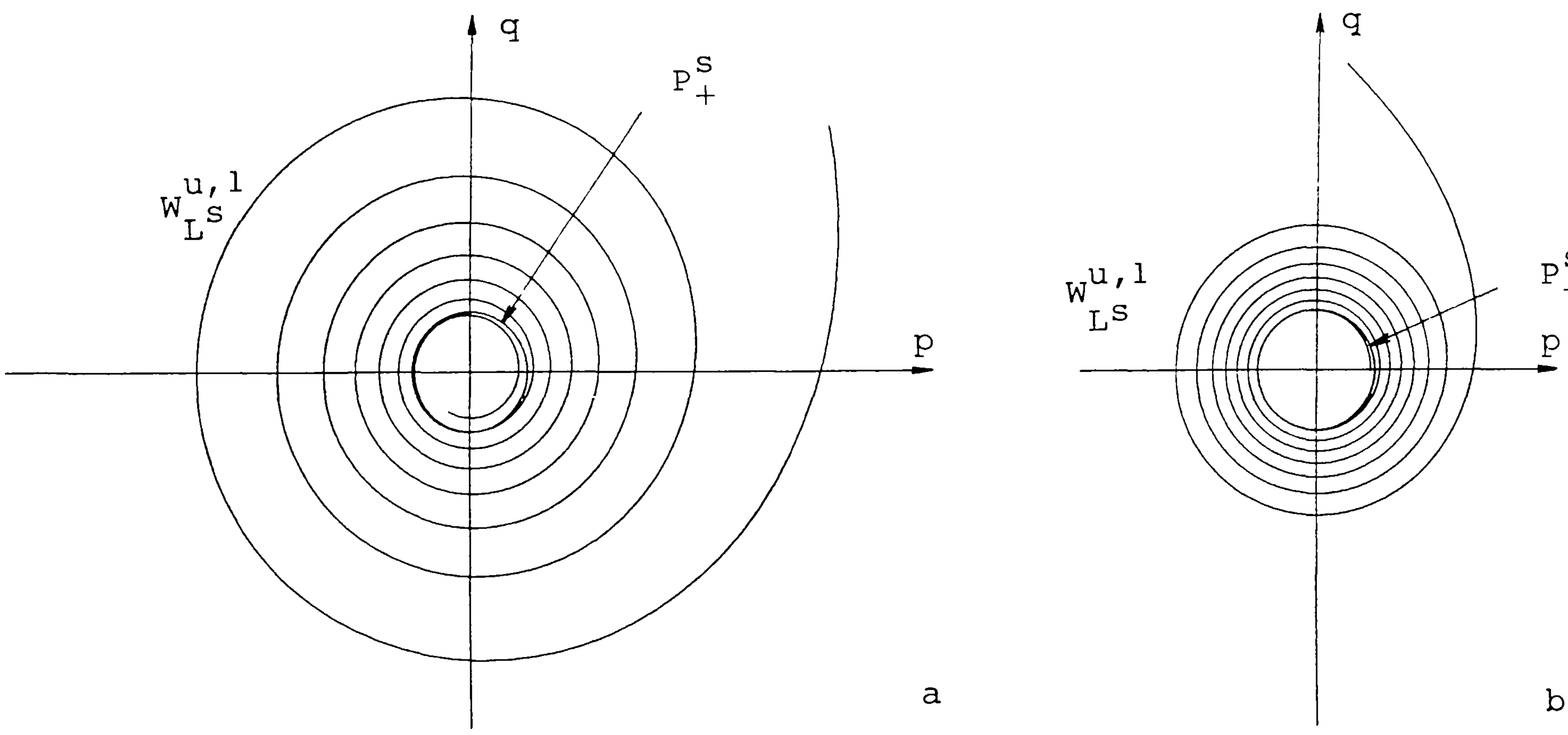

Fig. A1. The intersections $W^{u,1}_{L^s} \cap \{y=0.5\}$ and $P^s_+ \cap \{y=0.5\}$ are drawn for (a) $\varepsilon=1$; (b) $\varepsilon=30$. In (a) the coordinates are $p=(x-0.4)\cos(2\bar{\varphi})$, $q=(x-0.4)\sin(2\bar{\varphi})$ and the window is $(-0.8, 0.8)(-0,6, 0.6)$. In (b) 0.45 is used instead of 0.4. The window is $(-0.2, 0.2)(-0.3, 0.3)$.

good spiraling properties, they intersect only once P^s_+ and the spiral is compressed when ε is increased. The region where the intersection with P^s_+ is produced is displayed again suitably magnified in Fig. A2 for different values of ε. Table AI gives values of $\bar{\varphi}$ (mod π) for which the intersection with P^s_+ is produced on $\{y=0.5\}$. Table AII gives an estimation in radians of the angle α measuring the transversality of $W^{u,1}_{L^s}$ *and* P^s_+ *on* $\{y=0.5\}$.

TABLE AI

ε	0.3	1	3	10	30
$\bar{\varphi}$	−0.60295	−0.68913	−0.84888	−1.14580	−1.99100

TABLE AII

ε	0.1	0.3	1	5	10	30
$10^3\alpha$	11.1	10.8	8.4	3.5	1.2	0.5

The intersection of $W^{u,1}_{L^s}$ with $\{y=0\}$ is an infinite spiral as shown in Section 2. Figure A3 shows a portion of this spiral for $\varepsilon=1$. In this representation P.O.$_+$ lies on the origin. Furthermore, from the quantitative point of view it has been predicted in Section 2, using only the dominant terms, that between the angle $\bar{\varphi}$ and the radius x the relation $\bar{\varphi}x^3=$constant should hold. Table AIII gives some values of $\bar{\varphi}$ (measured in revolutions) and of x (measured in arbitrary units) and the product $\bar{\varphi}x^3$ for $\varepsilon=1$.

TABLE AIII

$\bar{\varphi}$	1	2	3	4	5	6	7
x	0.916	0.722	0.647	0.598	0.563	0.536	0.513
$\bar{\varphi}x^3$	0.769	0.753	0.813	0.855	0.892	0.924	0.945
$\bar{\varphi}$	8	9	10	11	12	13	14
x	0.493	0.477	0.464	0.452	0.440	0.429	0.420
$\bar{\varphi}x^3$	0.959	0.977	0.999	1.016	1.022	1.026	1.037

This gives evidence about the fact that, for a fixed $\bar{\varphi}$ (mod π) the successive values of x behave roughly as constant $\times\, n^{-1/3}$, $n\in N$, going slowly to zero.

The next computation is that of $W^{u,2}_{L^s}$ cut by the $v=0$ plane. Figure A4 shows the results for $\varepsilon=0.3$ and $\varepsilon=3$, but they are qualitatively the same throughout the

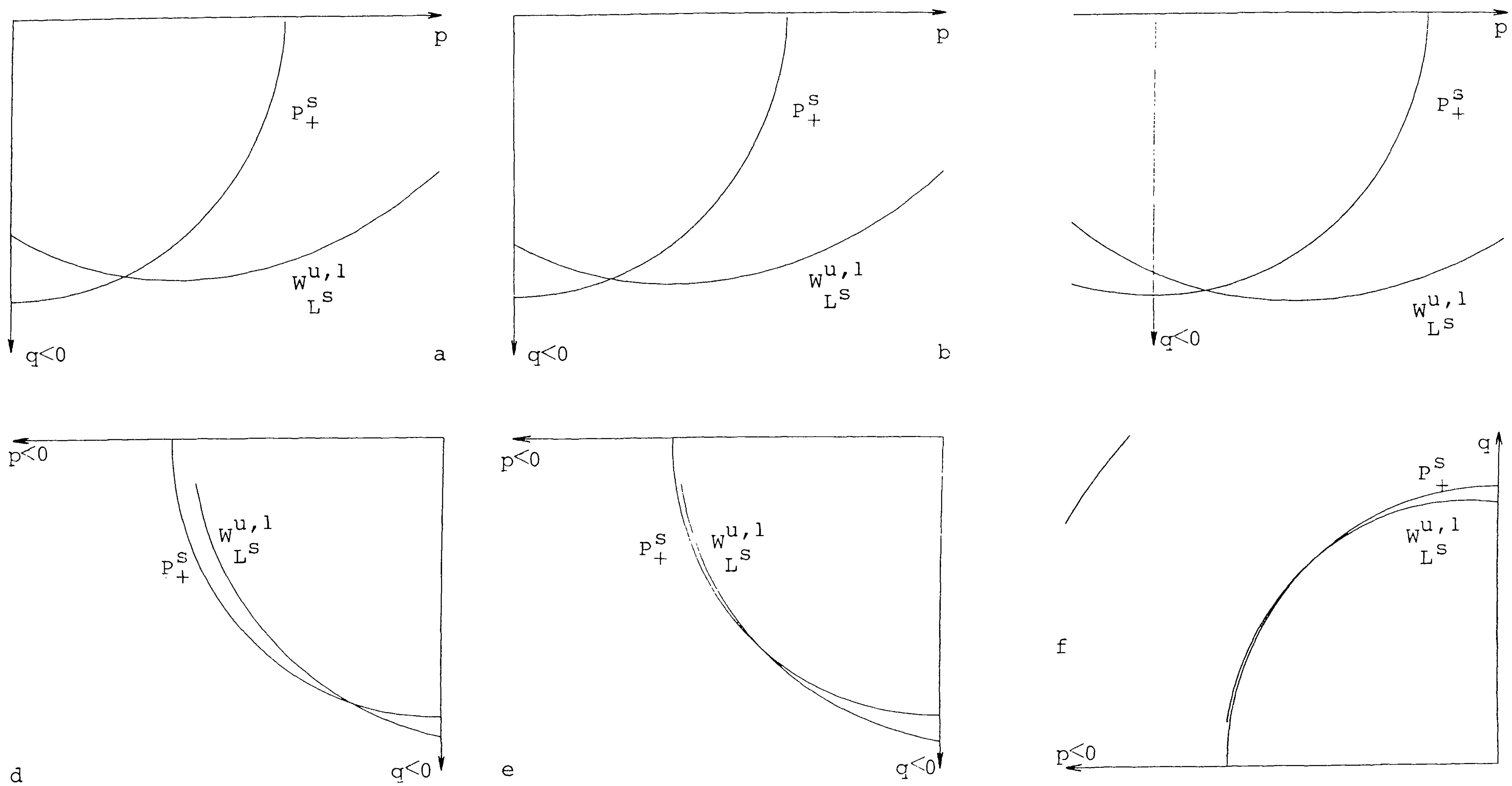

Fig. A2. A magnification of the intersections shown in A1. In all the figures the variables drawn are $p=(x-0.49)\,cos(2\bar{\varphi})$, $q=(x-0.49)\sin(2\bar{\varphi})$. The values of ε and the corresponding windows are: (a) $\varepsilon=0.1$, $(0,0.016)$ $(-0.012,0)$; (b) $\varepsilon=0.3$, $(0,0.016)$ $(-0.012,0)$; (c) $\varepsilon=1$, $(-0.003,0.013)$ $(-0.012,0)$; (d) $\varepsilon=5$. $(-0.016,0)$ $(-0.012,0)$; (e) $\varepsilon=10$, $(-0.016,0)$ $(-0.012,0)$; (f) $\varepsilon=30$, $(-0.016,0)$ $(0,0.012)$.

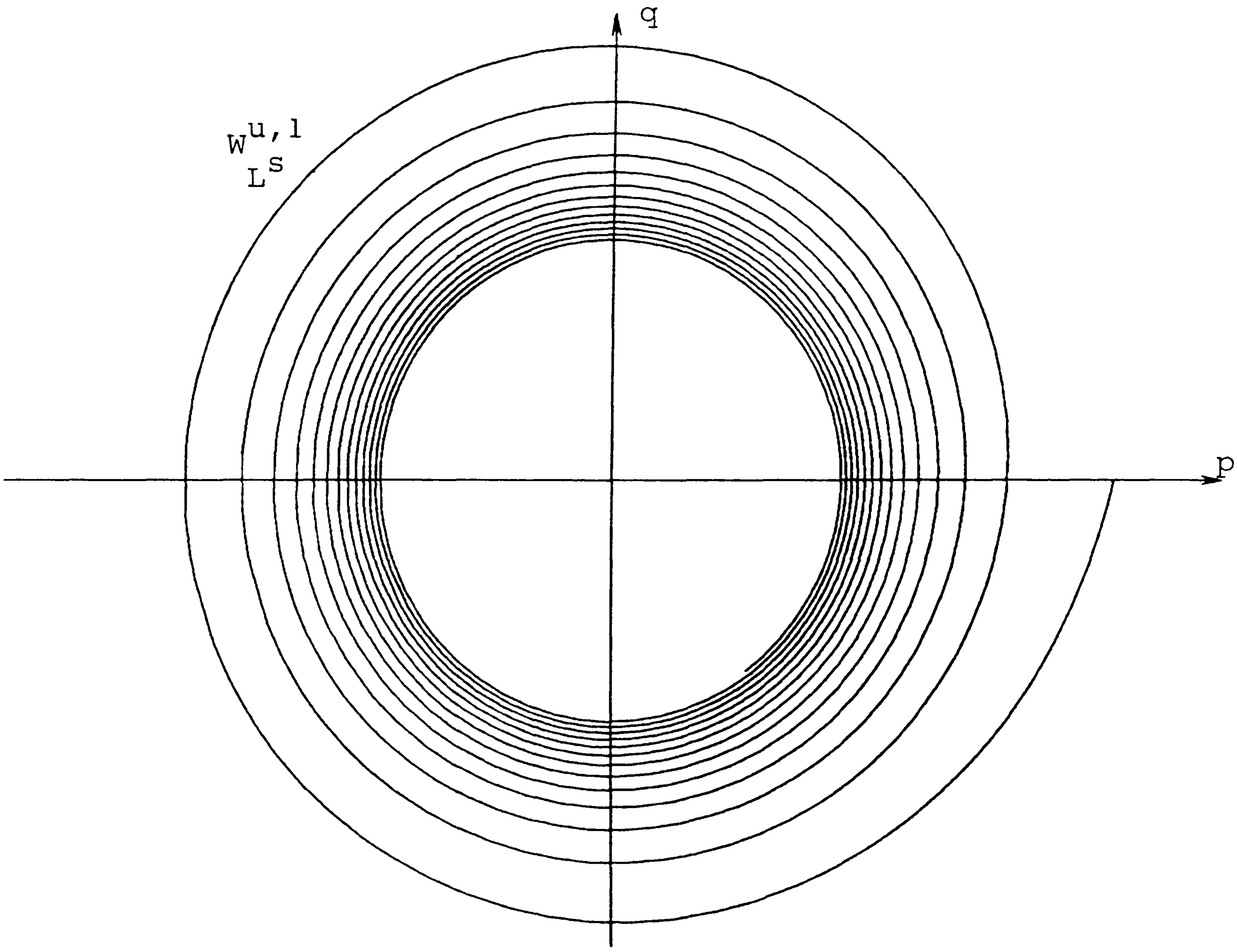

Fig. A3. The intersection $W^{u,1}_{L^s} \cap \{y=0\}$ is given for $\varepsilon = 1$. The variables are $p = x\cos(2\bar{\varphi})$, $q = x\sin(2\bar{\varphi})$. Window: $(-1.28,\ 1.28)(-0.96, 0.96)$.

range of our computations $[0.1, 10]$. To detect the nice spiraling behavior we have drawn also the symmetrical curves. As it should be the spiral has a geometric behaviour and it compresses faster the greater the value of ε. As we know, for $\varepsilon = 55/4$ there is no spiral and the curve enters directly to the origin. For the sake of completeness in the case $\varepsilon = 3$ we have included the intersection with $v = 0$ of $W^{u,1}_{L^s}$ and the symmetrical curves. As stated in Section 7 these curves are broken and they are made of an infinity of arcs. The successive arcs get strongly compressed because they are related to Table AIII. Furthermore the starting point of each one of the arcs (which end on the curve $\dot{v} = 0$) is only in the region $w < 0$ for a finite number of arcs.

The last set of computations refers to the real behaviour of the regions given in Figure 9.1 entering in the symbolic dynamics description. In this figure there appear the arcs ξ_i, $i = 1, 2, 3, 4$, as defined in Section 8 and four more arcs joining the points $l^{i,1}$, and $m^{i,1}$, $l^{i,2}$ and $m^{i,2}$, $l^{s,2}$ and $m^{s,2}$, $l^{s,1}$ and $m^{s,1}$. We have taken the last four arcs as $\Phi(c_1^1)$, $\Phi(c_1^2)$, $\Phi^{-1}(c_1^1)$ and $\Phi^{-1}(c_1^2)$ (respectively) and are denoted by η_1, η_2, η_3 and η_4 (respectively). These curves are suitable for our purposes because they are already continuous. Hence, using the terminology of Section 9 we have $m^2 = 2$. The

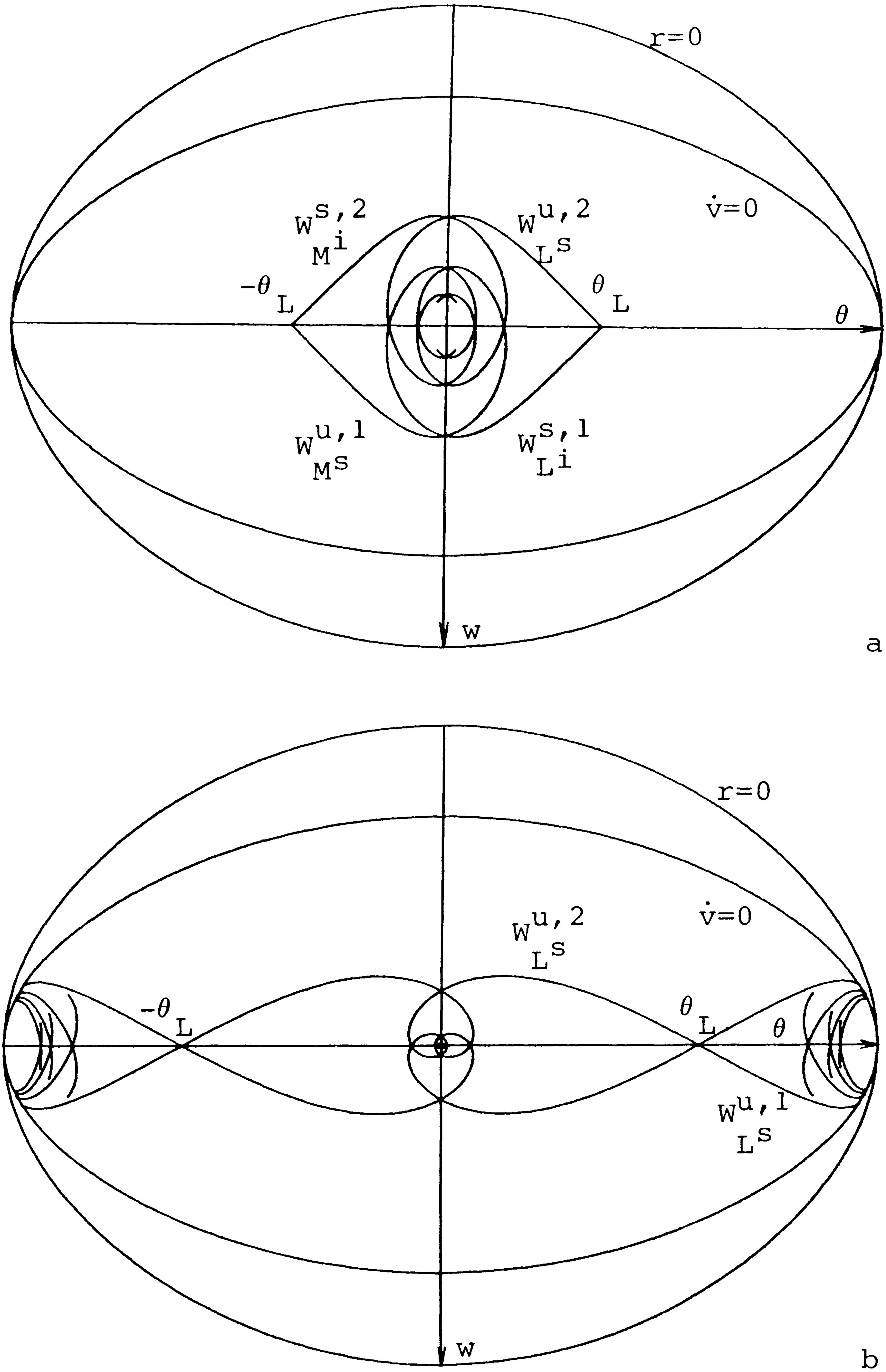

Fig. A4. (a) Intersection with the plane $v = 0$ of the branch $W^{u,2}_{L^s}$ and the symmetrical ones for $\varepsilon = 0.3$; (b) *Idem* for $\varepsilon = 3$, including the branch $W^{u,1}_{L^s}$ and the symmetrical ones.

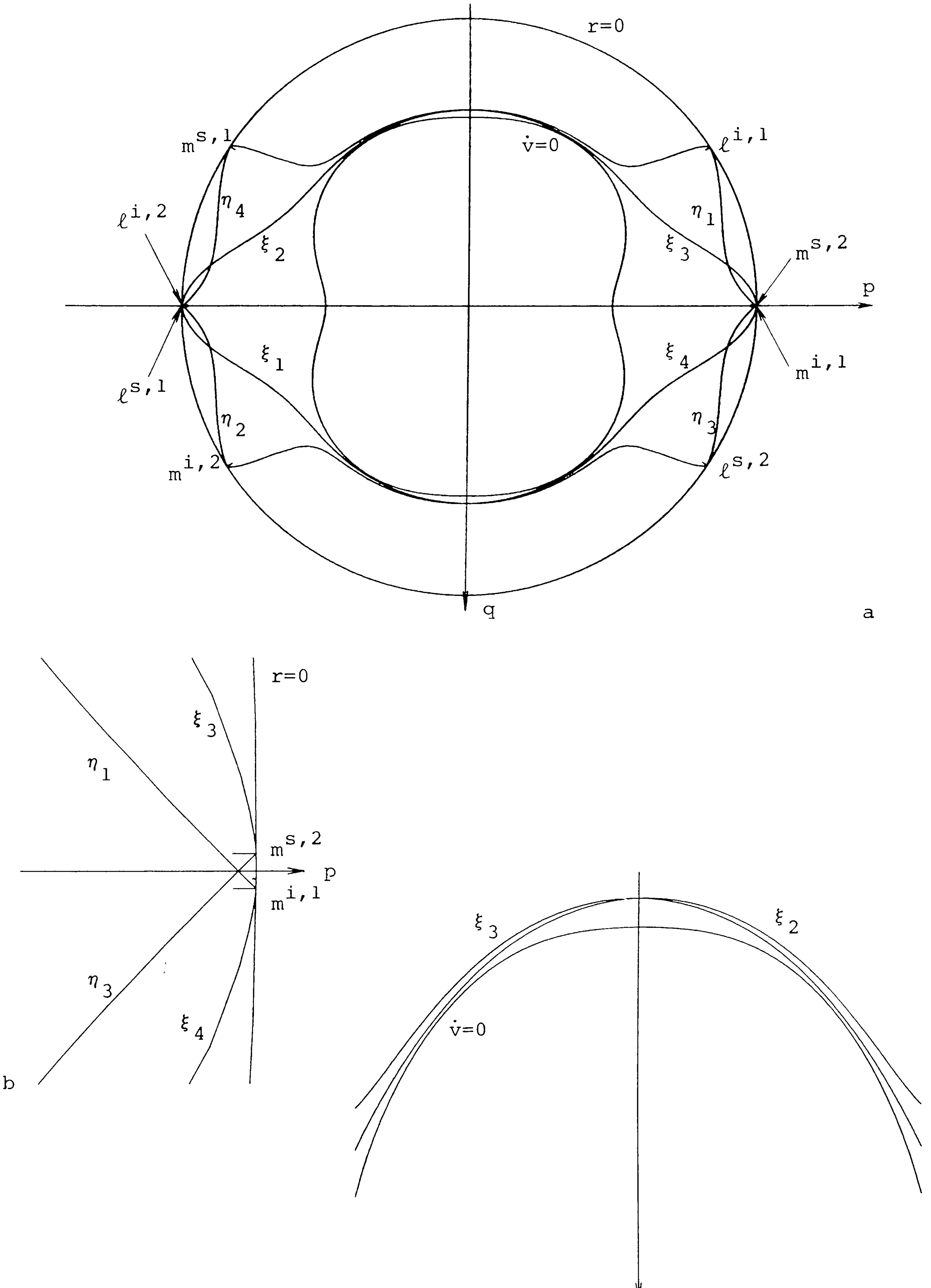

Fig. A5. The curves ξ_i and η_i, $i = 1, 2, 3, 4$ in the plane $v = 0$ for $\varepsilon = 0.3$. Relative position with respect to the curves $r = 0$ and $\dot{v} = 0$. Small marks denote the points $l^{\star,\star}$ and $m^{\star,\star}$. The coordinates used are $p = \rho \cos(\psi)$, $q = \rho \sin(\psi)$, where $\rho = 1 - \pi^{-1} \arctan(2.5r)$, $\psi = \arctan(w/\theta)$. (a) The full figure; (b) and (c) two magnifications with windows $(0.9, 1.01)(-0.045, 0.045)$ and $(-0.5, 0.5)(0.325, 0.7)$, respectively.

extreme points of the arcs ξ_i, η_i, $i = 1, 2, 3, 4$ are the points of the type $l^{\star,\star}$ and $m^{\star,\star}$. Table AIV gives some values of $l^{s,1}$ and $l^{s,2}$ for different values of ε. The other points are obtained by symmetry.

TABLE AIV

	ε	0.1	0.3	1	3	10	30
$l^{s,1}$	θ	−1.5707462	−1.5707796	−1.5673631	−1.4897127	−1.2822462	−1.1529981
	w	0.0100106	0.0057763	−0.0828644	−0.4024794	−0.7544038	−0.9008319
$l^{s,2}$	θ	1.5006676	1.2365198	0.5099078	−0.0528583	−0.4864930	−0.7408949
	w	0.3743560	0.8100443	1.3212062	1.4132256	1.3296450	1.2147961

Figures A5 to A7 show the curves ξ_i, η_i, $i = 1, 2, 3, 4$ as well as the curves $r = 0$ and $\dot{v} = 0$ all of them in the $v = 0$ plane, for $\varepsilon = 0.3$, 1 and 3, showing the three different cases. In Fig. A5 we see that the ξ_i curves are near the $\dot{v} = 0$ curve, but they are already continuous, in agreement with the Conjecture in Section 8. In Fig. A6 it is seen that the curves ξ_1 and η_2 intersect in two points (and a similar thing is true for the symmetrical pairs). Using only continuity reasons it is not strictly true that they should intersect as displayed in Fig. 9.1, but this does not affect the definition of regions A_j. In a similar way, in Fig. A7 the curves ξ_1 and η_2 intersect in three points. For continuity reasons they should intersect at least in one point. However, the number of extra intersections depends on ε and the two extra points dissappear for ε slightly greater than 3.

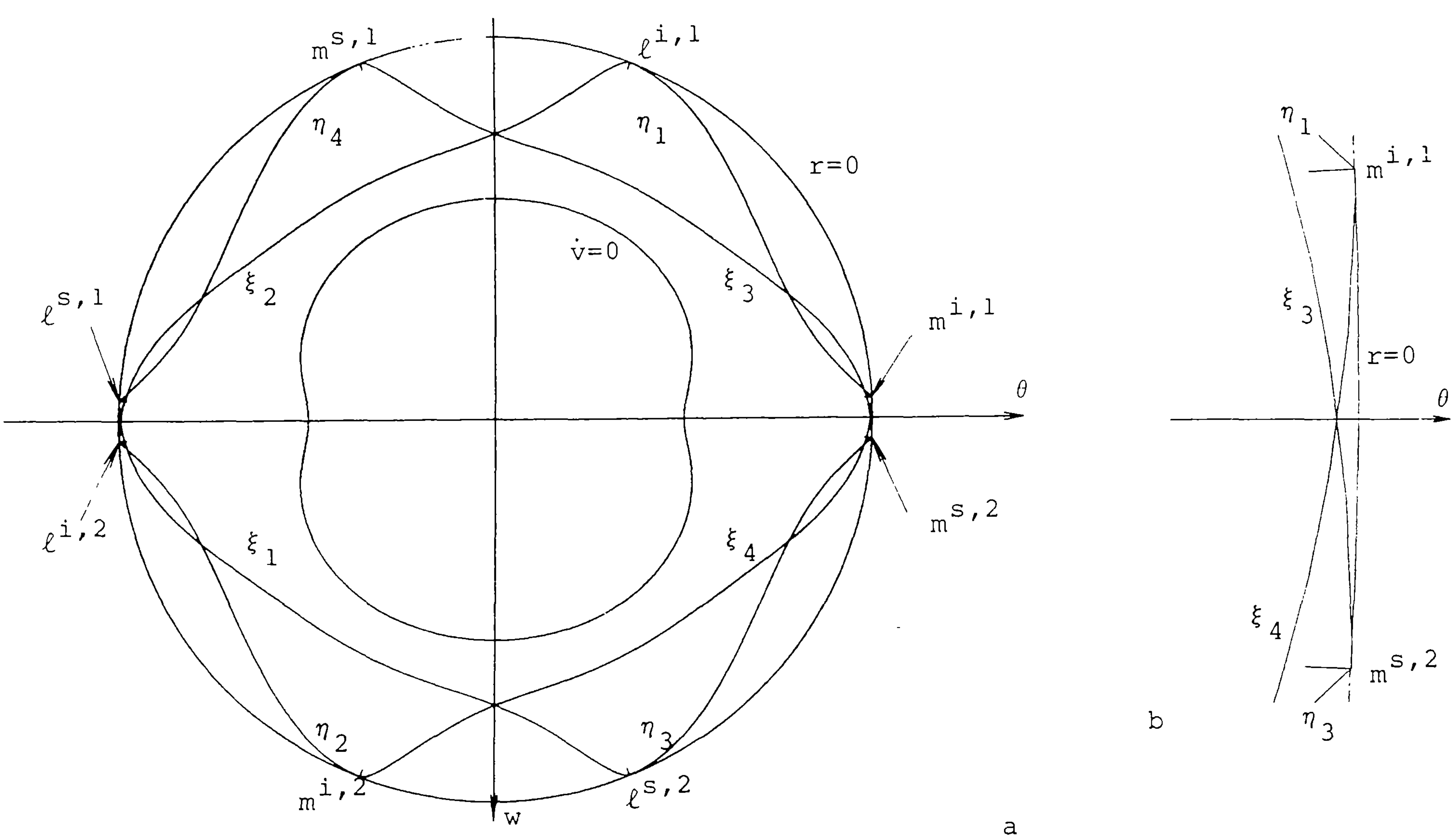

Fig. A6. (a) Same as Figure A5(a) for $\varepsilon = 1$; (b) A magnification with window $(0.96, 1.02)(-0.06, 0.06)$.

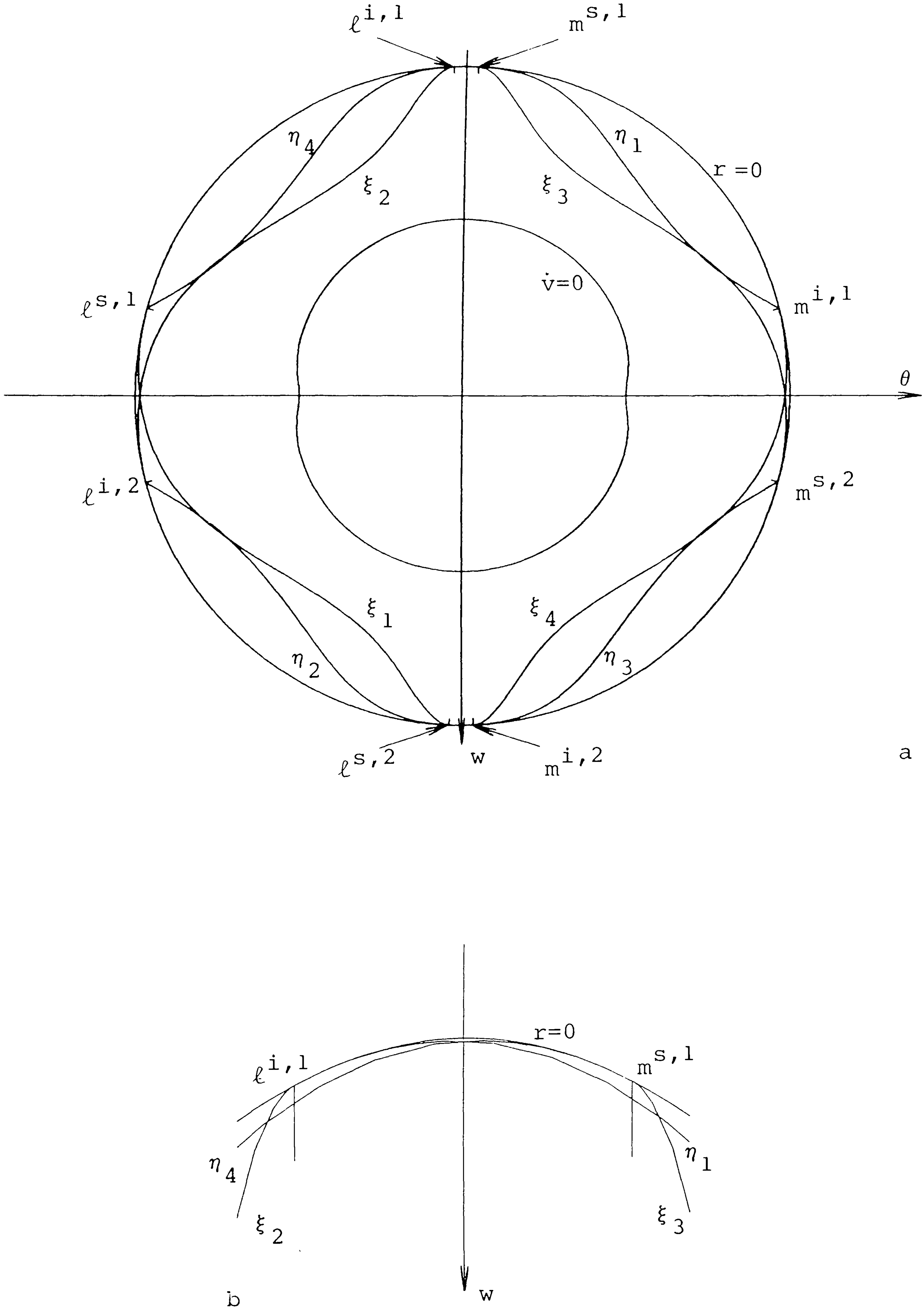

Fig. A7. (a) Same as Figure A5(a) for $\varepsilon = 3$; (b) A magnification with window $(-0.05, 0.05)\,(0.996, 1.0015)$.

Appendix B: The Fictitious Orbits s_j, $j = 1, 2, 3, 4$.

The global flow of the planar isosceles three-body problem gives rise, after adding the boundaries at triple collision and at infinity, to a 3-dimensional closed ball taking out two open 3-dimensional balls and four lines s_j, $j = 1, 2, 3, 4$, as displayed in Fig. 4.1. The line s_1 goes from one of the points deleted from the 2-dimensional sphere corresponding to triple collision, a point related to an infinitely close binary, to one of the points deleted from one of the 2-dimensional spheres at infinity, a point related to hyperbolic motion of the binary with respect to the third body with infinite escape velocity. The lines s_j, $j = 2, 3, 4$, are obtained by symmetry.

The purpose of this Appendix is to explain the behaviour of the flow near those lines and to see that they are natural boundaries that can be added to the global flow to get, as fully compactified phase space, a 3-dimensional closed ball minus two 2-dimensional open balls. Physically those lines can be seen as orbits between infinity and triple collision travelled at infinite velocity. The two equal masses are at distance zero. Hence the energy of the binary formed by them is $-\infty$ and therefore the energy of the system formed by the binary and the third body is $+\infty$.

Before going into the details we make a remark on the limiting case. Let $-h$, $h > 0$, be the energy of the binary $-h = \dot{x}_1^2/4 - 1/x_1$. Then the period of the binary is $(\pi/2)h^{-3/2}$. The remaining energy gives $(\varepsilon/(2+\varepsilon))\dot{x}_2^2 - 4\varepsilon\,(x_1^2 + 4x_2^2)^{-1/2} = h - 1$ and hence, when x_2 goes to infinity $\dot{x}_{2,\infty} = ((2+\varepsilon)(h-1)/\varepsilon)^{1/2}$.

In one oscillation of the binary, i.e., between two consecutive binary collisions, the distance between the binary and the third body, for big values of x_2, increases by an amount $O(h^{-1})$. To slow down the motion in order to detect the oscillations of the binary, for instance, scaling time to reach a finite limiting period, implies that the escape of the binary from the third particle is stopped when h goes to infinity.

As we are interested in motion near a rather close binary we introduce suitable variables in a neighborhood of the collision which can be used both in the regions near infinity and near triple collision.

Let x, y, ξ, η be the variables introduced in (2.1) to describe the motion near infinity and κ the independent variable used there. We also use the variable r as defined in (1.4) and the constant $d = \varepsilon(4(2+\varepsilon)^{1/3})^{-1}$.

We define the variables X, Y, $\hat{\xi}$ by

$$X = x\sqrt{\frac{4dr}{1 + r + 4drx^2}},$$

$$Y = y\sqrt{\frac{4dr}{1 + r + 4dry^2}}, \tag{B.1}$$

$$\hat{\xi} = \xi\sqrt{\frac{1 + r}{r(1 - Y^2)}},$$

and the independent variable $\hat{\kappa}$ by $d\hat{\kappa} = (r(1-Y^2)/(1+r))^{1/2}\, d\kappa$. We denote again by $'$ the differentiation with respect to $\hat{\kappa}$. Then the following equations of motion are obtained

$$
\begin{aligned}
X' &= -\frac{(2+\varepsilon)^{1/2}}{4\varepsilon^{3/2}} X^3 Y(1-Y^2)\hat{\xi}^2 + \frac{1}{2\rho^3} X^7(1-X^2)(1-Y^2)^2\hat{\xi}^3\eta + \\
&\quad + \frac{2\varepsilon^{3/2}}{(2+\varepsilon)^{1/2}\rho^3} X^5(1-X^2)^2 Y(1-Y^2)\hat{\xi}^2, \\
Y' &= -\frac{(2+\varepsilon)^{1/2}}{4\varepsilon^{3/2}} X^4(1-X^2)^{-2}(1-Y^2)^3\hat{\xi}^2(1+u^2)^{-3/2} + \\
&\quad + \frac{1}{2\rho^3} X^6 Y(1-Y^2)^3\hat{\xi}^3\eta + \frac{2\varepsilon^{3/2}}{(2+\varepsilon)^{1/2}\rho^3} X^4(1-X^2)Y^2(1-Y^2)^2\hat{\xi}^2, \\
\hat{\xi}' &= \eta - \frac{(2+\varepsilon)^{1/2}}{4\varepsilon^{3/2}} X^4(1-X^2)^{-2} Y(1-Y^2)^2\hat{\xi}^3(1+u^2)^{-3/2} - \\
&\quad - \frac{1}{2\rho^3} X^6(1-Y^2)^3\hat{\xi}^4\eta - \frac{2\varepsilon^{3/2}}{(2+\varepsilon)^{1/2}\rho^3} X^4(1-X^2)Y(1-Y^2)^2\hat{\xi}^3, \\
\eta' &= -\hat{\xi}[Y^2 + (1-X^2/\rho)(1-Y^2)] + X^2(1-X^2)^{-1}(1-Y^2)\hat{\xi}(1+u^2)^{-3/2},
\end{aligned}
\tag{B.2}
$$

where

$$
\rho^2 = \tfrac{1}{2}X^4(1-Y^2)^2\hat{\xi}^4 + (8\varepsilon^3/(2+\varepsilon))(1-X^2)^2
$$

and

$$
u = \frac{1}{4\varepsilon} X^2(1-X^2)^{-1}(1-Y^2)\hat{\xi}^2.
$$

The variable r is obtained from

$$
(1+r)^2 = \tfrac{1}{2}\hat{\xi}^4(1-Y^2)^2 + (8\varepsilon^3/(2+\varepsilon))X^{-4}(1-X^2)^2, \tag{B.3}
$$

and the energy relation is written as

$$
\begin{aligned}
&\eta^2 + \hat{\xi}^2[Y^2 + (1-X^2/\rho)(1-Y^2)] = \\
&\quad 1 + X^2(1-X^2)^{-1}(1-Y^2)\hat{\xi}^2 \\
&\quad [1 + \tfrac{1}{16}X^4(1-X^2)^{-2}(1-Y^2)^2\hat{\xi}^4]^{-1/2}.
\end{aligned}
\tag{B.4}
$$

If $X < X_1 < 1$ then the equations (B.2) are regular. The condition $X < X_1$ is equivalent to the condition that the variable θ, defined in (1.4), is bounded from below by some positive constant. We make the hypothesis $X < X_1 < 1$ from now on. Later on we shall see that in the region considered this is satisfied. We are interested in very fast escape motions, i.e., big values of y and therefore, according to (B.1), in values of Y close to 1. Let $\bar{Y} = 1 - Y$. From (B.4) we obtain that $|\eta|$, $|\hat{\xi}|$ are bounded by expressions of the type $1 + O(\bar{Y})$. It is easely seen that the equations of motion can be rewritten in the form

$$X' = \frac{(2+\varepsilon)^{1/2}}{2\varepsilon^{3/2}} X^3 \bar{Y} \hat{\xi}^2 \left[-1 + \left(\frac{2+\varepsilon}{8\varepsilon^3} \right)^{1/2} X^2 (1 - X^2)^{-1} + O(\bar{Y}) \right],$$

$$\bar{Y}' = -\frac{2+\varepsilon}{2\sqrt{2\varepsilon^3}} X^4 (1 - X^2)^{-2} \bar{Y}^2 \hat{\xi}^2 (1 + O(\bar{Y})), \tag{B.5}$$

$$\hat{\xi}' = \eta + O(\bar{Y}^2),$$

$$\eta' = -\hat{\xi} + O(\bar{Y}).$$

The triple collision manifold is obtained putting $r = 0$ in (B.3). If furthermore $Y = 1$ then a value $X = X_0$ is obtained and for this value one has $((2+\varepsilon)/(8\varepsilon^3))^{1/2} X^2 (1 - X^2)^{-1} = 1$. The region of interest is contained between X close to X_0 (triple collision manifold) and $X = 0$ (infinity). Hence, as said before, there is $X_1 < 1$ such that $X < X_1$. Let ψ the argument of $\hat{\xi} + \sqrt{-1}\eta$ and define a radius R as Y^{-1}. Figure

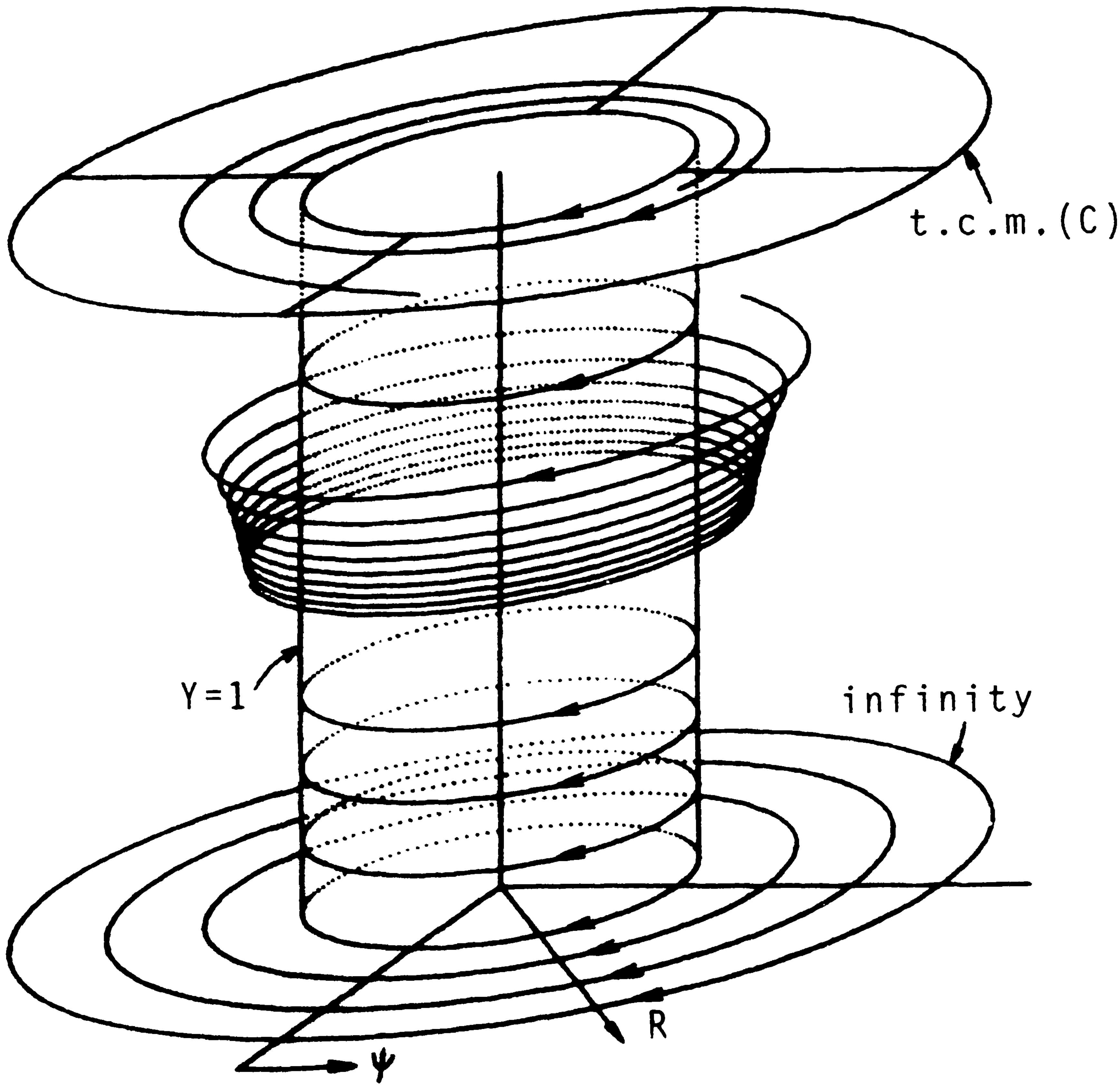

Fig. B1.

B.1 displays the phase space for Y close to 1, where R and ψ have been used as polar coordinates and X as a vertical one.

For $\bar{Y}=0$ one has $X'=\bar{Y}'=0$, $\hat{\xi}'=\eta$, $\eta'=-\hat{\xi}$ and we obtain a cylinder foliated by periodic orbits each one for a different value of X. If $X=0$ one also has $X'=\bar{Y}'=0$, $\hat{\xi}'=\eta$, $\eta'=-\hat{\xi}$ but now the value of X remains 0 for all the orbits and Y takes any value in a neighbourhood of 1. We obtain an annulus foliated again by periodic orbits.

The fact that $\bar{Y}'$ is non positive for X close to X_0 and in fact it is negative unless $\hat{\xi}=0$ (it is zero for $\hat{\xi}=0$ due to the unavoidable scaling of time to regularize binary collisions) shows a spiraling behavior on the triple collision manifold towards $X=X_0$, $Y=1$. This is a way of rewritting the spiraling along the horns in Fig. 1.3.

The cylindrical annulus limited by the triple collision manifold and infinity with vertical walls $\bar{Y}=0$ and $\bar{Y}=\bar{Y}_0$, $\bar{Y}_0$ small enough, is positively invariant according to the equations (B.5). If $X<X_0-O(\bar{Y})$ we have $X'<0$ and the flow approaches the cylinder $Y=1$ going downwards. Only in a thin neighbourhood of the triple collision manifold the variable X goes up and down following closely the form of the triple collision manifold in these variables. We claim that any orbit entering the cylindrical annulus goes down to infinity ending in one of the periodic orbits of the bottom annulus. To prove the claim it is enough to remark that this orbit can not go to one of the periodic orbits which foliate the cylinder $Y=1$. This would imply that a physical orbit (i.e. coming from some finite values of x_1, x_2, $\dot{x}_1$, $\dot{x}_2$) would reach a finite value of $x_2\neq 0$ with an infinite value of $\dot{x}_2$ which is an absurdity.

Further information is given by the Poincaré map through $\psi=\pi/2$ (recall that due to the regularization this means to consider the values of X, $\bar{Y}$ after two successive collisions). Let X, $\bar{Y}$ be the initial point and let X_n, $\bar{Y}_n$ be the image under the Poincaré map. We can easily obtain from (B.5) the expression

$$\begin{aligned} X_n &= X-\pi\frac{(2+\varepsilon)^{1/2}}{2\varepsilon^{3/2}}X^3\bar{Y}\left[1-\left(\frac{2+\varepsilon}{8\varepsilon^3}\right)^{1/2}X^2(1-X^2)^{-1}+O(\bar{Y})\right],\\ \bar{Y}_n &= \bar{Y}-\pi\frac{2+\varepsilon}{2\sqrt{2\varepsilon^3}}X^4(1-X^2)^{-2}\bar{Y}^2(1+O(\bar{Y})). \end{aligned} \tag{B.6}$$

The map (B.6) can be seen as the time one flow of a vector field in the X, $\bar{Y}$ variables. Figure B.2 shows the orbits of that vector field.

Finally we can shrink the cylinder $Y=1$ to a line. In fact, going back to the variable ξ or x_1 we get $\xi=x_1=0$ because $Y=1$. This is precisely the line s_1. Using again as independent variable the physical time t it is obvious that the line is travelled at an infinite velocity because

$$\frac{\mathrm{d}X}{\mathrm{d}t}=\frac{(2+\varepsilon)^{1/2}}{4\varepsilon^{3/2}}\rho^3(\rho^2-X^2)^{-3/2}X^3(1-Y^2)^{-1/2}$$

$$\left[-1+\left(\frac{2+\varepsilon}{8\varepsilon^3}\right)^{1/2}X^2(1-X^2)^{-1}+O(\bar{Y})\right].$$

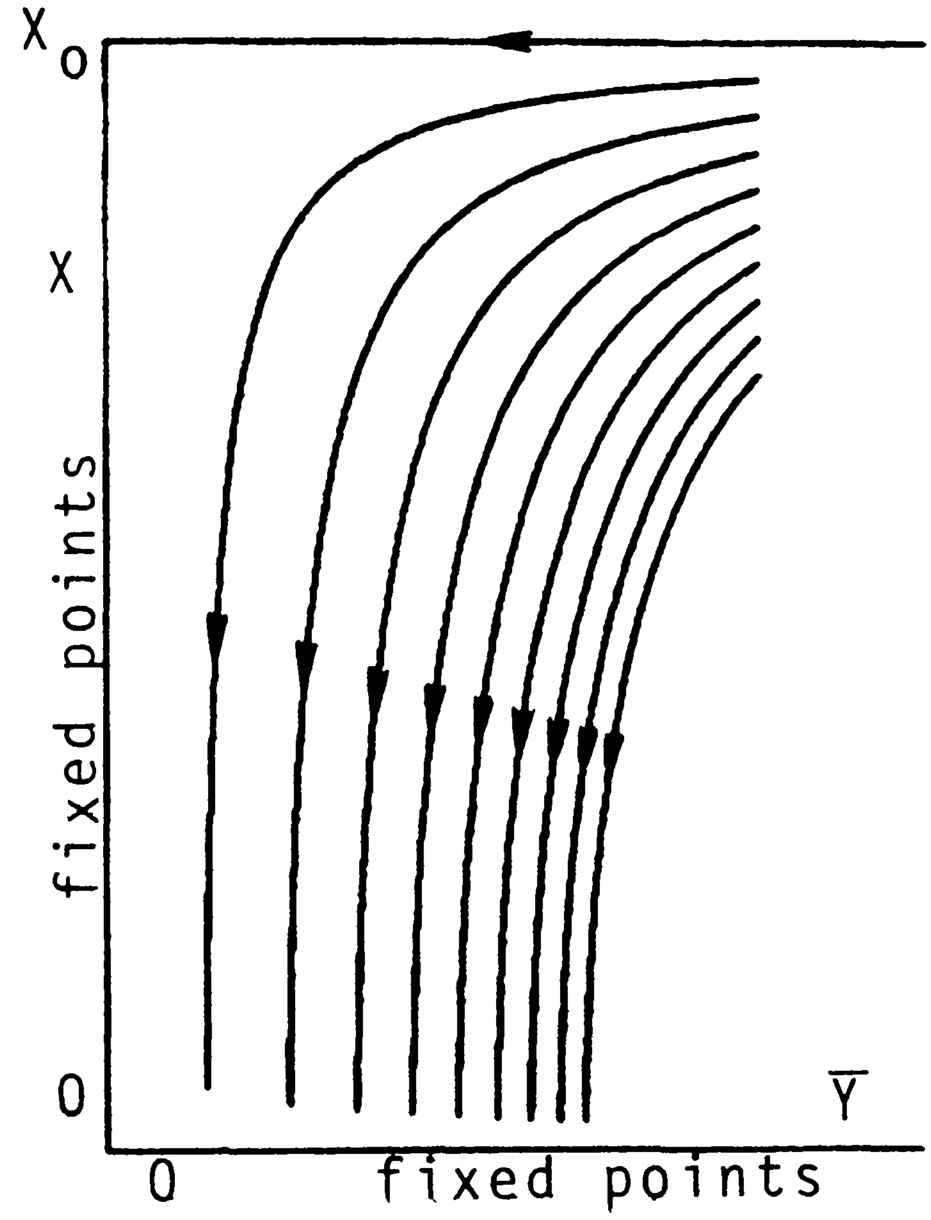

Fig. B2.

References

1. Broucke, R.: 'On the Isosceles Triangle Configurations in the Planar General Three-Body Problem', *Astron. Astrophys.* **73**, 303–313 (1979).
2. Devaney, R.: 'Triple Collision in the Planar Isosceles Three-Body Problem', *Inventiones Math.* **60**, 249–267 (1980).
3. Devaney, R.: 'Reversible Diffeomorphisms and Flows', *Trans. Amer. Math. Soc.* **218**, 89–113 (1976).
4. Lacomba, E., Simó, C.: 'Boundary Manifolds for Energy Surfaces in Celestial Mechanics', *Cel. Mechanics* **28**, 37–48 (1982).
5. Moser, J.: *Stable and Random Motions in Dynamical Systems.* Princeton (1973).
6. McGehee, R.: 'Triple Collision in the Collinear Three-Body Problem', *Inventiones Math.* **27**, 191–227 (1974).
7. McGehee, R.: 'A Stable Manifold for Degenerate Fixed Points with Applications to Celestial Mechanics', *J. Diff. Equations* **14**, 70–88 (1973).
8. Moeckel, R.: 'Orbits of the Three-Body Problem which Pass Infinitely Close to Triple Collision', *Amer. J. Math.* **103**, 1323–1341 (1981).
9. Moeckel, R.: *Heteroclinic Phenomena in the Isosceles Three-Body Problem*, preprint.
10. Simó, C.: 'Analysis of Triple Collision in the Isosceles Problem', in *Classical Mechanics and Dynamical Systems.* 203–224, Marcel Dekker (1981).
11. Simó, C., Llibre, J.: 'Characterization of Transversal Homothetic Solutions in the *n*-Body Problem, *Archive for Rational Mechanics and Anal.* **77**, 189–198 (1981).
12. Devaney, R.: 'Singularities in Classical Mechanical Systems', in *Ergodic Theory and Dynamical Systems, Proceedings of the Maryland Special Year*, A. Katok (ed.), 211–333, Birkhauser (1981).
13. Moeckel, R.: 'Chaotic Dynamics Near Triple Collision', to appear in *Ergodic Theory and Dynamical Systems.*